MANUFACTURING STRUCTURALLY INTEGRATED THREE DIMENSIONAL PHASED ARRAY ANTENNAS

A Thesis
Presented to
The Academic Faculty

by

Shannon R. Pine

In Partial Fulfillment
of the Requirements for the Degree
Master of Science in Mechanical Engineering

© Georgia Institute of Technology
May 2006

MANUFACTURING STRUCTURALLY INTEGRATED THREE DIMENSIONAL PHASED ARRAY ANTENNAS

APPROVED:

Jonathan Colton, Advisor
School of Mechanical Engineering
Georgia Institute of Technology

John Muzzy
School of Chemical & Bimolecular Engineering
Georgia Institute of Technology

Daniel Baldwin
School of Mechanical Engineering
Georgia Institute of Technology

John Schultz
Georgia Tech Research Institute

Date approved by advisor: April 5, 2006

ACKNOWLEDGMENTS

I thank my advisor, Dr. Jonathan Colton, for all of the support and guidance which were generously provided throughout this project. His advice, assistance and keen wit were invaluable to this work, and greatly appreciated. I would also like to thank Dr. John Schultz for providing technical information on the antenna designs. I also thank Dr. John Muzzy and Dr. Daniel Baldwin for serving on my thesis committee.

I would like to thank the Rapid Prototyping and Manufacturing Institute (RPMI) for use of equipment during this project. Thanks go to Andrew Layton for the rapid prototyping technical assistance provided.

I would like to thank my office mates Hoyeon Kim and Brian Nealis for many conversations which helped to make the last two years more enjoyable. I would also like to acknowledge two undergraduates, Charlie Graham-Brown and Nicholas Khaw, who assisted with this project. Their contributions and humor were much appreciated. Special thanks go to Hoyeon and Nicholas for allowing me to utilize their unsurpassed photographic abilities.

"I bend but do not break."

Jean de La Fontaine

TABLE OF CONTENTS

LIST OF TABLES

LIST OF FIGURES

NOMENCLATURE

Symbol	Meaning
β	Searle parameter
b	Bend width (inch)
Rx	Neutral axis radius of curvature (inch)
t	Thickness (inch)
r_p	Punch radius (inch)
ε	Strain
σ	Stress (psi)
σ_{max}	Maximum material stress (psi)
σ_{yield}	Material yield stress (psi)
K	Material linear strain hardening constant (psi)
v	Poisson's ratio
M_b	Bending moment (lbf-inch)
M_e	Recovery moment (lbf-inch)
$\sigma_{recovery}$	Recovery stress (psi)
E	Modulus of elasticity (psi)
ε_{final}	Final strain
ε_{bent}	Bent strain
$\varepsilon_{recovery}$	Recovery strain
ε_{spring}	Spring strain
h_c	Compression height (inch)
α	Bend angle (degree)
r'_p	Punch radius after recovery (inch)

SUMMARY

A phased array antenna differs from a conventional antenna, such as a dish antenna, in that it coherently adds radiation from multiple radiating elements instead of mechanical positioning to direct the signal. When transmitting and receiving information from a source while in motion, a phased array antenna can continuously adjust its signal to focus on the source. New antenna designs focus on integrating phased array antennas into the structure of the antenna platform, as advanced antenna platforms require the antenna to take up less and less real estate. With further development of phased array antennas, new designs become increasingly complex. This thesis developed and studied a number of manufacturing techniques for these new structurally integrated antennas.

Several possible manufacturing techniques are developed and analyzed for each antenna design to determine the methods suitable to manufacture the antennas. The manufacturing techniques include forming flex-circuit like material into different configurations that incorporate the geometry of the antenna design. In one design the flex circuit material is folded into hollow rectangular straws that contain a portion of the geometry of the antenna. A second design that utilizes the flex circuit material is created by constructing bent planes and L-shapes that contain a portion of the antenna geometry. These components are then assembled and the voids filled with rigid foam to create an antenna.

Another antenna design is manufactured by affixing coaxial cables to hollow plastic hemispheres. These hemispheres and rods are cast into epoxy for support. Layers of

copper wire mesh and fiberglass cloth are cast into the epoxy structure to compliment the performance on the antenna and the strength of the antenna, respectively.

Stereolithography is another manufacturing technique that is investigated. In this method a solid model of the antenna's lattice structure is created and a part is manufactured from photopolymer resin on a 3D Systems SLA 3500 machine. This part is then coated with a conductive material.

A requirement of the antenna design is that it be conductive, on the order of three Ohms from corner to corner. The antennas are subjected to an electrical test to determine if they meet the three ohm conductivity requirement. The antenna must be able to support itself through the manufacturing procedure and subsequent assembly procedures, until it is encased. The materials that are used to support the antenna structure must have a low dielectric constant so that the antenna functions properly. The antennas also are tested to see how well they can send and receive signals.

The straw and the bends and L-shape flex circuit concepts had a corner to corner resistance of 1.7 Ohms and 2.75 Ohms, respectively. The nickel coated SLA antenna had a corner to corner resistance of 300 Ohms. The silver coated SLA antenna had a corner to corner resistance of 0.85 Ohms. The silver and nickel antennas were tested to determine their antenna gain. The silver coated SLA antenna outperformed the nickel by having a larger area under the gain plot.

1 INTRODUCTION

1.1 Problem Description

A phased array antenna differs from a conventional antenna, such as a dish antenna, in that it coherently adds radiation from multiple radiating elements instead of mechanical positioning to direct RF energy. When transmitting and receiving information from a source while in motion, a phased array antenna can continuously adjust its signal to focus on the source. New antenna designs focus on integrating phased array antennas into the structure of the antenna platform, as advanced antenna platforms require the antenna to take up less and less real estate. With further development of phased array antennas, new designs become increasingly complex. The manufacturing techniques to facilitate the integration of complex antenna designs into the structure of an antenna platform must be developed, as traditional manufacturing operations, such as injection molding, machining and bulk deformation processes, are not well suited to create the small details and complex three dimensional lattice designs of the antennas.

Innovative solutions need to be developed that allow the manufacture of complex antennas, thereby enabling testing to be performed on actual devices. The results from testing physical models can buttress analytical models and lead to better antenna designs. This work developed and studied suitable methods for manufacturing three-dimensional, structurally-integrated antennas.

1.2 Problem Background

Future designs of naval vessels will need to minimize their signatures. One of the largest obstacles to this minimization is the large, odd shape of antennas on naval vessels as shown in Figure 1-1.

Figure 1-1 Typical Antenna Design

Figure 1-1 is an example of a navigational radar antenna that rotates and has a narrow path of visibility, or gain, perpendicular to the antenna, at its given position. In addition to their large, oddly shaped structures, these antennas have a refresh rate limited by their mechanical rotation speed.

Several complex designs that reduce the radar signal of the antenna and lessen the time for detection of threats have been developed. This was accomplished by creating a design that combines the functionality of a three dimensional antenna incorporated into the structure of the naval vessel. In this design, a three

dimensional antenna is encased in a composite structure, which then becomes an assembly part of the naval vessel as shown in Figure 1-2.

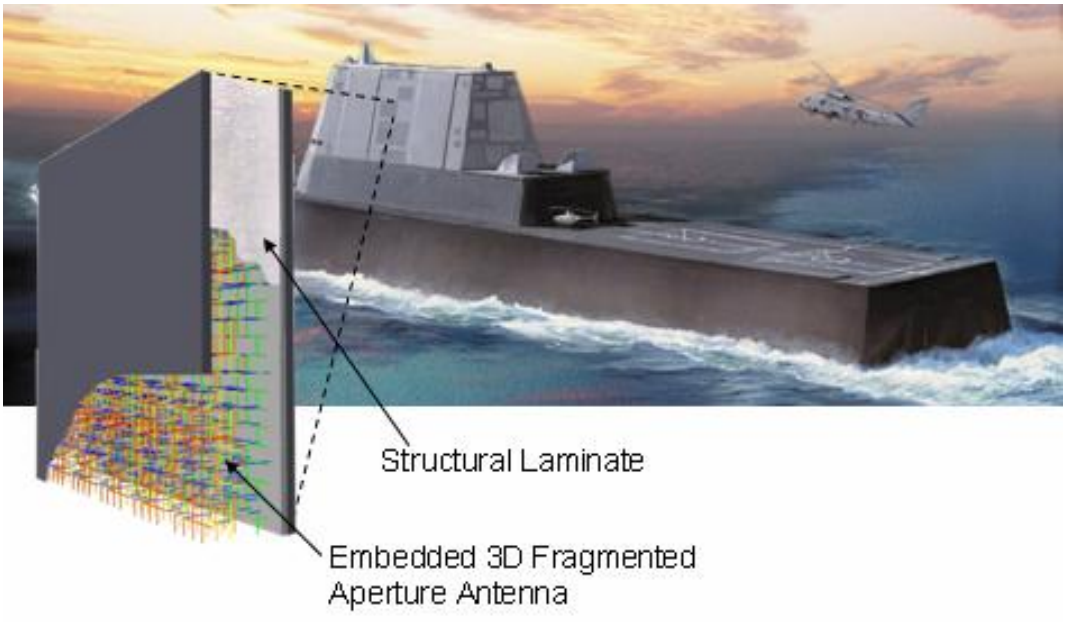

Figure 1-2 Antenna Design

1.3 Project Goals

The goal of this work was to investigate innovative methods to manufacture these structurally integrated antennas and then build models of the antennas. The antenna designs were provided in the form of wire frame drawings and a list of antenna nodal points and with the following requirements: Each individual three dimensional antenna must be conductive, on the order of three ohms resistance from corner to corner; the antennas must be strong enough to support themselves and maintain conductivity throughout subsequent manufacturing operations; and the materials used to create the antennas must be of a low enough dielectric constant for the three dimensional antennas to function properly.

The antenna designs included in this work were two epoxy encapsulated hemispheres designs, a fragmented slot antenna design, and two three dimensional antenna designs. One design of the epoxy encapsulated hemispheres antenna is shown in Figure 1-3.

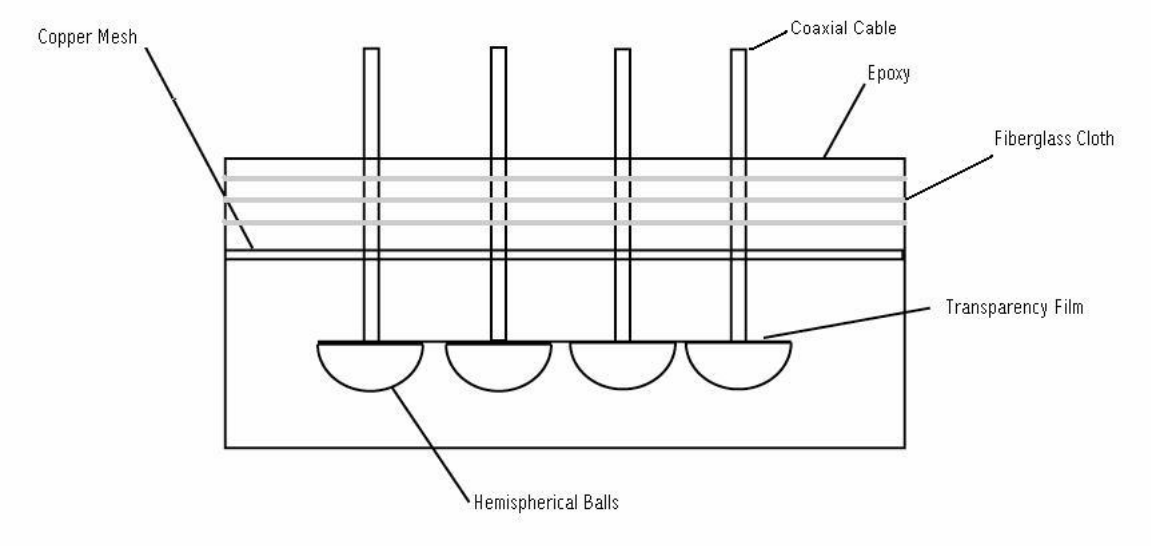

Figure 1-3 Epoxy Encapsulated Hemispheres Antenna (Side View)

This antenna design features plastic hemispherical shells sealed with transparency film which creates voids to locate radiators that are connected to copper jacketed coaxial cables. These antenna parts are cast into an epoxy structure with copper mesh, which serves as a reflective backplane for the radiators, and fiberglass cloth, which increases the mechanical properties of the structure.

A second design of the epoxy encapsulated hemispheres antenna is shown in Figure 1-4.

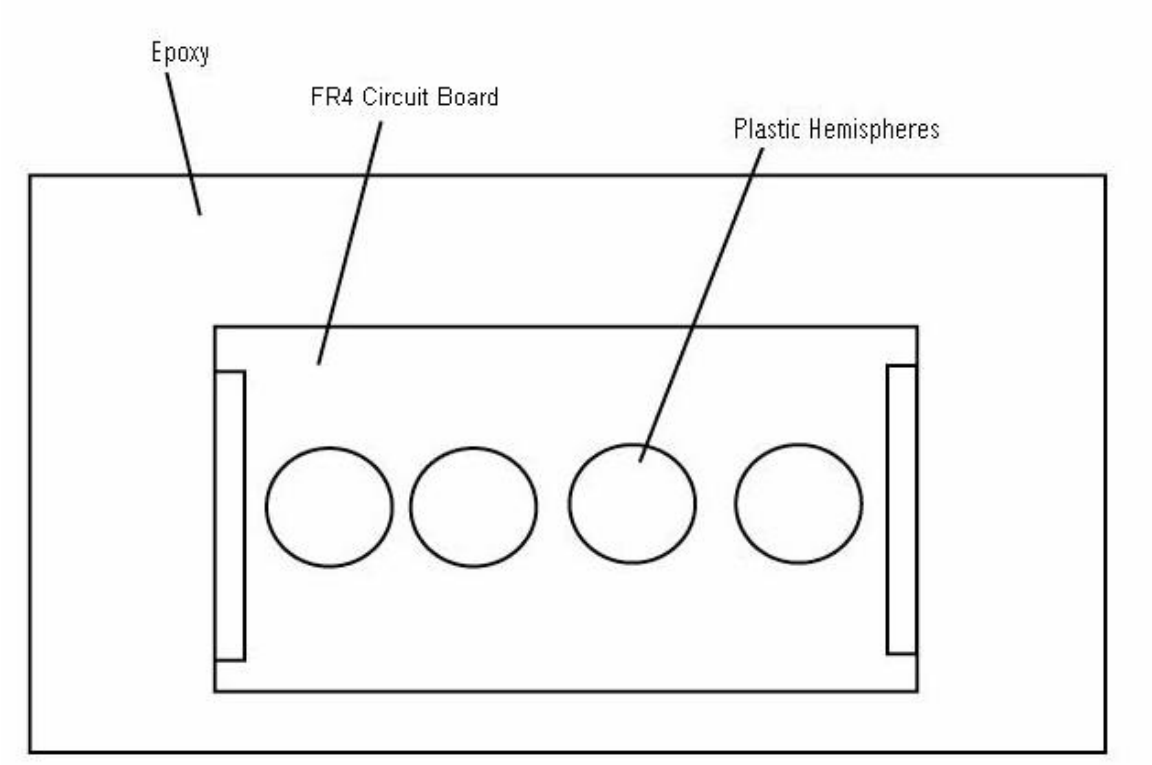

Figure 1-4 FR4 Circuit Hemispheres Antenna (Top View)

This antenna design features plastic hemispherical shells sealed to FR4 circuit board which creates voids to locate radiators that are electrically connected to the circuit board. These antenna parts are cast into an epoxy structure.

The fragmented slot antenna design is shown in Figure 1-5.

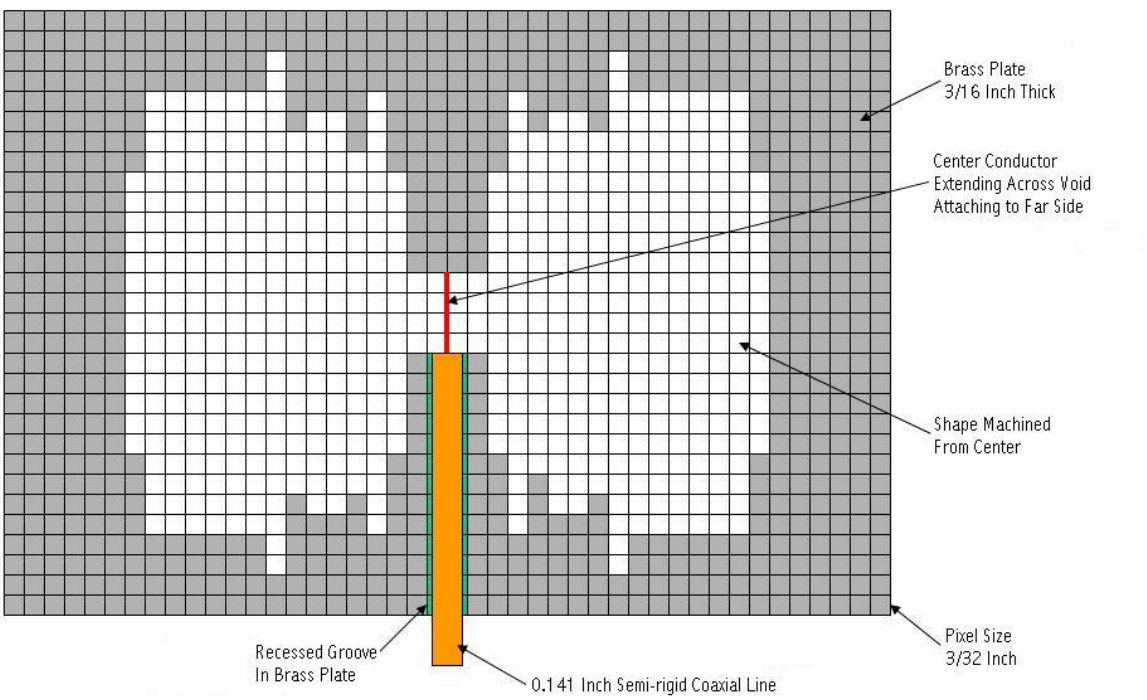

Figure 1-5 Fragmented Slot Antenna (Top View)

The fragmented slot antenna design comprised a brass plate, copper jacketed coaxial cable, conductive and non conductive epoxies and acrylic sheet. The brass plate was machined via wire EDM to remove a portion of the center of the plate resulting in a geometric structure that could function as an antenna. A recessed groove was milled in the brass plate with a CNC milling machine to allow the copper jacketed coaxial cable to locate in the center of the plate. The center conductor of the copper jacket coaxial cable extended across the void in the plate and was soldered to the side opposite the recessed groove. The space between the copper jacketed coaxial cable and the recessed groove was filled with conductive epoxy. The void in the center of the plate, where material was removed by the EDM operation, was filled with epoxy.

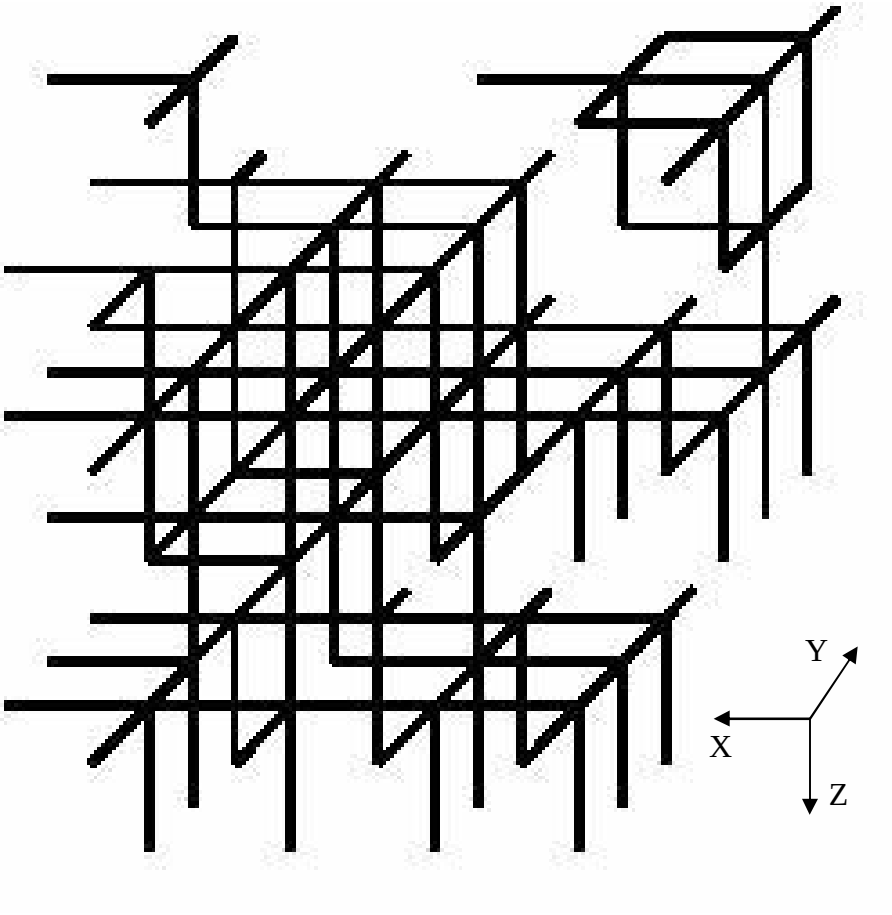

Figure 1-6 First Three Dimensional Antenna Design

The first three dimensional antenna design is shown in Figure 1-6. Each line in this figure represents an antenna element. The length and diameter of each element segment are 1.5 cm and 1.5 mm, respectively. The antenna design is in the shape of a rectangular prism with dimensions of 6 cm in the Y direction, by 7.5 cm in the X direction by 7.5 cm in the Z direction. The antenna elements are to be conductive, and the space in between the elements is to be filled with a material possessing a low dielectric constant. The first design consists of an array of 150 elements joined together forming one single part.

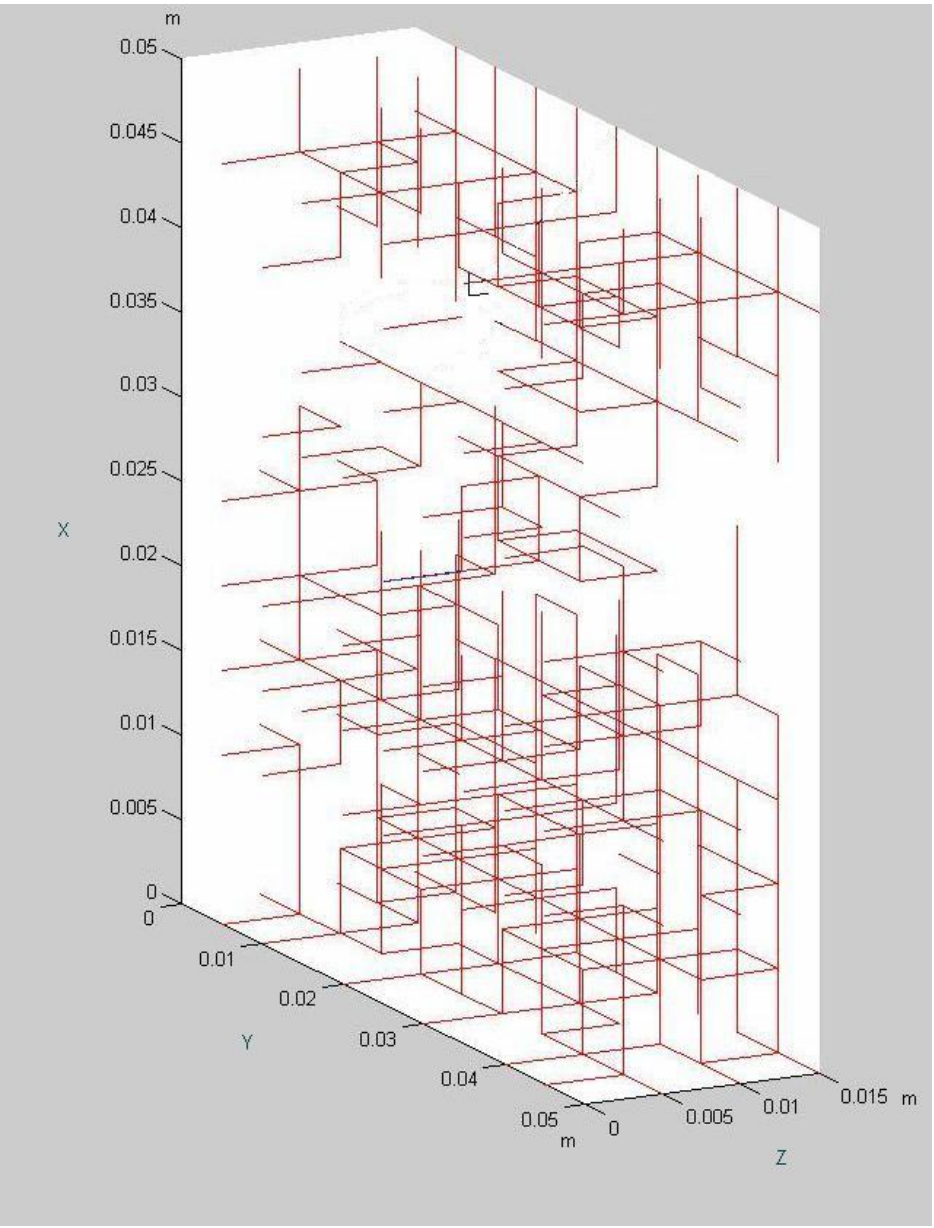

Figure 1-7 Second Three Dimensional Antenna Design

A second three dimensional antenna design is shown in Figure 1-7. Each line in this figure represents an antenna element. The length and diameter of the antenna elements are 0.5 cm and 1.5 mm, respectively. The antenna design is in the shape of a rectangular prism with dimensions of 5 cm in the Y direction, by 5 cm in the X

direction by 1.5 cm in the Z direction. The antenna elements are to be conductive, and the space in between the elements is to be filled with a material possessing a low dielectric constant.

1.4 Thesis Overview

Chapter 1 discussed designs of structurally integrated antennas, discussed the challenges associated with their manufacture, and presented the focus of this work. Background information was provided as to the importance of this research.

Chapter 2 discusses the makeup and properties of the flex circuit material. Available varieties of the flex circuit material are provided. A method of creating circuit traces on flex circuit is detailed. Methods used to manufacture antennas, including epoxy encapsulation, rapid prototyping, and bending operations are discussed.

Chapter 3 details the development and theory of an experimental bending method. An analytical bending model is developed. Material models for polyimide film and copper foil are discussed. Bending limits of the flex circuit material are calculated. Theoretical values of the final strain and recovery strain from the bending of flex circuit is provided. A spring based bulging model is developed.

Chapter 4 details the experimental procedures used to test the bending of the flex circuit material. A bending fixture is designed and a bending procedure is

developed. Epoxy encapsulation testing is performed. Models of epoxy encapsulated antenna designs are constructed. Concepts for three dimensional antenna designs manufactured from flex circuit are discussed. Models of three dimensional antennas constructed from flex circuit material are created. Methods of manufacturing three dimensional antennas via rapid prototyping are presented.

Chapter 5 presents the results of the experimental procedures discussed in Chapter 4. Results of the experimental bending tests of the flex circuit is provided and analyzed. The predicted values of stain, for the bending of flex circuit material, are compared to the experimental bending results. An evaluation of the flex circuit material, after bending, is conducted. Discussion of models of the epoxy encapsulated antenna designs is provided. Models of three dimensional antennas manufactured from flex circuit material are discussed. Testing results of three dimensional antennas manufactured via SLA are provided and discussed.

Chapter 6 provides a brief summary of the findings of this work. Recommendations for continuing research on three dimensional antenna manufacturing are provided.

2 BACKGROUND

2.1 Introduction

In this chapter, the makeup of flexible circuit material is discussed. A method of circuit formation is presented. Manufacturing methods that are used in this work are discussed.

2.2 Flexible Circuit Material

Flexible circuit material (flex circuit) is used in this work as a material to construct three dimensional antennas. This material is made from polyimide film, copper foil and a binder which come in a variety of thicknesses.

2.2.1 Material

Flex circuit is a composite of polymer film, copper foil and a binder. With origins dating to early 1900's the use of this material has seen double digit growth in recent years [14]. The flex circuit material used in this work is manufactured by DuPont under the brand name of Pyralux flexible composites. The Pyralux flex circuit is constructed of DuPont Kapton polyimide film, annealed, rolled or electro-deposited copper, and a modified C-Staged acrylic adhesive. The flex circuit is available in a variety of thickness combinations of polyimide, copper and adhesive. The flex circuit also can have one or two exposed sides of copper, with the multiple sides

being used for multiple layered circuit applications. An example of the combinations of polyimide, copper and adhesive available is shown in Table 2-1 [2].

Table 2-1: Available Flex Circuit Material Combinations

Product Code	Copper oz/ft^2 (g/m^2)	Adhesive Thickness Mil (μm)	Kapton Thickness Mil (μm)
LF7002R	1 (305)	0.5 (13)	0.5 (13)
LF7004R	0.5 (153)	1 (25)	0.5 (13)
LF7008R	2 (610)	0.5 (13)	1 (25)
LF7011R	1 (305)	0.5 (13)	1 (25)
LF7012R	0.5 (153)	0.5 (13)	0.5 (13)
LF7037R	1 (305)	1 (25)	0.5 (13)
LF7038R	2 (610)	1 (25)	0.5 (13)
LF7062R	0.5 (153)	0.5 (13)	1 (25)
LF7092R	1 (305)	0.5 (13)	2 (51)
LF7097R	1 (305)	2 (51)	1 (25)
LF8510R	0.5 (153)	1 (25)	1 (25)
LF8520R	0.5 (153)	1 (25)	2 (51)
LF9110R	1 (305)	1 (25)	1 (25)
LF9120R	1 (305)	1 (25)	2 (51)
LF9130R	1 (305)	1 (25)	3 (76)
LF9150R	1 (305)	1 (25)	5 (127)
LF9210R	2 (610)	1 (25)	1 (25)
LF9220R	2 (610)	1 (25)	2 (51)

Pyralux coverlay is a composite material made of the same materials as the flex circuit, without the copper. Once the circuit is etched onto the copper of the flex circuit material, the coverlay is used as a protective coating. The coverlay serves as a barrier to oxidation as well as a mechanism to help protect the integrity of the circuit. The coverlay is available in a variety of thickness combinations of polyimide and adhesive shown in Table 2-2 [2].

Table 2-2: Available Coverlay Material Combinations

Product Code	Adhesive Thickness Mil (μm)	Kapton Thickness Mil (μm)
LF0110	1 (25)	1 (25)
LF0120	1 (25)	2 (51)
LF0130	1 (25)	3 (76)
LF0150	1 (25)	5 (127)
LF0210	2 (51)	1 (25)
LF0220	2 (51)	2 (51)
LF0230	2 (51)	3 (76)
LF0250	2 (51)	5 (127)
LF0310	3 (76)	1 (25)
LF1510	0.5 (13)	1 (25)
LF7001	0.5 (13)	0.5 (13)
LF7013	1 (25)	0.5 (13)
LF7034	0.5 (13)	1 (25)
LF7082	2 (51)	0.5 (13)

Pyralux flexible circuit material is manufactured to comply with IPC specification IPC-4202/1: “Flexible Metal-Clad Dielectrics for use in Fabrication of Flexible Printed Wiring” with general material specifications shown in Table 2-3 [2].

Table 2-3: IPC Specification and Typical Material Values

Property	IPC Specification	Typical Value
Peel Strength, min. lb/in (kg/cm) As received After solder	 8 (1.4) 7 (1.3)	 10 (1.8) 9 (1.6)
Dimensional Stability, max., Percent	0.15	0.10
Dielectric Constant, max. (at 1 MHz)	4.0	3.6
Dissipation Factor, max. (at 1 MHz)	0.03	0.02
Volume Resistivity, min. megaohm-cm (ambient)	10^7	10^9
Surface Resistivity, min. megaohm-cm (ambient)	10^6	10^8

2.2.2 Circuit Formation

The flexible circuit material is treated with antioxidant coatings that must be removed before circuit formation. The exposed copper side of the flexible circuit material needs to be cleaned and roughened. This can be accomplished by mechanical or chemical means.

The mechanical preparation process involves scrubbing the exposed copper of the flexible circuit material with 3F grit acid pumice slurry. Scrubbing by hand or by mechanical rotary brush is acceptable. Care must be taken when scrubbing to not distort the material. To lessen the distortion, the flexible circuit material can be backed with a rubber support pad while scrubbing. After the scrubbing process is complete, the flexible circuit material is rinsed with water and dried with forced air.

The chemical preparation process involves cleaning the exposed copper of the flexible circuit material with a general acid or alkaline cleaner to remove oils, dirt, and fingerprints. A 10% H_2SO_4 bath, at a temperature of 120ºF (49ºC), for 1 minute, is then used to remove the antioxidant coating [2]. A persulfate or peroxide-sulfuric base microetch then is used to roughen the surface. A 10% H_2SO_4 rinse is then used to clean the flexible circuit material of any residue from the microetch [2]. The material then is dried with forced air.

After cleaning, photoresist material should be laminated to the copper side of the flexible circuit material within a few hours to minimize time-based oxidation. The user should follow the recommendations provided by the manufacturer of the photoresist for the lamination procedure. Generally, for optimal quality, a heated roller method of lamination is preferred, provided that roll temperatures in excess of approximately 230ºF (110ºC) are not used [2].

The flexible circuit material with photo resist then is exposed to a fixed point UV light source. A pattern of the desired circuit is used between the light source and the photoresist. The photoresist reacts with the light in the areas allowed by the pattern. The unexposed photoresist is then removed by washing in development solution, according to the development recommendation of the manufacturer.

The desired circuit now is protected by the exposed photoresist, and the undesirable copper can be removed from the flexible circuit material by etching. A solution of ammoniacal, cupric chloride or ferric chloride can be used for the etching process. After etching a warm water rinse and forced air drying process will remove any residue from the etching process and dry the flexible circuit material, respectively. The exposed photoresist then can be removed by any common stripping procedure.

2.3 Manufacturing Methodologies

Manufacturing methods that are used in this work are presented in this section. Epoxy encapsulation, rapid prototyping, and bending operations are discussed.

2.3.1 Epoxy Encapsulation

Epoxy encapsulation is a required manufacturing procedure for the hemispheres antenna design as well as the fragmented slot antenna design. Epoxies are thermosetting polymers comprised of two components, termed A and B, when combined in the correct proportions react to form a solid. Component A is an epoxy resin and component B is an epoxy curing agent. Epoxies exhibit excellent adhesive properties due to the formation of strong polar bonds with contacting surfaces [4]. When cured, epoxies are strong, hard, possess good dimensional stability, and are heat and chemical resistant. In addition, epoxies are good electrical insulators in neat form, or can be doped to become good electrical conductors. Epoxies have a relatively low

viscosity when the components are mixed, giving them excellent flow properties and allowing them to be easily poured into a mold. Epoxies can be cured at room or elevated temperatures and have pot lives between a few minutes and several hours depending on the curing conditions and specific component compositions.

A critical aspect of epoxy encapsulation is the control of material shrinkage during the curing process. Shrinkage of the epoxy during curing is not desirable as it causes voids to form in the epoxy and causes the epoxy to expose the object being encapsulated. The amount of shrinkage is related to the amount of heat produced by the curing process. The curing process is exothermic, generating heat during the curing process. As the reaction progresses the heat generated increases the temperature of the material. An increase in the temperature of the material increases the reaction rate, thereby producing more heat as the reaction continues.

The measured rate of cure is referred to as the gel time and the measured amount of heat generated is the peak exotherm [5]. The shorter the gel time and the larger the mass of epoxy to cure are, the higher the exotherm is [5]. The rate of cure is controlled by the chemical makeup of the epoxy components and the temperature of the material. The rate of cure can be controlled by altering the chemical composition of the components or by altering the ratio in which the components are combined, as well as reducing

the temperature of the material. For a lower rate of reaction one would mix less hardener with the epoxy resin, however a large reduction of the amount of hardener could lead to the part not fully curing. The ratio of surface area to volume can also control the rate of reaction, as a larger ratio will allow more heat to leave the material, lowering the temperature of the material; thereby causing a lower rate of reaction.

2.3.2 Rapid Prototyping

Rapid prototyping is a manufacturing procedure that was used in this work to make three dimensional antennas. Previously when a prototype part was desired, the machining process and casting pattern development could have taken weeks or even months to produce a prototype. With the advent of rapid prototyping processes, circa 1980, one could turn a three dimensional CAD drawing into a prototype part in a matter of hours. One of the main differences between rapid prototyping processes and traditional manufacturing processes is that many of the rapid prototyping processes are additive, meaning that the parts are made from adding material rather than removing material from a billet. Various metal, polymer, and ceramic materials can be utilized in rapid prototyping processes.

In rapid prototyping the user must convert a three dimensional CAD drawing of the user's part into a format that is compatible with rapid prototyping technology. The intermediate file type that is used to transition from the three

dimensional CAD is an STL file. The STL file utilizes triangles to represent the surfaces of the CAD drawing. Each triangle that represents the surface meets adjacent triangles along common edges, sharing two common vertices with each adjacent triangle.

STL files are imported into rapid prototyping software where they are used to generate the machine motions. The STL file is sliced into individual layers, and the layers are used to create an outline of the part at that layer, with the rapid prototyping software generating the machine path needed to construct that layer. This process of part slicing and machine path creation from individual layers is fundamentally identical for different additive rapid prototyping processes, including stereolithography (SLA), selective laser sintering (SLS), fused deposition modeling (FDM), and laminated object manufacturing (LOM).

Stereolithography is a type of rapid prototyping process that uses a solid state UV laser to solidify liquid photopolymer resins. The photopolymer resin is stored in a vat in the machine. A platform, which is capable of vertical motion, resides in the vat of liquid photopolymer. The platform is positioned for the first layer, and the laser traces over the area that needs to be solidified. The platform then is lowered, a fresh layer of photopolymer is spread over the previous layer, and the process is repeated until the part is complete. A point of interest is the need for supports for overhanging edges. The beginning

layers of a part overhang require a support structure so that the layers do not sag or tear away from the main body of the part.

Selective laser sintering is a rapid prototyping process that uses a carbon dioxide laser to sinter powdered material to form a part. The powdered material is stored in a reservoir that feeds the machine. A platform, similar in application to the platform used in stereolithography, is used. A layer of powdered material is spread onto the platform and then sintered to form the first layer of the part. The platform is then lowered and another layer of powder is spread over the platform and sintered. The process continues until the part is complete. A main difference between selective laser sintering and stereolithography is that the use of supports is not needed in SLS because the unfused powder supports the overhanging layers.

2.3.3 Bending

One of the most popular manufacturing operations is bending. This work bends flex circuit material to build three dimensional antennas. In bending the geometry of a material is formed by the local deformation of the material in the immediate area of the bend. Several models can be used to approximate the material behavior while it undergoes bending. These models are generally based on inner moment calculations to determine permanent and elastic material deformations as well as elastic recovery.

An important consideration when developing a bending model is to determine if a plane strain or plane stress condition exists, depending on the material geometry. A beam is considered to have a small width, as compared to its thickness, which allows the transverse stresses to be considered negligible while anticlastic bending occurs along the width of the bend. However, in a plate, the width of the bend is large compared to the thickness of the material and the transverse stresses along the width of the plate can not be considered negligible, and they prevent the anticlastic bending along the width of the plate. A plane stress situation is generally used for beam bending models when the thickness of the material to be bent is greater than approximately $1/20^{th}$ of the bend width. A plane strain situation is generally used for plate bending models when the thickness of the material to be bent is less than approximately $1/20^{th}$ of the bend width [7]. Chapter 3 provides the theory behind the bending of the flex circuit. The development of an analytical model for bending of flex circuit is discussed there.

2.4 Summary

In this chapter the makeup and properties of the flex circuit material were discussed. Available varieties of the flex circuit material were provided. A method of creating circuit traces on flex circuit was detailed. Methods used to manufacture antennas, including epoxy encapsulation, rapid prototyping, and bending operations were discussed.

Chapter 3 details the theory behind the experimental bending method. An analytical bending model is developed. Material models for polyimide film and copper foil are discussed. Bending limits of the flex circuit material are calculated. Theoretical values of the final strain and recovery strain from the bending of flex circuit is provided. A spring based bulging model is developed.

3 THEORY

3.1 Introduction

A method of making antennas by bending flexible circuit material is used in this work. The development of methods of bending the flex circuit as well as an analytical model for predicting the bending behavior of the flex circuit is discussed. Material models for the flex circuit are provided and bending limits of the materials are calculated.

3.2 Development of Flex Circuit Bending Method

The flex circuit material used in this work is Pyralux LF9120R which is a single-sided copper-clad laminate with a copper thickness of 1 Mil, a polyimide thickness of 2 Mil and an adhesive thickness of 1 Mil. This is laminated to Pyralux LF0120 coverlay with a polyimide thickness of 2 Mil and an adhesive thickness of 1 Mil [2].

This flex circuit material has copper traces that represent the geometry of the antenna. Every copper trace on the flex circuit corresponds to an antenna element. Figure 3-1 shows how the flex circuit traces represent antenna geometry.

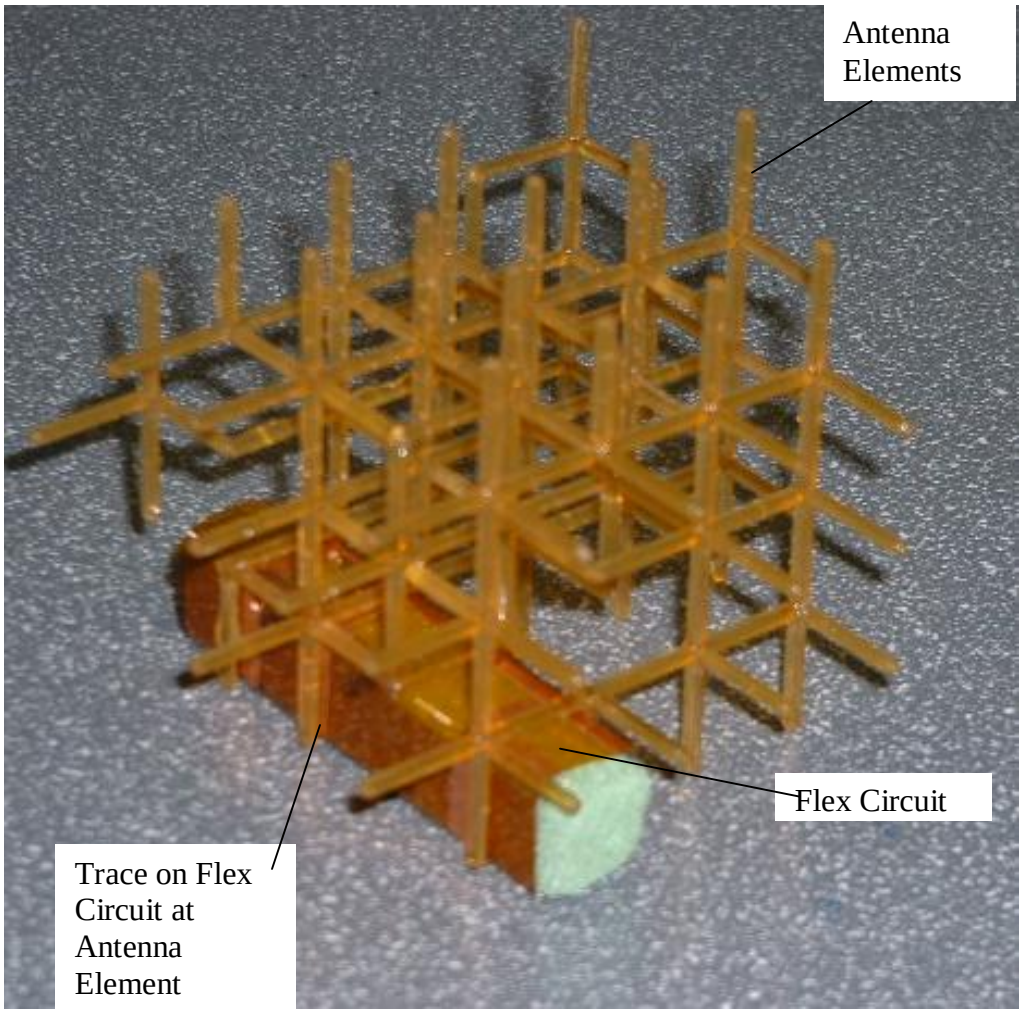

Figure 3-1 Antenna Geometry

The flex circuit material needs to be bent to 90 degrees to complete the antenna geometry. Two common bending operations are the punch and die and the sweeping method. Although these methods may be useful in many applications, they are not suitable for bending very thin materials as they cannot generate the amount of strain needed for a suitable amount of plastic deformation to occur in the Pyralux. Therefore an alternative method of bending was developed.

One method that was developed is a compressive bending method as shown in Figure 3-2.

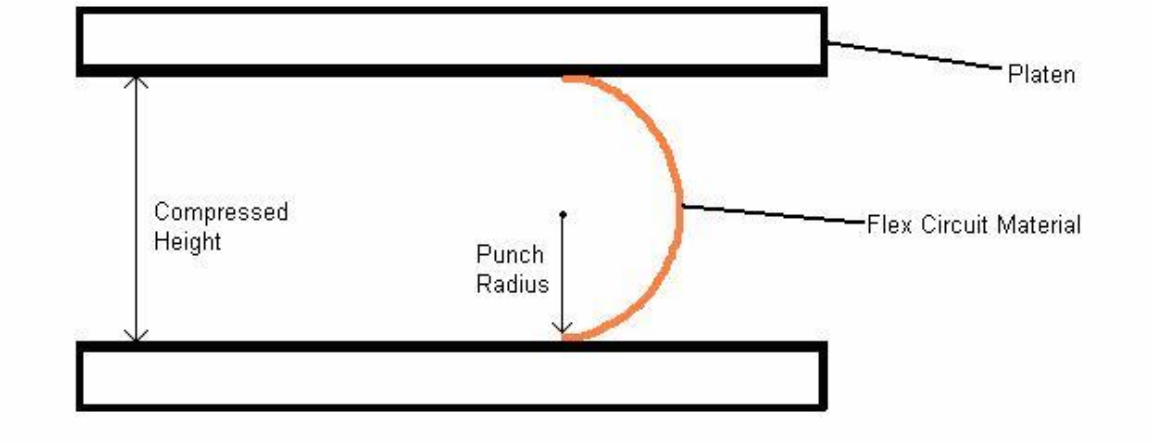

Figure 3-2 Compressive Bending Method

In this method the material is bent into a U-shape with the sides of the U parallel to the platens of a press. The platens are closed to a compressed height that generates a desired bend angle in the material. This method requires experimental testing of the bending of the material to develop an empirical relationship between the compression height and the bend angle of the material, as well as the development of an analytical model to predict the final bend angle resulting for a specific compression height.

Another method of bending that was developed is a rolling method. In this method the flex circuit material is wrapped around a spacer as shown in Figure 3-3.

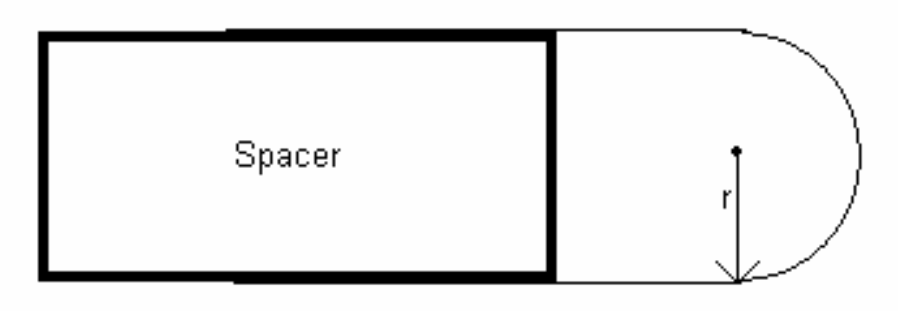

Figure 3-3 Flex Circuit with Spacer

The spacer and flex circuit assembly is then rolled between two rollers. The resulting bend radius is half of the thickness of the spacer. The thickness of the spacer determines the resulting bend angle of the flex circuit material. In a production atmosphere, the rolling method is preferred to the compression method because it is quicker. In this work the compression method was used for material testing because it allows for more control over the bending conditions.

3.3 Development of Analytical Bending Model

An analytical model for the bending of a thin sheet using a strain hardening material model is detailed in this section. The strain hardening material model was chosen because the polyimide and copper materials exhibit strain hardening properties. The first consideration in developing the bending model is to determine if plane strain or plane stress conditions exist, depending on the material geometry. A beam is considered to have a small bending width with respect to the thickness. This assumption allows the transverse stresses to be considered negligible, in addition, anticlastic bending occurs along the width of the bend. However, in a plate, the width of the bend is large compared to the thickness of the material and the

transverse stresses along the width of the beam can not be considered negligible; this prevents the anticlastic bending along the width of the bend. A plane stress situation is generally used for bending models when the thickness of the material being bent is on the order of $1/20^{th}$ of the bend width or greater [7].

Plane strain was assumed for this model as the geometric requirements for plane strain, where the thickness of the material is much less than the width of the bend, were met. This assumption can be verified by using the Searle parameter, β, where b is the width of the bend, R_x is the radius of curvature of the neutral axis, and t is the thickness, shown in Equation 3-1.

$$\beta = \frac{b^2}{R_x \times t}$$

Equation 3-1

It has been shown that a plane strain condition exists when the Searle parameter is greater than or equal to 100 and that the structural rigidity increases by a factor of $1/(1-\nu^2)$ [7].

The minimum bend width of this material is 0.591 inch, which is the length of a single antenna element. The thickness of the flex circuit material is 0.007 inch. By using Equation 3-1, it is determined that the bending of the flex circuit material occurs under a plane strain condition for all compression heights less than 0.506 inch.

The engineering strain distribution in a material undergoing a bending operation is given by Equation 3-2 where r_p is the punch radius and t is the thickness.

$$\varepsilon = \frac{1}{\left(\frac{2r_p}{t} + 1\right)}$$

Equation 3-2

The maximum stress of the material, $\sigma_{max,}$ can be calculated using the engineering strain, with Equation 3-3 where K is a linear strain hardening material model factor.

$$\sigma_{\max} = \frac{\sigma_{yield} + K\varepsilon}{1 - \nu^2}$$

Equation 3-3

The factor of $\left(1-\nu^2\right)$ is included due to the plane strain assumption.

A strain hardening stress distribution for a single material is shown in Figure 3-4.

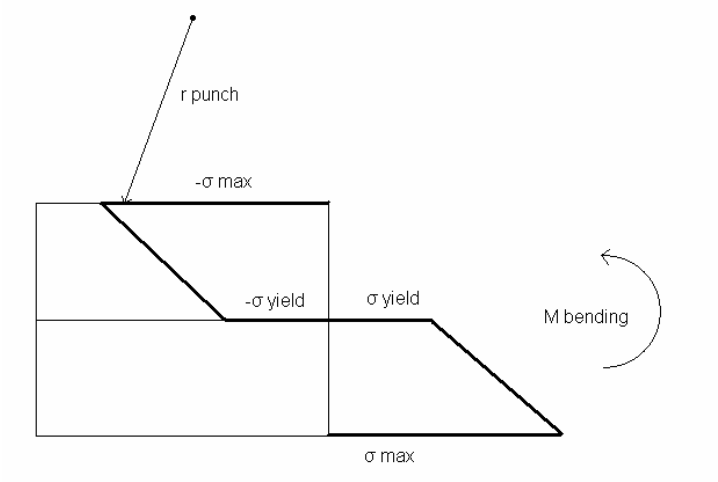

Figure 3-4 Material Stress Distribution

The equation for the bending moment can then be derived by integrating the stress distribution over the thickness of the material as shown in Equation 3-4.

$$M_b = \frac{\sigma_{yield} \times b \times t^2}{12}\left(1 + 2\frac{\sigma_{\max}}{\sigma_{yield}}\right)$$

Equation 3-4

When the material is released, it undergoes a recovery process. This process is assumed to be elastic as shown in Figure 3-5.

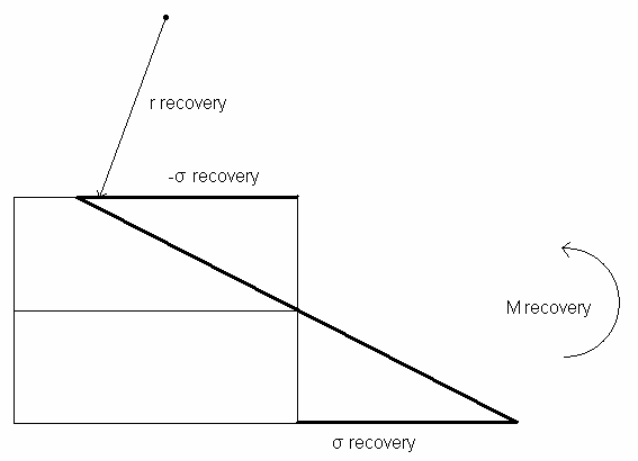

Figure 3-5 Elastic Recovery

The moment created by this stress distribution, M_e is equal in magnitude to M_b. The equation for M_e can then be derived by integrating the stress distribution over the thickness of the material as given by Equation 3-5.

$$M_e = \frac{t^2 \times b \times \sigma_{recovery}}{6}$$

Equation 3-5

From Equation 3-5 one can solve for the recovery stress $\sigma_{recovery}$, and calculate the recovery strain as given by Equation 3-6.

$$\varepsilon_{recovery} = \frac{1}{E}\left(\frac{6M_b}{t^2 b}\right)$$

Equation 3-6

The total amount of strain in the material after the recovery process, i.e., the permanent deformation of the material, can be calculated from the recovery strain and the strain in the material before the recovery process, shown in Equation 3-7.

$$\varepsilon_{final} = \varepsilon_{bent} - \varepsilon_{recovery}$$

Equation 3-7

This equation can be combined with geometric compatibility equations to calculate the final bending angle of the material.

This analytical model of bending analysis can be expanded to include laminated composite materials such as flex circuit material. The flexible circuit material is a composite of thin copper and polyimide sheets laminated together with an acrylic adhesive as shown in Figure 3-6.

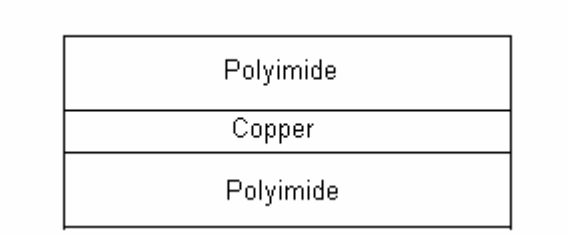

Figure 3-6 Flexible Circuit Material Cross-section

It was assumed that the layers of copper and polyimide were perfectly joined and the thickness of the adhesive can be included with that of the polyimide. An elastic

strain hardening material model was used in this bending analysis. Figure 3-7 shows a general stress distribution of the flex circuit material when it is bent.

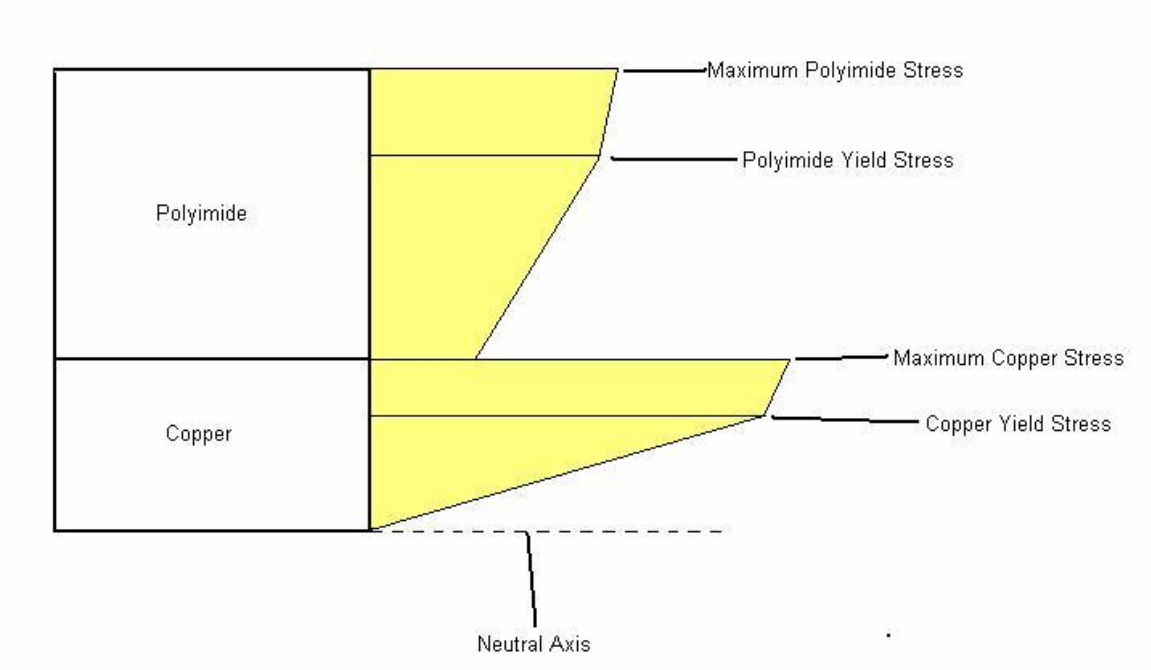

Figure 3-7 Flex Circuit Stress Distribution

A program was created using Matlab that calculated the bending moment by integrating the stress distribution of the material over the thickness of the material.

The recovery of this material when released is assumed to be elastic and is shown in Figure 3-8.

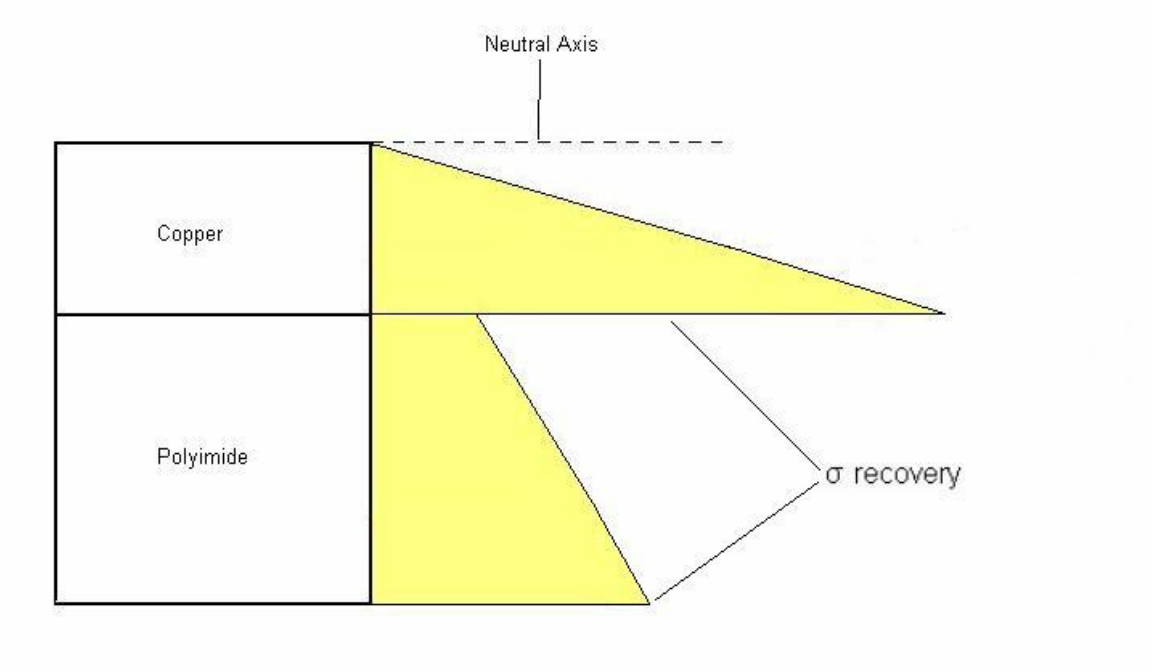

Figure 3-8 Flex Circuit Elastic Recovery

The elastic recovery moment was calculated by integrating the stress distribution over the material thickness using the Matlab program. The elastic recovery strain was calculated using the Matlab program over a range of bend radii to determine the springback of the material. The source code for this program is included in Appendix A.

Figure 3-9 shows the theoretical final bending strain predicted by the model, and Figure 3-10 shows the theoretical springback strain predicted by the model.

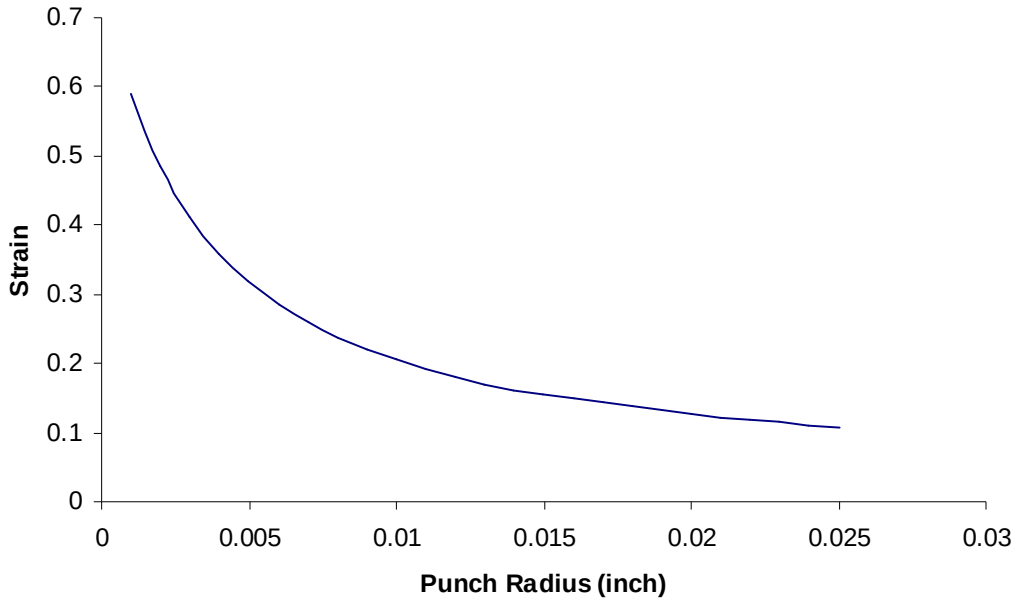

Figure 3-9 Theoretical Final Strain

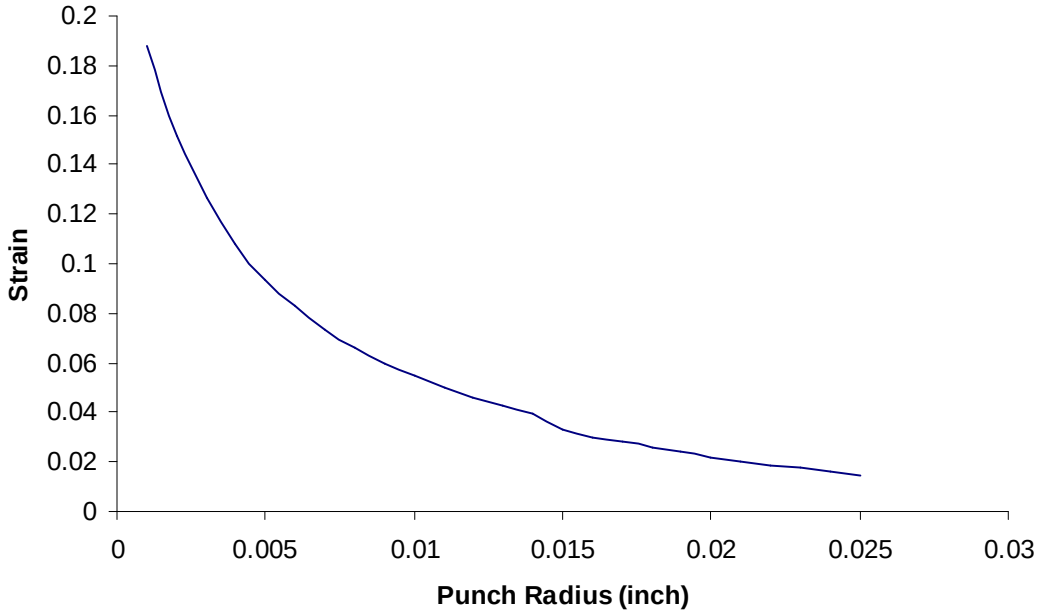

Figure 3-10 Theoretical Recovery Strain

When first comparing the predicted values of final and recovery strain to the experimental data, it was apparent that the material was bulging during the bending process, which is discussed in section 5.2. A bulging model was developed that approximated the material bulging as a spring in series with the polyimide material on the inside of the bend of the flex circuit, as shown in Figure 3-11.

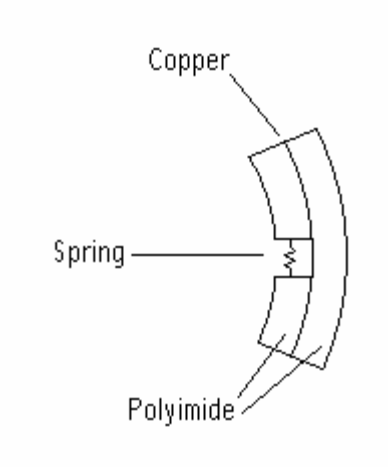

Figure 3-11 Spring Bulging Model

The spring in the bulging model will increase the recovery strain of the material by storing elastic energy during the bending process. The amount of recovery strain that the spring stores was determined empirically from the testing data and the theoretical model. The amount of recovery strain that the spring stores is shown in Figure 3-12.

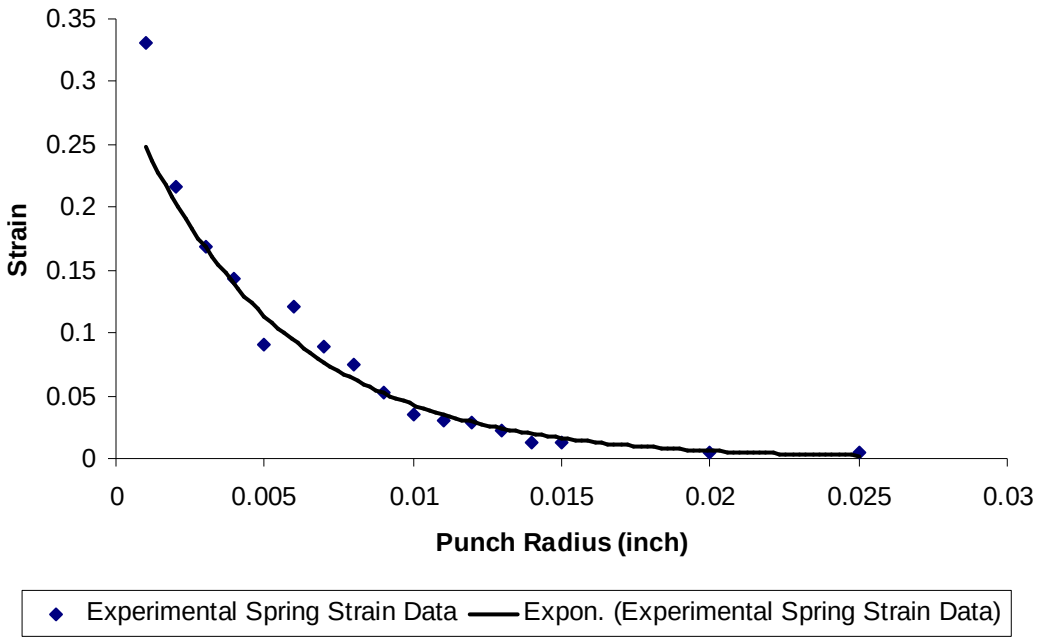

Figure 3-12 Spring Recovery Strain

An equation for recovery strain generated by the spring model was derived from a regression line that fit the measured data.

$$\varepsilon_{Spring} = 0.3017e^{-195.24 r_P}$$

Equation 3-8

This spring model was incorporated into the Matlab bending model. The corrected theoretical final strain is shown in Figure 3-13, and the corrected theoretical recovery strain is shown in Figure 3-14.

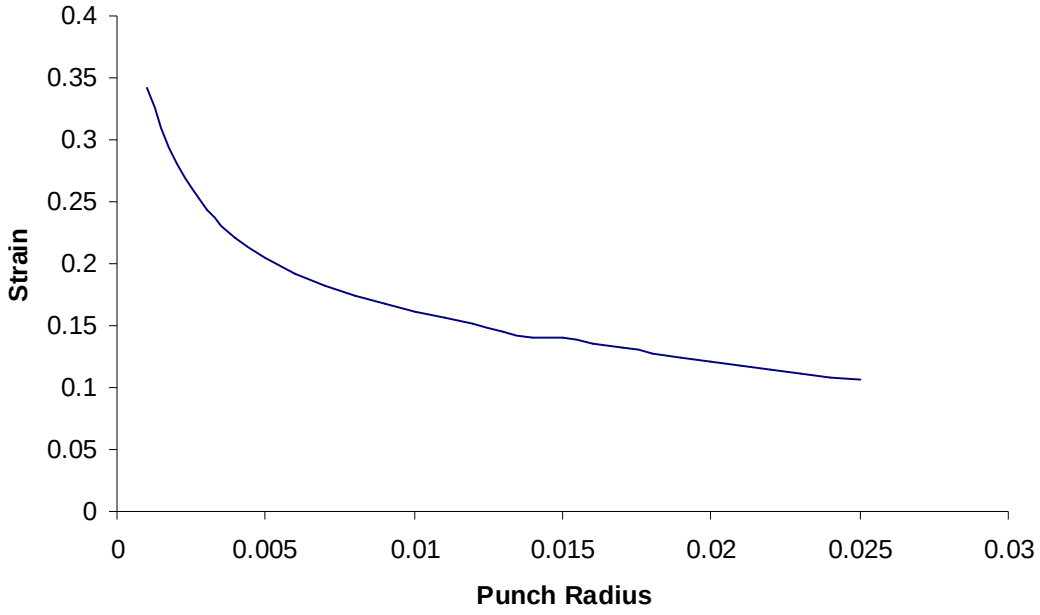

Figure 3-13 Bulging Corrected Final Strain

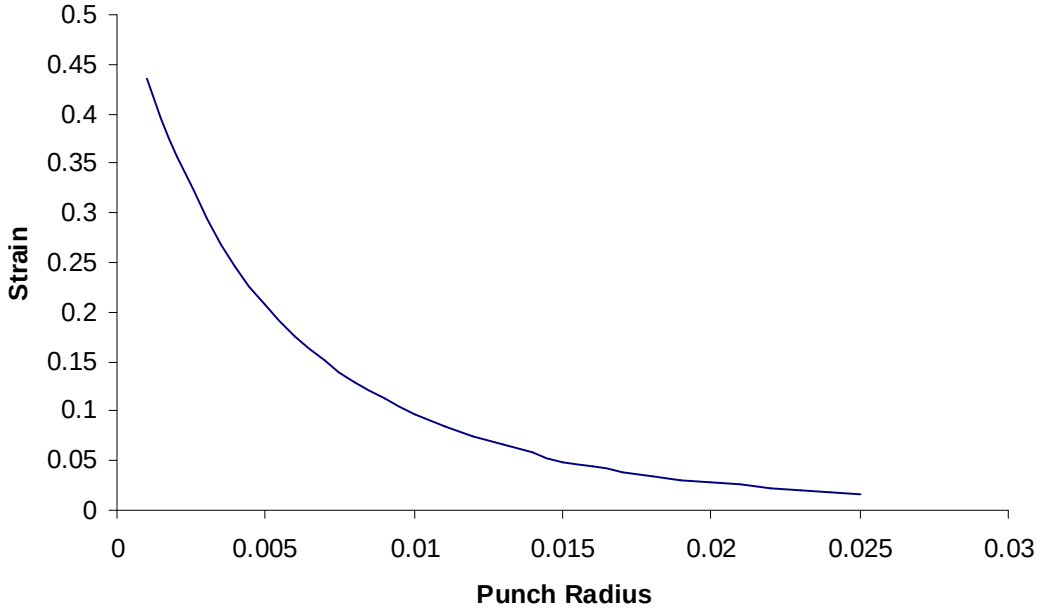

Figure 3-14 Bulging Corrected Recovery Strain

Further discussion of the bulging issue is found in section 5.2.

3.4 Development of Material Models

Material models for copper and polyimide, which comprise the flex circuit material, were developed for use in the analytical bending model. A strain hardening material model was chosen because the polyimide and copper materials exhibit strain hardening properties.

3.4.1 Copper Material Model

An elastic linear strain hardening material model for copper was needed for the analytical bending model. The material model developed was a linear strain hardening type represented by Equation 3-9.

$$\sigma = K\varepsilon + \sigma_{yield}$$

Equation 3-9

In Equation 3-9, K is the linear strain hardening constant. Figure 3-15 shows the copper material model used.

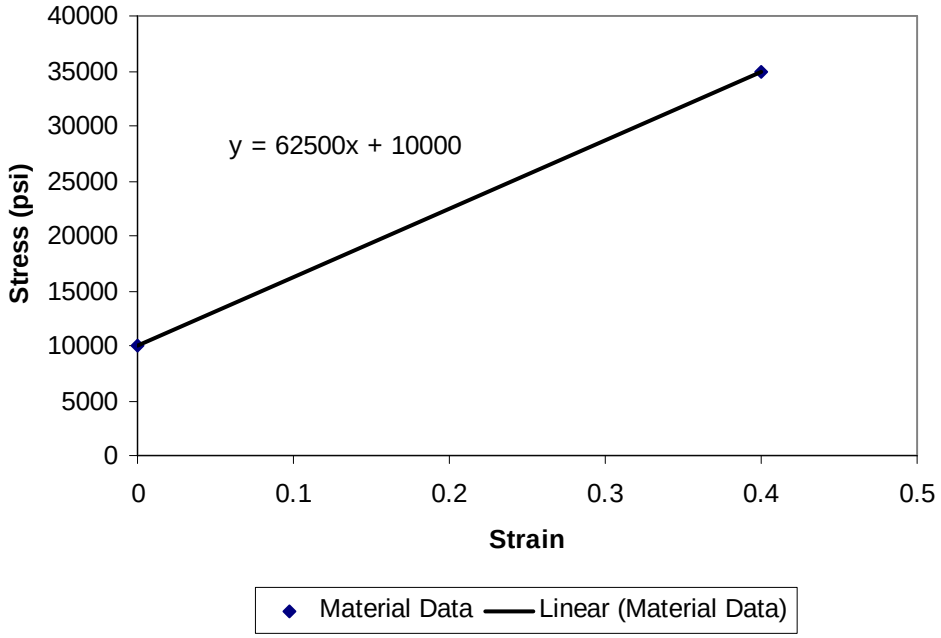

Figure 3-15 Copper Material Model

The copper used in the flex circuit material is annealed electrical copper sheet. The copper material model was created using data obtained from annealed electrical copper manufactured by H Cross Company located in Weehawken, NJ [8]. Although this company may not be the copper supplier for the flex circuit material, the mechanical properties for their product are expected to be similar to the material used in the flex circuit as both are high purity annealed electrical copper. The copper material data was plotted and a linear fit was performed. The linear strain hardening constant, *K*, for copper was determined to be 62500 psi. This material model is valid for values of strain above yield, 10000 psi, and below the maximum elongation of copper, 0.4.

3.4.2 Polyimide Material Model

An elastic linear strain hardening material model for polyimide was needed for the analytical bending model. The material model developed was a linear strain hardening type represented by Equation 3-9. Figure 3-16 shows the polyimide material model used.

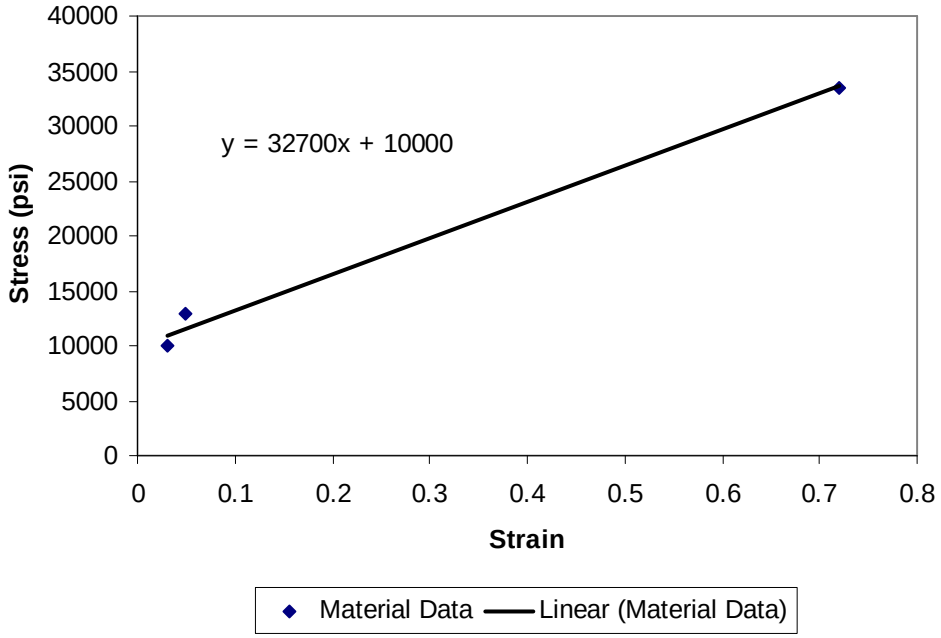

Figure 3-16 Polyimide Material Model

The polyimide material model was created using data obtained from Kapton film, manufactured by E. I. du Pont de Nemours and Company located in Wilmington, Delaware [9]. This Kapton film is the same polyimide material that is used in the flex circuit. The polyimide material data was plotted and a linear fit was performed. The linear strain hardening constant, *K*, for polyimide was determined to be 32700 psi. This material model is valid for

values of strain above yield, 10000 psi, and below the maximum elongation of polyimide, 0.72.

3.5 Calculation of Bending Limits

A lower limit of the punch radius is needed to insure that the mechanical limits of the material being bent are not exceeded. An upper limit of the punch radius is needed to ensure that the material being bent reaches a state of plastic deformation to achieve a non-recoverable change in the shape of the material. Bending limits were calculated for both the polyimide and copper components of the flex circuit to determine limits for the compression height. Table 3-1 shows the material data used to calculate the bending limits of the copper [8].

Table 3-1 Copper Material Data

σ_{yield}	10000 (psi)
Max Elongation	0.4
E	17 e6 (psi)
t	0.001 (inch)

Table 3-2 shows the material data used to calculate the bending limits of the polyimide [9].

Table 3-2 Polyimide Material Data

σ_{yield}	10000 (psi)
Max Elongation	0.72
E	370000 (psi)
t	0.007 (inch)

Solving Equation 3-10 for $r_{p,}$ the minimum punch radius can be determined.

$$MaxElongation = \ln\left[\frac{r_p + t}{r_p + \frac{t}{2}}\right]$$

Equation 3-10

The minimum punch radius for the copper material, alone, was determined to be 0.00052 inch. However, due to the 0.003 inch thick layer of polyimide on the inside of the bend of the composite material, the minimum punch radius for the copper is 0.003 inch larger than the minimum punch radius for the composite material. This results in a minimum punch radius that the copper will experience of 0.003 inch, even if the material is bent onto itself. As a result, the copper will not exceed its maximum elongation of 0.4. Figure 3-17 depicts this minimum copper radius.

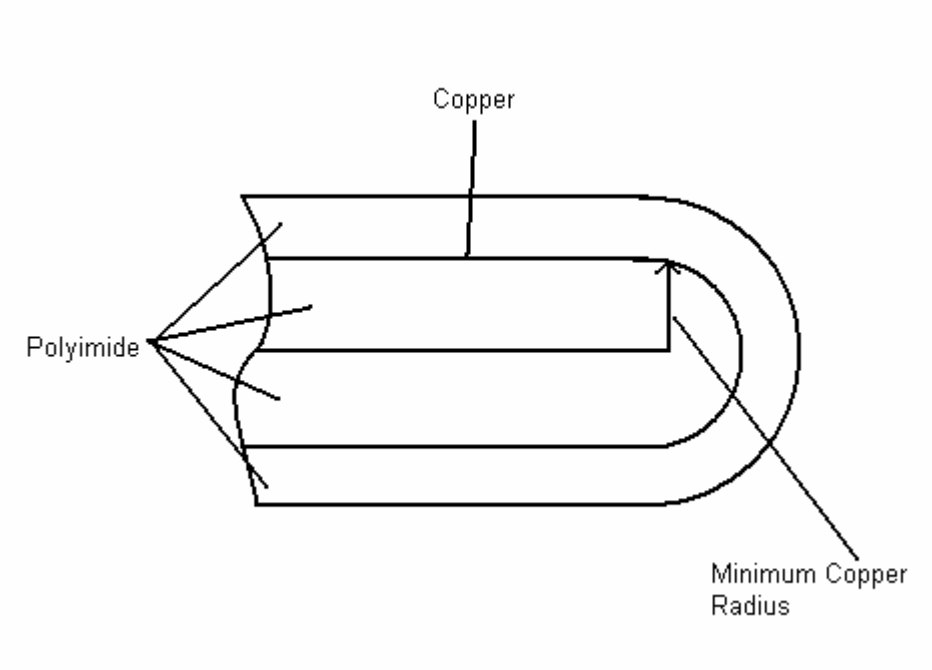

Figure 3-17 Minimum Copper Punch Radius

The minimum punch radius for the polyimide was determined to be 0 inch. This is because the polyimide does not exceed its maximum elongation of 0.72 when it is folded onto itself. When evaluating the two calculated minimum punch radii, it is obvious that there is no lower limit for the punch radius. The flex circuit material can be folded completely back onto itself and neither the copper nor the polyimide material will reach or exceed its maximum elongation. The minimum compression height is therefore set at twice the thickness of the material, 0.014 inch.

Solving Equation 3-11 for $r_{p,}$ the maximum punch radius can be determined by ensuring that the material transitions into the plastic region.

$$\frac{\sigma_{yield}}{E} < \frac{1}{\frac{2 * r_p}{t} + 1}$$

Equation 3-11

The maximum punch radius for the polyimide was determined to be 0.126 inch. This determines that the punch radius must be less than 0.126 inches for any permanent deformation to take place in the polyimide. The maximum punch radius for the copper was determined to be 0.850 inch. However, due to the layer of polyimide on the inside of bend of the composite material, the largest punch radius that will cause any plastic deformation in the copper is 0.847 inch. This situation is shown in Figure 3-18.

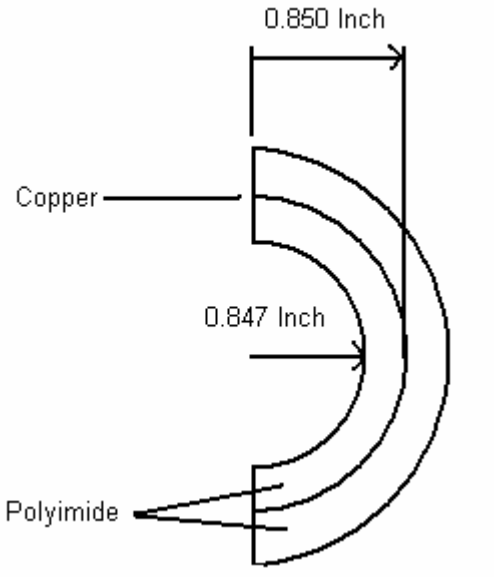

Figure 3-18 Maximum Copper Punch Radius

The smaller of the two maximum punch radii is selected as the maximum punch radius for the flex circuit material, as plastic deformation will take

place in both the copper and polyimide at that punch radius. The maximum compression height was set at 0.126 inch.

3.6 Summary

In this chapter the theory behind the experimental bending method was discussed. An analytical bending model was discussed and provided. Material models for polyimide film and copper foil were presented. Bending limits of the flex circuit material were calculated. Theoretical values of the final strain and recovery strain from the bending of flex circuit were provided. A spring based bulging method was developed.

Chapter 4 details the experimental procedures used to test the bending of the flex circuit material. A bending fixture is designed and a bending procedure is developed. Epoxy encapsulation testing is performed. Models of epoxy encapsulated antenna designs are constructed. Concepts for three dimensional antenna designs manufactured from flex circuit are discussed. Models of three dimensional antennas constructed from flex circuit material are created. Methods of manufacturing three dimensional antennas via rapid prototyping are presented.

4 EXPERIMENTAL PROCEDURES

4.1 Introduction

Several designs for structurally integrated antennas were studied. These designs included an epoxy encapsulated hemisphere design, a fragmented slot design, and two different three dimensional designs. Different ways of manufacturing the antenna designs were developed. The manufacturing processes were evaluated by making models of the designs. As some of the antenna designs were to be encased in epoxy, epoxy encapsulation testing was performed. As some of the antenna designs were to be made by bending flex circuit material, bending tests were conducted on the flex circuit material. If a concept and manufacturing method were determined to be successful, a prototype antenna was produced.

4.2 Epoxy Testing

A common feature of some of the antenna designs was that they were encased in epoxy to increase their structural properties. The epoxy used in this work was Magnolia 943 manufactured by Magnolia Plastics Inc. located in Chamblee, Georgia. The ratio of resin to hardener was mixed 2:1 by volume or 100:42 by mass, per manufacturer specification. The requirements of the epoxy encapsulation were that the epoxy structure be as clear as possible and free from major voids. The epoxy was required to be free from voids because they cause variation in the dielectric constant of the epoxy. The epoxy was required to be clear so that it could be subjected to optical testing. Initial experiments were conducted to determine the

conditions that were the most conducive to satisfying the requirements. In the testing, the molds that were used were bread baking pans. These molds had a fair amount of draft which assisted in the removal of the part from the mold. The molds were coated with a silicone spray before casting the epoxy, which further facilitated releasing the part from the mold. Clearco High Performance Silicone Spray and Spray-on S00305 Heavy Duty Silicone Mold Release were the two silicone sprays used.

The masses of resin and hardener were measured, using an Ohaus model TS12OS digital balance manufactured by Ohaus Corporation, Florham Park, New Jersey, in two expanded polystyrene (EPS) cups. Hardener was added to the resin. It was found that care must be taken when mixing the resin and hardener to not entrain air. A solution to this was to slowly stir the mixture, instead of using a whipping stirring motion. Also it was beneficial to not change the vertical height of the stirrer while stirring. For the mixture to fully cure the two components must be very well mixed.

The epoxy mixture was poured from the EPS cup into the mold. It was beneficial to maintain an angle of the cup such that the flow of epoxy out of the cup into the mold was laminar. It was also beneficial to maintain the smallest pour height above the mold as possible. When the epoxy was poured into the mold it was leveled with the stirrer, and any bubbles that were noticed were removed or popped with the stirrer. It was found that good clarity and minimal porosity was obtainable

when the thickness of the epoxy was less than one inch, with increasing clarity and decreasing porosity achieved as the thickness of the layer decreased. Multiple layers were implemented when the desired thickness of the final product was greater than the maximum layer thickness.

4.3 Epoxy Encapsulated Hemispheres

The epoxy encapsulated hemispheres were implemented as two separate designs. Both designs relied on radiators to send and receive signals. To function properly, these radiators needed to be encased in a hollow of a protective structure comprised of a dielectric material. The protective structure was required to be as translucent and as free from voids as possible, while providing protection to the enclosed radiators. Epoxy was selected as the material that would best meet these requirements. The hollows were created with hemispherical plastic shells. The hemispherical shells were polypropylene hollow float balls with a diameter of 0.787 inch manufactured by Orange Products, Inc. in Allentown Pennsylvania. The hemispherical shells were hollow plastic spheres that were then cut in half with a hand saw. The hemispherical shells serve as a cavity designed to hold radiators that send and receive signals.

The first design used copper jacketed coaxial cable attached directly to the hemispheres, and the second design used a circuit board to attach the hemispheres. A schematic of the first antenna design is shown in Figure 4-1.

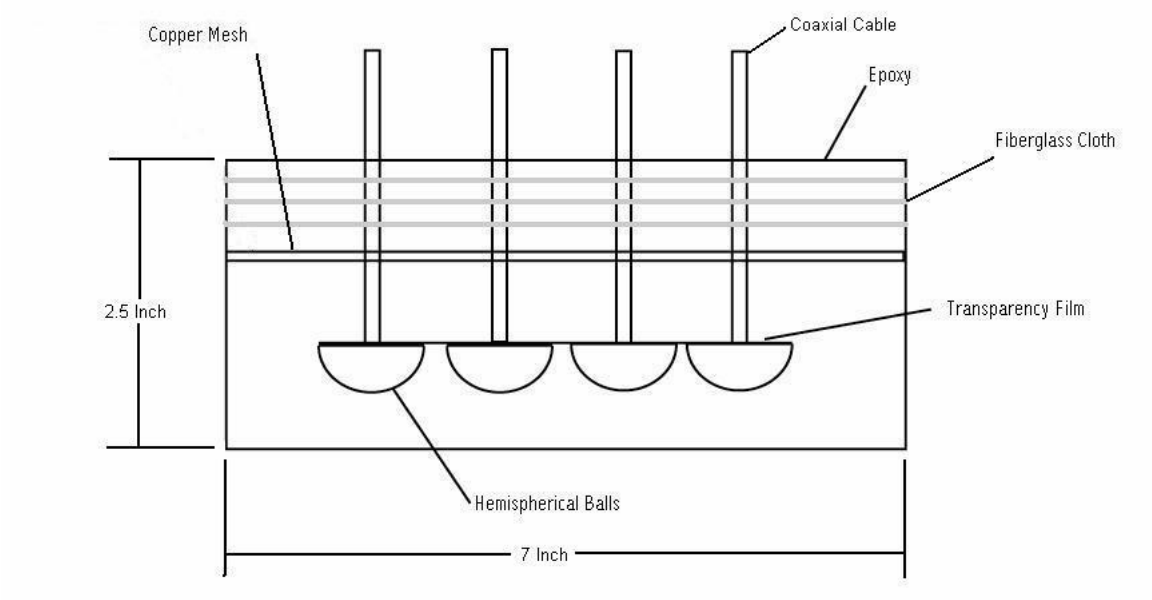

Figure 4-1 Epoxy Encapsulated Hemispheres (Side View)

The first antenna design mock-up consisted of four copper jacketed coaxial cables attaching to the hollow hemispherical balls, which in an actual device allow the transfer of signals to and from the radiators. A thin film transparency was glued to the surface of the hemispheres with cyanoacrylate to seal the hemispheres and isolate the radiator from the surrounding composite structure, while allowing a connection between the radiators and copper jacketed coaxial cables. The copper jacketed coaxial cables were attached to the thin film transparency, fixed into position, and encapsulated into an epoxy structure. A layer of copper mesh was added to serve as a reflective back plane for the radiators. Additional layers of fiberglass cloth were added to increase the strength of the structure.

The encapsulation of the hemisphere and copper jacketed coaxial cable antenna model had to be performed in several steps. If the assembly was encapsulated all at once, the curing of the epoxy would generate too much heat, causing dimensional

distortion, porosity and discoloration. As the epoxy structure was required to be translucent and free of voids, a rapid curing process was avoided. A rapid curing process was avoided by casting the epoxy structure of the antenna model in several thin layers. Careful selection of the layers also allowed for ease of assembly. A bread baking pan was used as a mold for the antenna structure. An initial layer of epoxy was poured into the pan and allowed to fully cure. This initial layer of epoxy allowed the copper jacketed coaxial cables and hemispheres to be easily placed at a uniform depth in the structure. A fixture as shown in Figure 4-2 was made to hold the copper jacketed coaxial cables into position while the second layer of epoxy was poured and during its curing process.

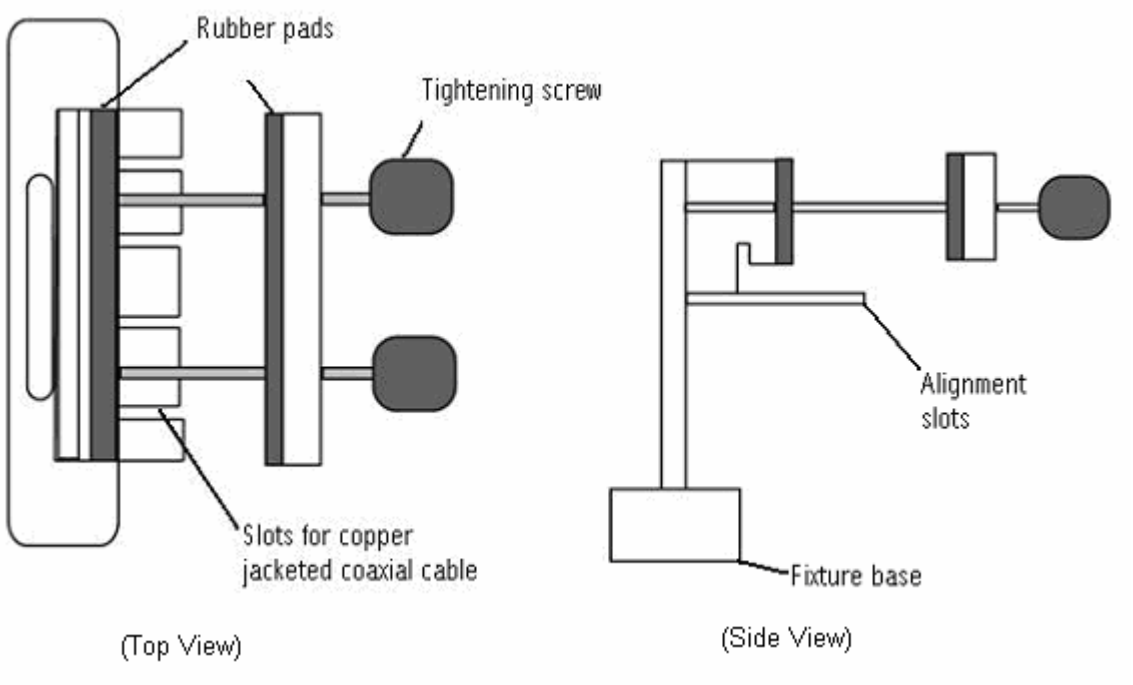

Figure 4-2 Fixture for Copper Jacketed Coaxial Cable and Hemispheres

The fixture consisted of a base and a mounting head that had slots to insert the copper jacketed coaxial cables. The cables were clamped between two rubber pads by turning the tightening screws. The fixture held the copper jacketed coaxial cables in place during the pouring process and curing of the second epoxy layer. When the second layer of epoxy was fully cured, the fixture was removed and the copper jacketed coaxial cables and hemispheres were maintained in proper alignment by the epoxy.

The copper mesh then was installed on top of the second layer, with holes cut in the mesh to allow the copper jacketed coaxial cables to pass through without contacting the copper mesh. This layer was allowed to cure fully. An additional optional layer of epoxy reinforced with fiberglass cloth could be added for an increase in structural properties of the protective structure. After the epoxy was fully cured, the part was removed from the mold. Figure 4-3 and Figure 4-4 show a part after the addition of the copper mesh layer, while Figure 4-5 shows the part after the addition of the fiberglass reinforced layer.

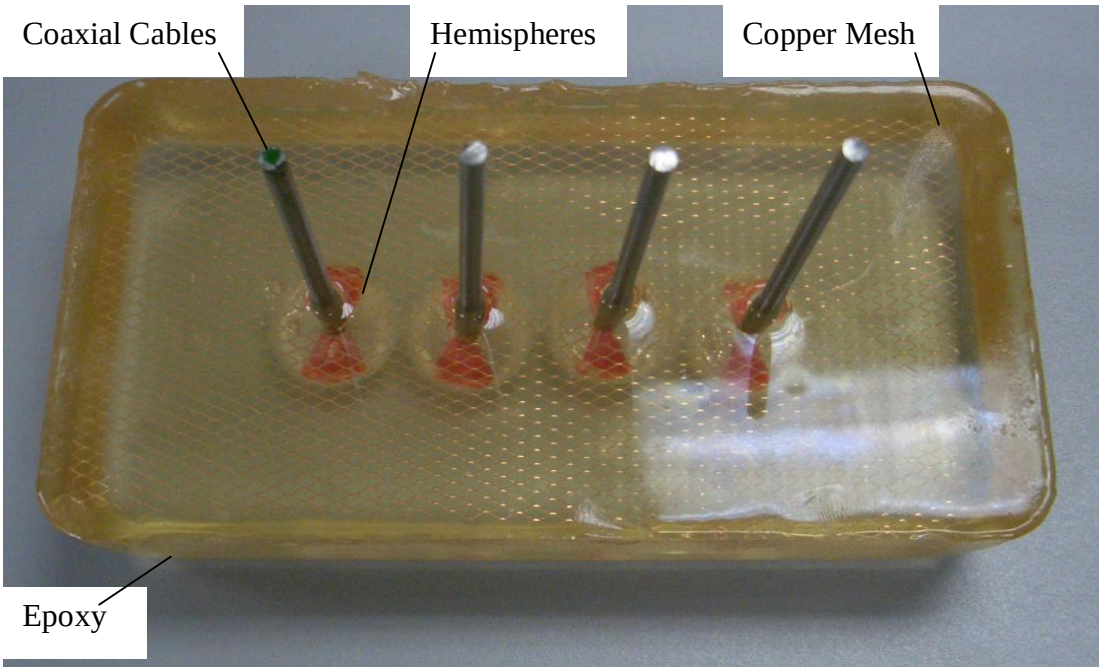

Figure 4-3 Copper Jacketed Coaxial Cable Hemisphere Antenna Model (Top View)

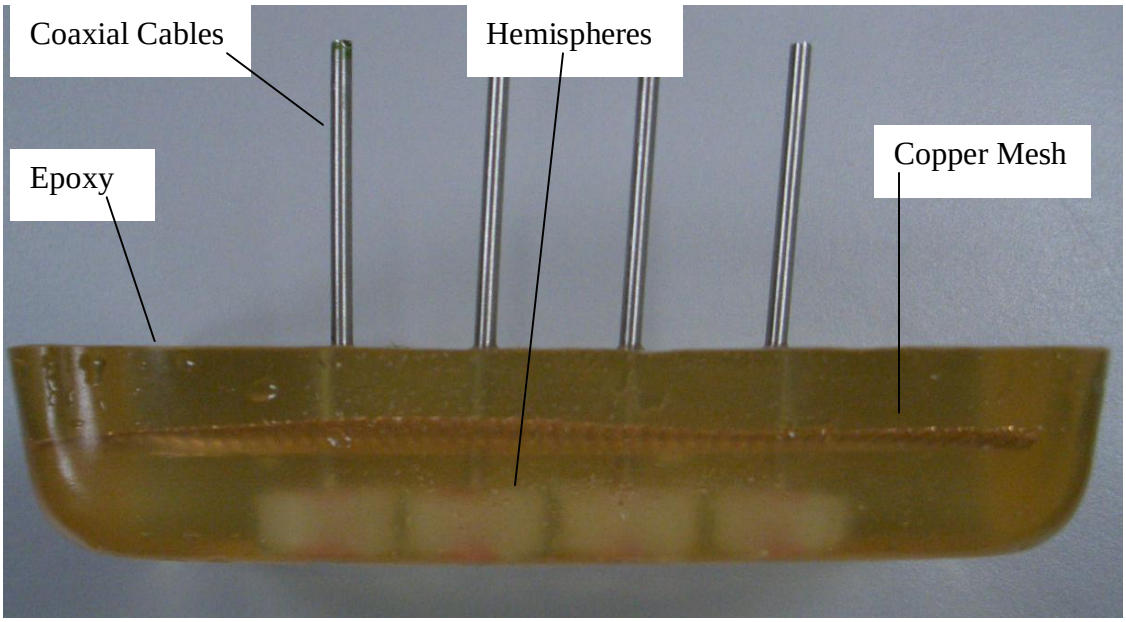

Figure 4-4 Copper Jacketed Coaxial Cable Hemisphere Antenna Model (Side View)

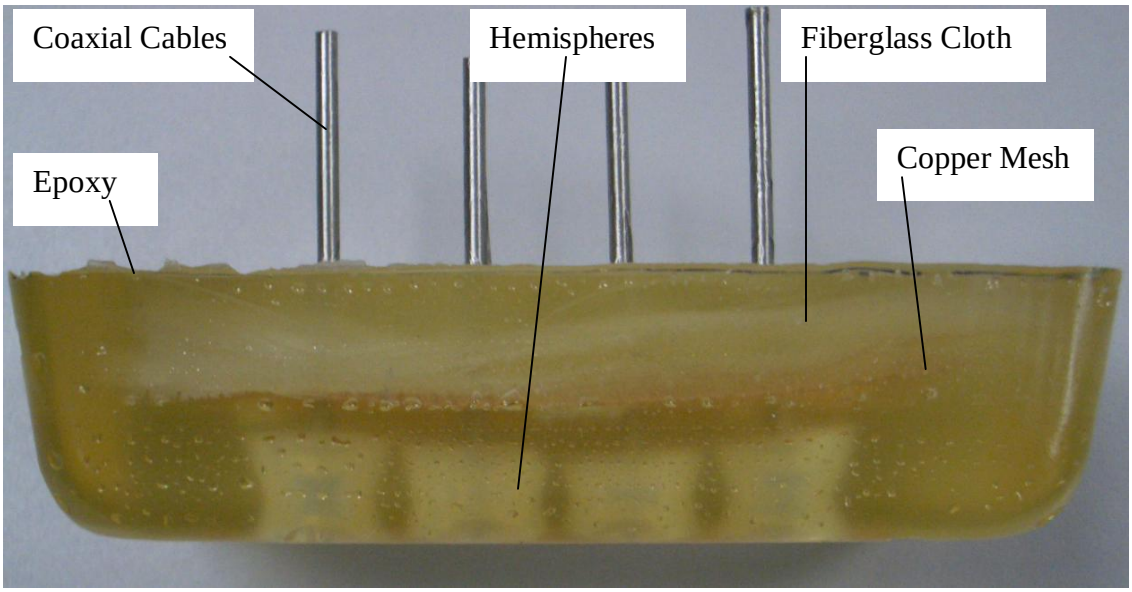

Figure 4-5 Hemisphere Model with Fiberglass Reinforcement (Side View)

The second design, a circuit board antenna design is shown in Figure 4-6 and Figure 4-7.

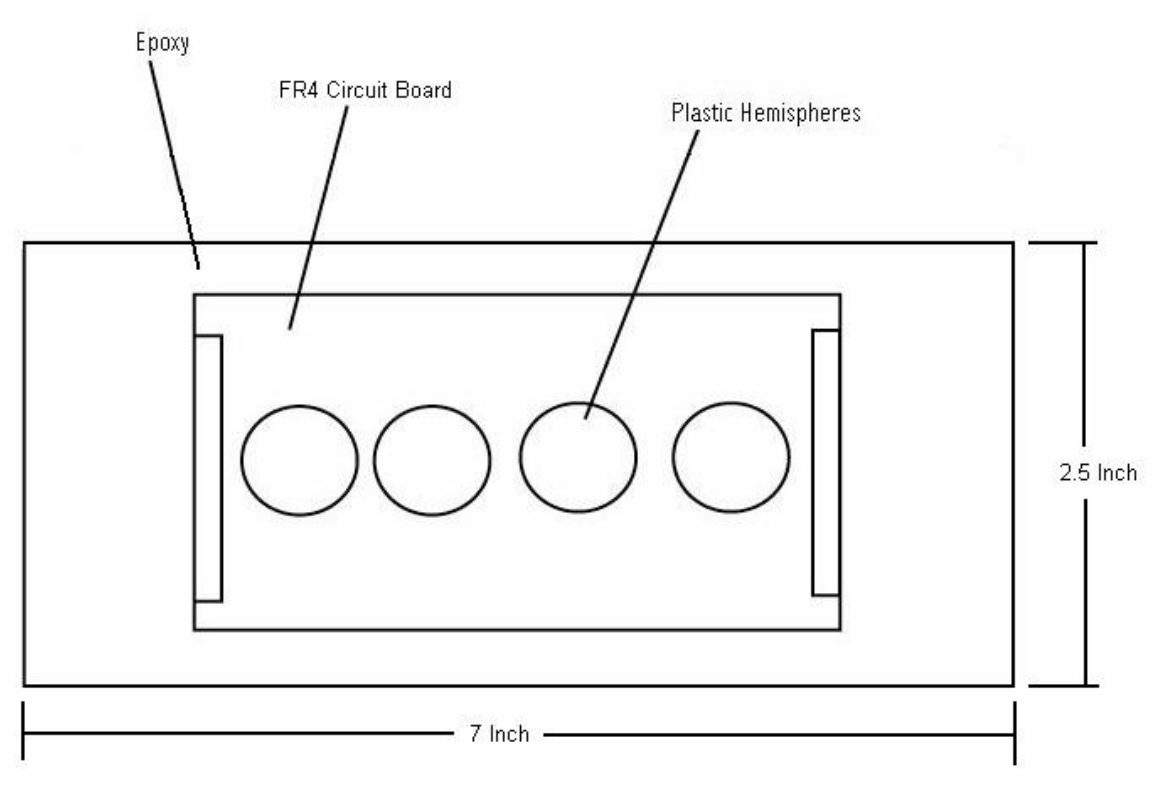

Figure 4-6 Circuit Board Antenna (Front View)

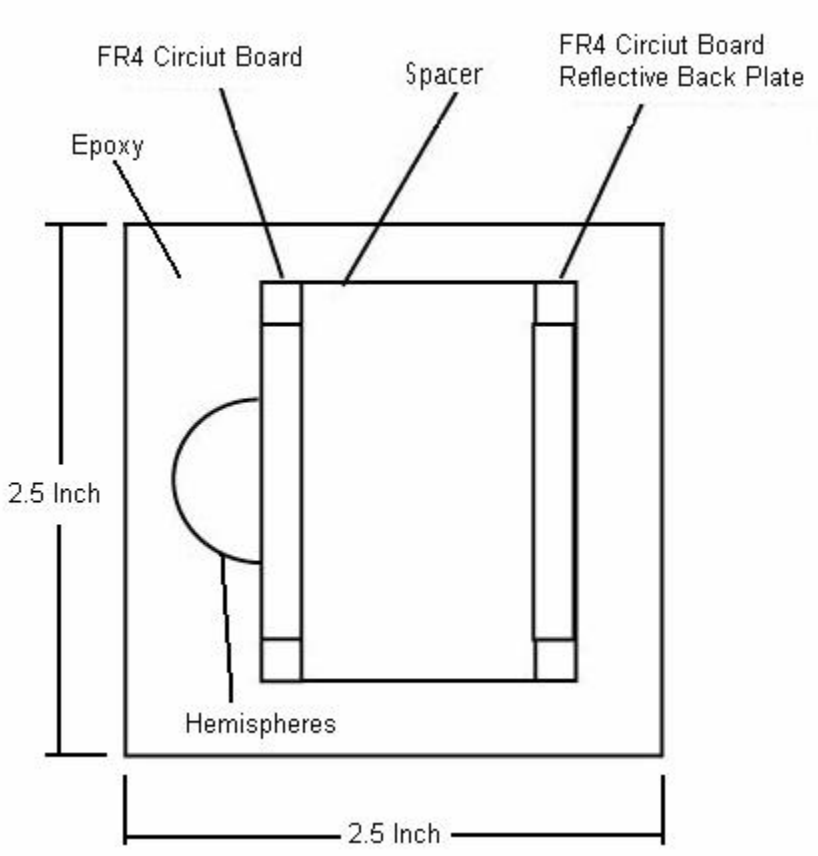

Figure 4-7 Circuit Board Antenna (Side View)

The model consisted of FR4 circuit board, plastic hemispheres, and a plastic spacer. In this design, radiators would be attached to specific locations on the circuit board. The hemispheres were attached over the radiator locations and sealed to the circuit board with cyanoacrylate. A second FR4 circuit board, which mimics the back plane, was attached with cyanoacrylate parallel to the plane of the FR4 circuit board that contained the hemispheres with cyanoacrylate using a plastic spacer. The antenna assembly was subsequently encased in epoxy. This design is different and somewhat superior to the first as different circuit designs allow for better performance tuning of the antenna. This design utilizes common electrical wiring

to connect the circuit to a radiator verses the copper jacketed coaxial cables utilized in the first design. The antenna assembly was subsequently encased in epoxy.

The encapsulation of the circuit board antenna assembly was performed in several steps. If the assembly was encapsulated all at once, the curing of the epoxy would generate too much heat, causing dimensional distortion and discoloration. As the epoxy structure was required to be translucent and free of voids, so a rapid curing process was avoided. A bread baking pan was used as a mold. A fixture, shown in Figure 4-8, was made to hold the circuit board in position while the epoxy was poured and during the curing process.

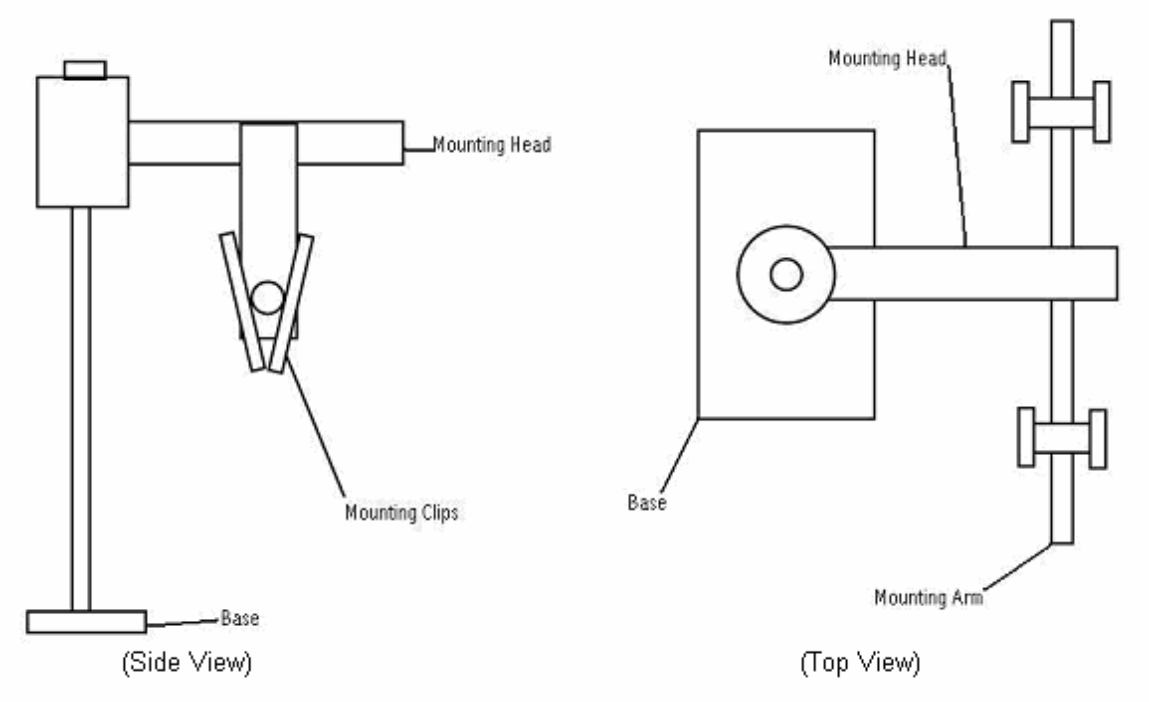

Figure 4-8 Circuit Board Encapsulation Fixture

After the first layer of epoxy was fully cured, the fixture could be removed and the antenna assembly would be maintained in proper alignment by the epoxy. Figure 4-9 shows a diagram of the layering method used.

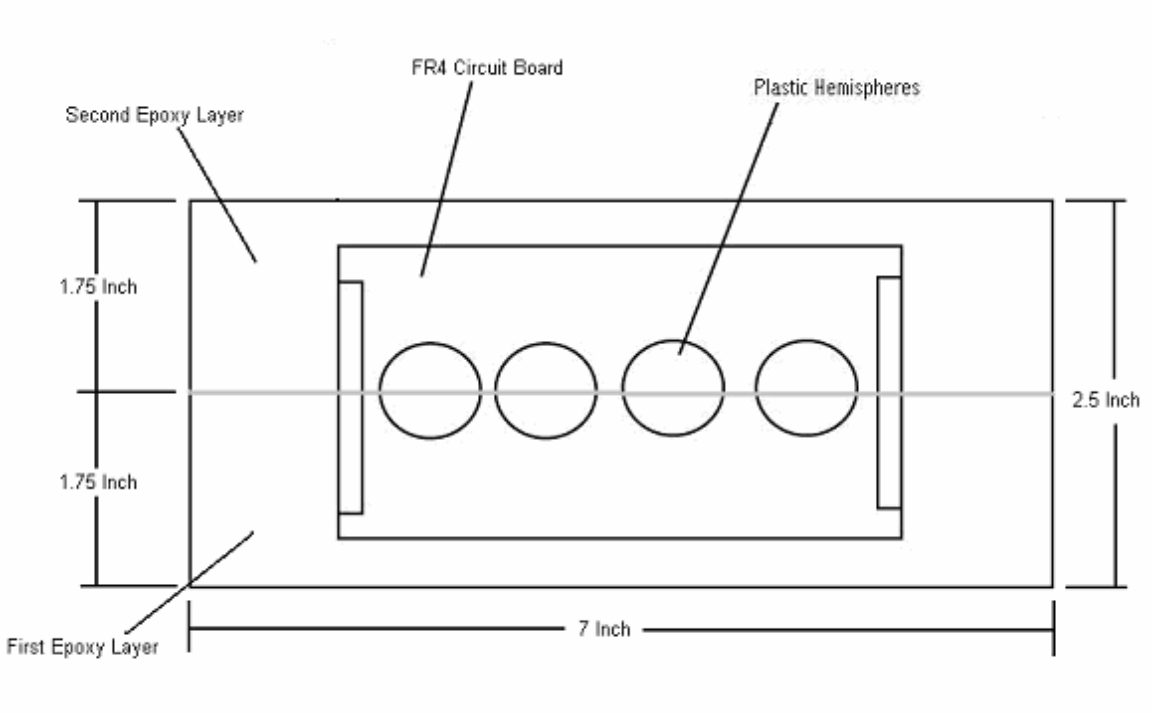

Figure 4-9 Epoxy Layering Method (Top View)

After all of the layers of epoxy had fully cured the antenna was removed from the mold. Figure 4-10, Figure 4-11, and Figure 4-12 show the completed part.

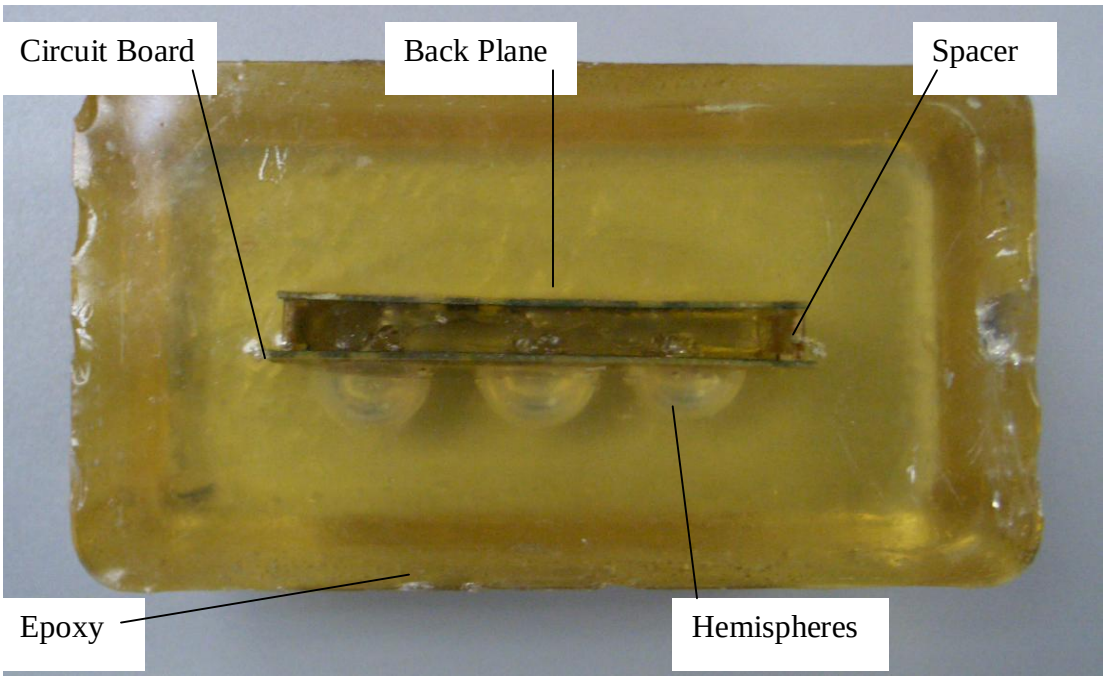

Figure 4-10 Circuit Board Hemisphere Antenna (Top View)

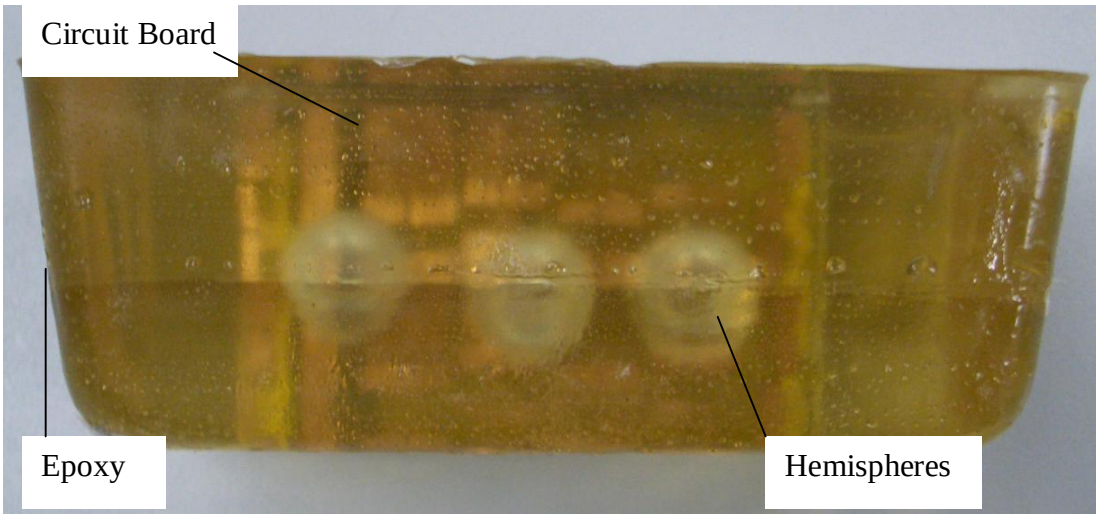

Figure 4-11 Circuit Board Hemisphere Antenna (Front View)

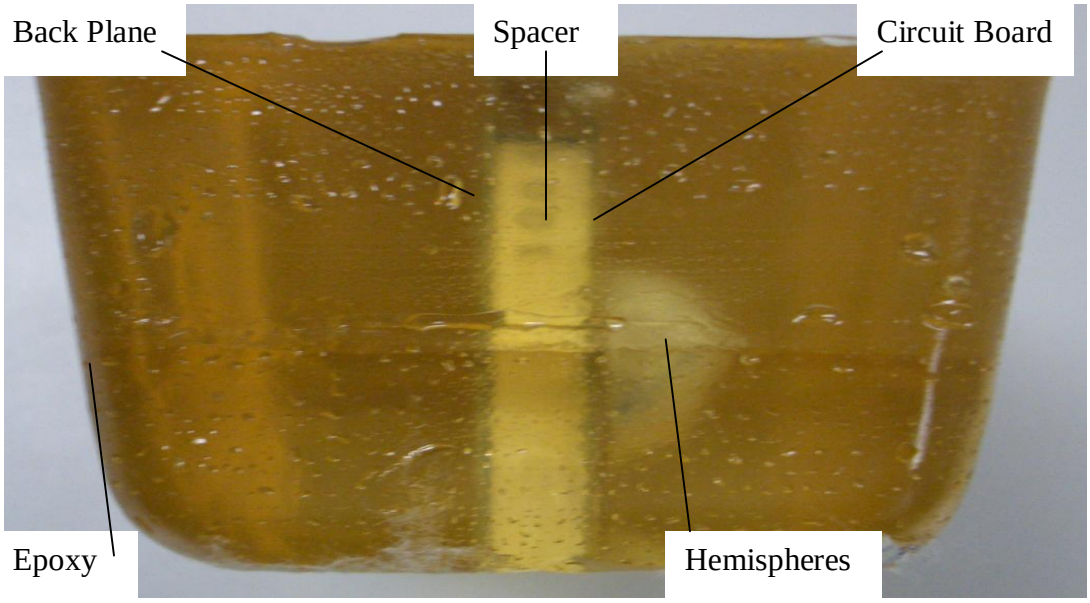

Figure 4-12 Circuit Board Antenna (Side View)

4.4 Fragmented Slot Antenna

A schematic of the fragmented slot antenna is shown in Figure 4-13.

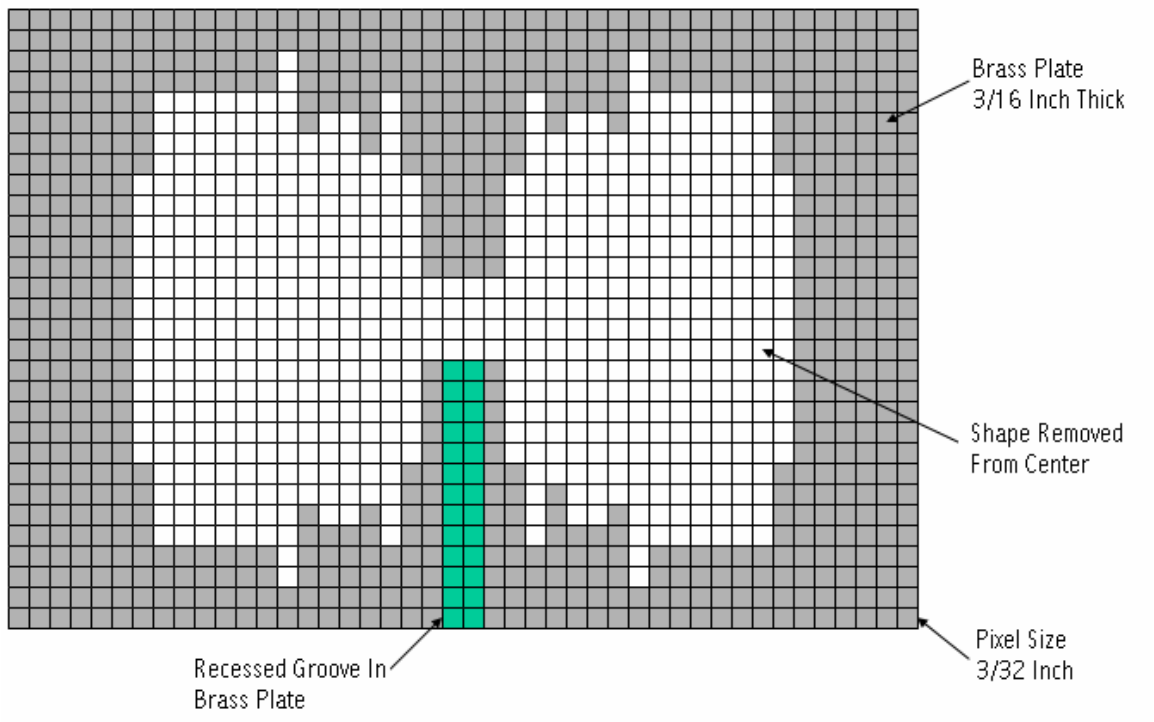

Figure 4-13 Fragmented Slot Antenna Schematic

The fragmented slot antenna design comprised a brass plate, copper jacketed coaxial cable, conductive and non conductive epoxies and acrylic sheet. The brass plate was machined via wire EDM to remove a portion of the center of the plate resulting in a geometric structure that could function as an antenna. A recessed groove was milled in the brass plate with a CNC milling machine to allow the copper jacketed coaxial cable to locate in the center of the plate.

Figure 4-14 shows a schematic of the fragmented slot antenna with the addition of the copper jacket coaxial cable.

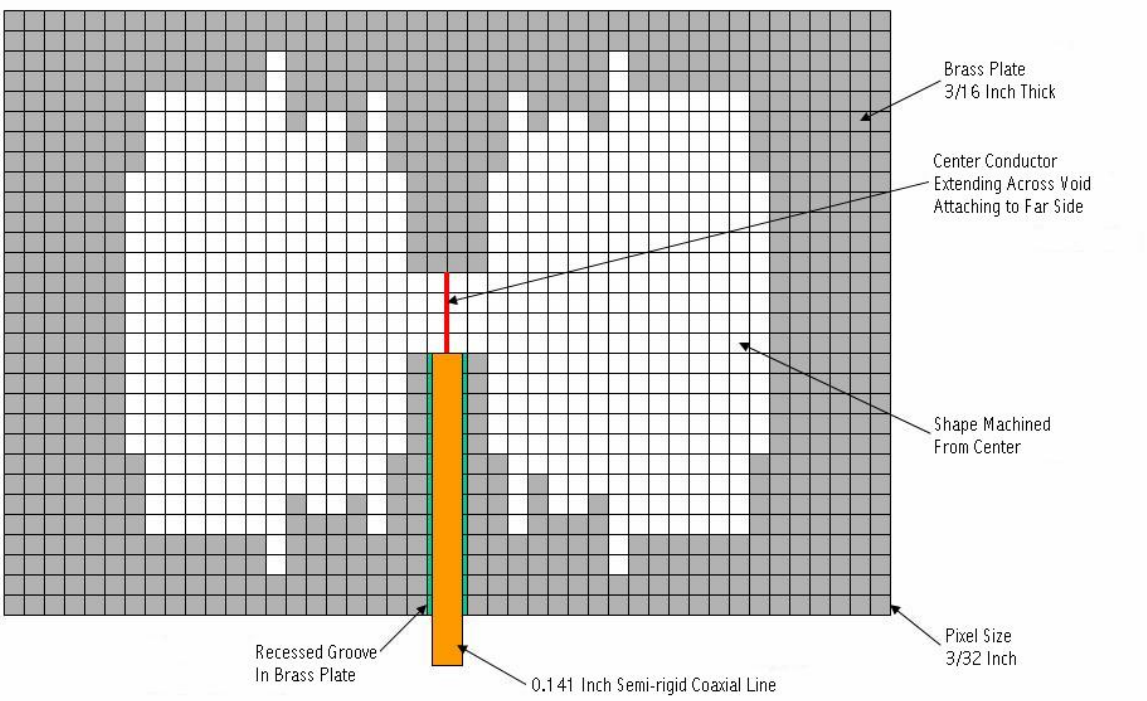

Figure 4-14 Fragmented Slot Antenna with Copper Jacketed Coaxial Cable

The center conductor of the copper jacketed coaxial cable was attached to the center of the plate with solder. The milled slot and area surrounding the copper jacketed coaxial cable were filled with conductive epoxy to join them mechanically and electrically. The epoxy also served to fill the void in the brass plate between the coaxial cable and the milled slot resulting in an uninterrupted surface on the brass plate.

The center of the brass plate, removed via EDM, was filled with unfilled epoxy and two acrylic sheets were placed over the brass plate, completing the assembly, as shown in Figure 4-15.

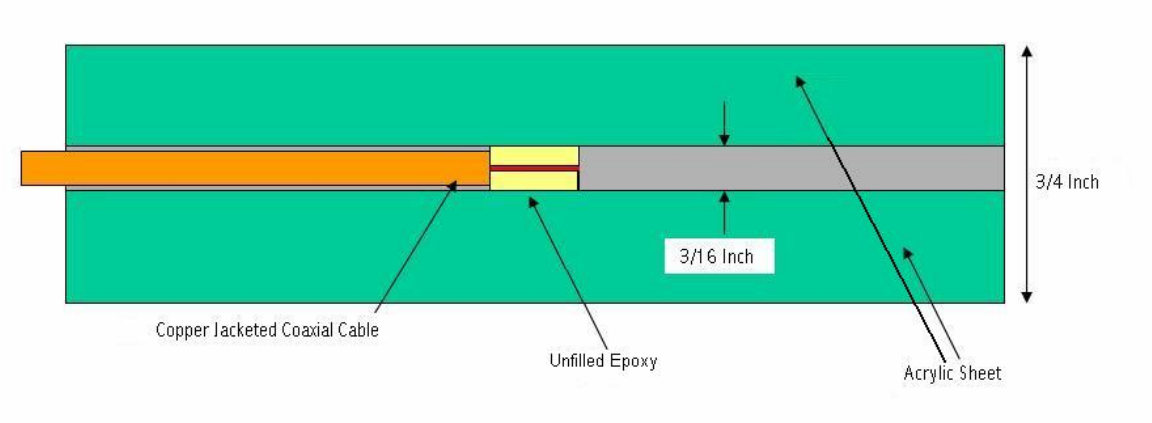

Figure 4-15 Completed Fragmented Slot Antenna Assembly

4.5 Three Dimensional Antenna

4.5.1 Designs

There were two designs that were provided for the three dimensional antenna models. The first design was provided as a wire frame drawing and is shown in Figure 4-16.

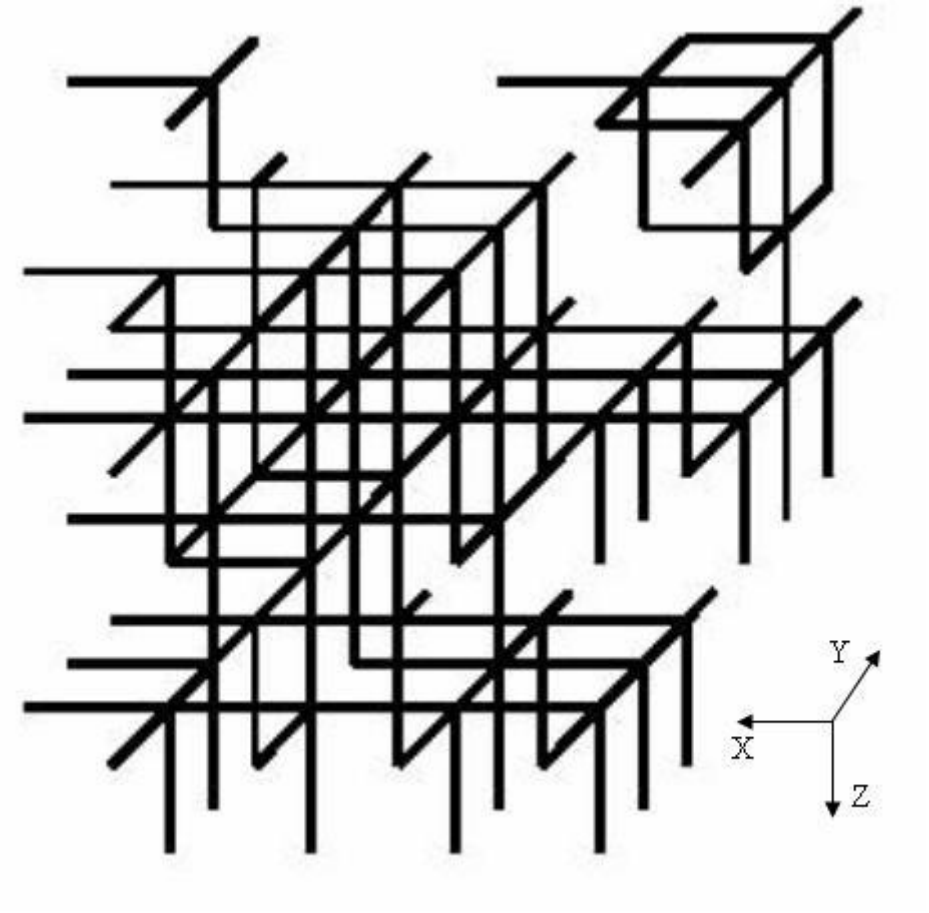

Figure 4-16 Three Dimensional Antenna First Design

Each line in the wire frame drawing represents an antenna element. The length of an antenna element is 1.5 cm and the diameter of an antenna element is 1.5 mm. The antenna design is in the shape of a rectangular prism with dimensions of 6 cm in the Y direction, by 7.5 cm in the X direction by 7.5 cm in the Z direction. The antenna elements are to be conductive, and the space in between the elements is to be filled with a material possessing a low dielectric constant. The first design consists of an array of 150 elements joined together forming one single part. The electrical resistance of the entire structure, measured from corner to corner was to be on the order of 10 ohms

or less. The conductive structure was designed to be encapsulated in a support structure with a low dielectric constant to increase the structural integrety of the antenna.

The second design was provided as a list of element location data. A sample of the data for the first ten elements is shown in Table 4-1, and the full set of element location data is provided in Appendix C.

Table 4-1 Element Location Data of Second Design

Element Number	X_0 (mm)	Y_0 (mm)	Z_0 (mm)	X_1 (mm)	Y_1 (mm)	Z_1 (mm)
1	0	5	0	5	0	0
2	10	5	0	5	0	0
3	10	5	5	5	0	0
4	0	5	10	5	0	0
5	10	5	10	5	0	0
6	0	5	15	5	0	0
7	5	5	15	5	0	0
8	0	5	20	5	0	0
9	5	5	20	5	0	0
10	0	5	25	5	0	0

In Table 4-1 each antenna element is numbered for identification. The starting and ending locations of the elements are defined by three dimensional Cartesian coordinates. The length and diameter of the antenna elements are 0.5 cm and 1.5 mm, respectively. The overall dimensions of the antenna design are 5 cm by 5 cm by 1.5 cm.

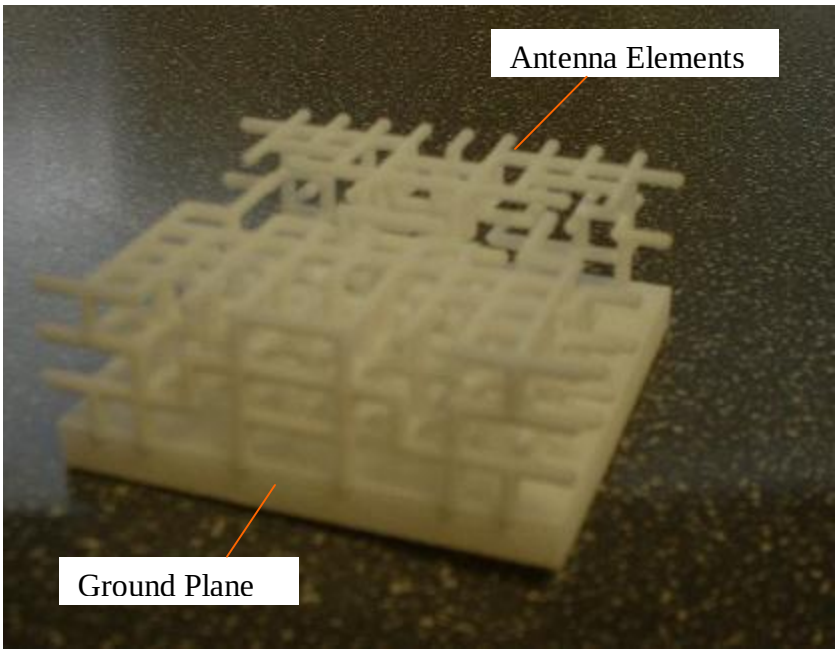

Figure 4-17 Second Three Dimensional Antenna Design

The second design is shown in Figure 4-17. The second design consisted of three independent arrays of elements. A ground plane united the three antenna pieces into one single part. Each element of the second design was required to be conductive, and the space in between the elements was required to be filled with a material possessing a low dielectric constant. The ground plane connected to the three antenna pieces mechanically and electrically.

The electrical resistance of the entire structure, measured from corner to corner was to be on the order of 10 ohms or less. The conductive structure was designed to be encapsulated in a support structure with a low dielectric constant to increase the structural properties of the antenna.

4.5.2 Flex Circuit Concept Development

A method of manufacturing these three dimensional antennas with flexible circuit material was devised and several concepts developed. The first three dimensional antenna design was selected to be used with the flex circuit manufacturing method as it was less complex and had fewer elements than the second design.

This method of manufacturing was developed from the idea of representing antenna elements with printed circuit traces on flexible circuit material. The development of the flex circuit manufacturing method included the study of several possible ways to assemble different circuit traces on planer flex circuit material thereby creating a three dimensional structure in which all of the antenna elements were represented by conductive copper traces. Several concepts were developed that utilized this method.

A straw concept was developed in which the flex circuit would be bent into rectangular straws. These straws contained copper circuit traces on the outside surface. These straws were joined together mechanically and electrically with conductive epoxy. To ease the joining process the straws were filled with EPS foam which assisted in maintaining the rectangular shape as well as provided additional support during the assembly process. When all of the straws were assembled, the circuit traces would represent the three dimensional antenna elements. A model of a straw is shown in Figure 4-18.

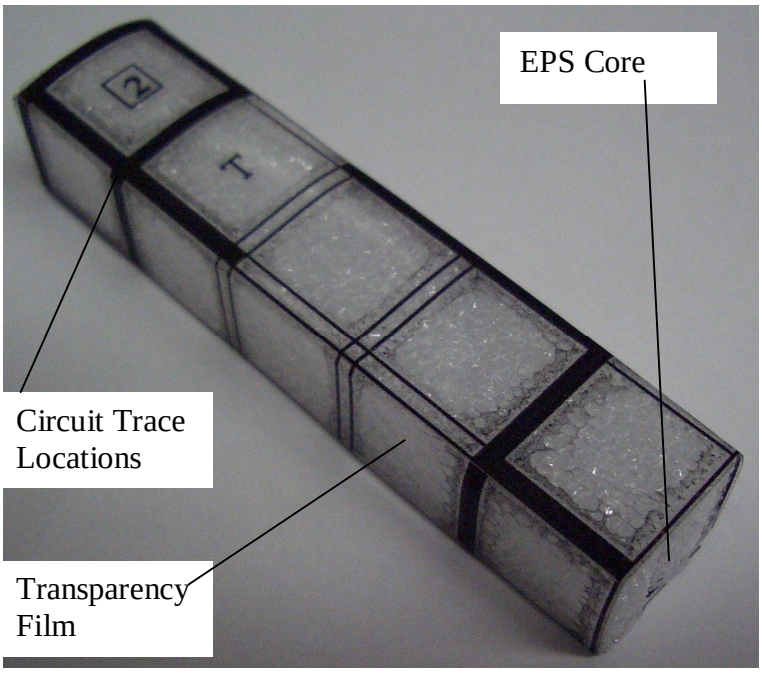

Figure 4-18 Flex Circuit Straw

In this model, the flex circuit is represented by transparency film and the copper trace locations are represented as thick lines. The transparency film straw was bent in four locations generating five equal length sides. The rectangular shape was achieved by overlapping the first and last side and bonding them with cyanoacrylate. The straw was given an EPS core to maintain proper shape and to increase the rigidity of the structure for ease of assembly.

Figure 4-19 shows the method in which the individual straws were assembled to form an antenna.

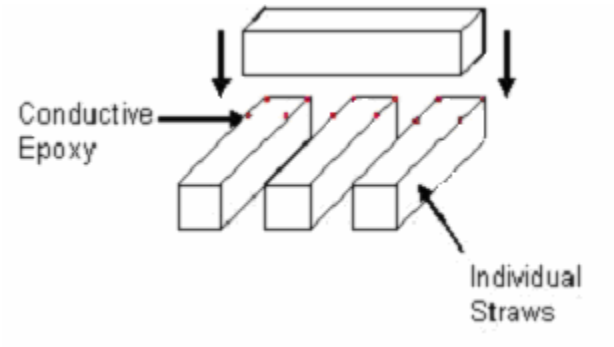

Figure 4-19 Assembly of Individual Straws

The individual straws were positioned so that the circuit traces represented the geometry of the antenna elements. Conductive epoxy was placed on the straws at all locations so that traces on one straw could join traces on a different straw. This provided sufficient mechanical and electrical connections between the individual straws.

Figure 4-20 shows multiple straws, each with unique circuit traces, assembled to generate the geometry of the antenna elements.

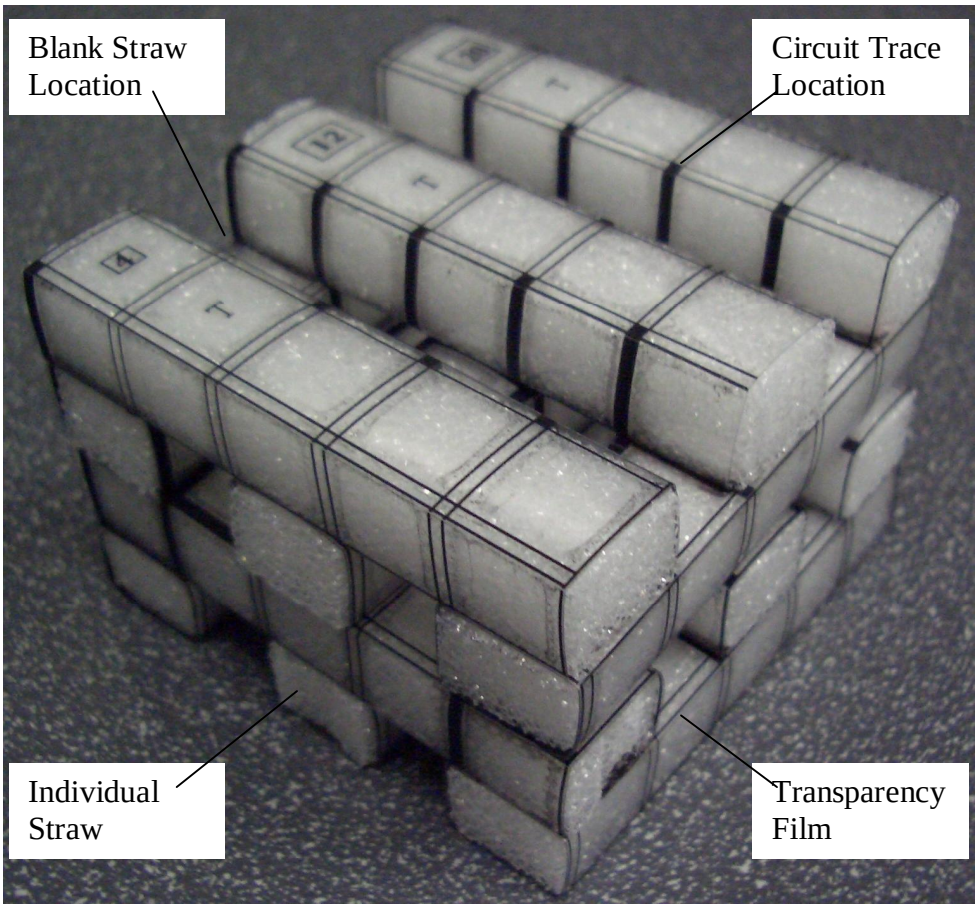

Figure 4-20 Assembled Straw Antenna Concept

In this model, the flex circuit material is represented by transparency film and the circuit traces are represented by dark lines on the transparency film. This model of the straw concept shows the layers of individual straws assembled perpendicular to each other with two possible straw locations blank per layer. It is possible to assemble the straws without the blank straw locations; however, the geometry of the antenna elements can be fully represented with the blanks included. If the blanks were filled with straws, the benefits would be a slight increase in the structural strength of the assembly and redundancy in the circuit traces with the expense of making more straws.

Another design developed was the slotted card concept, shown in Figure 4-21.

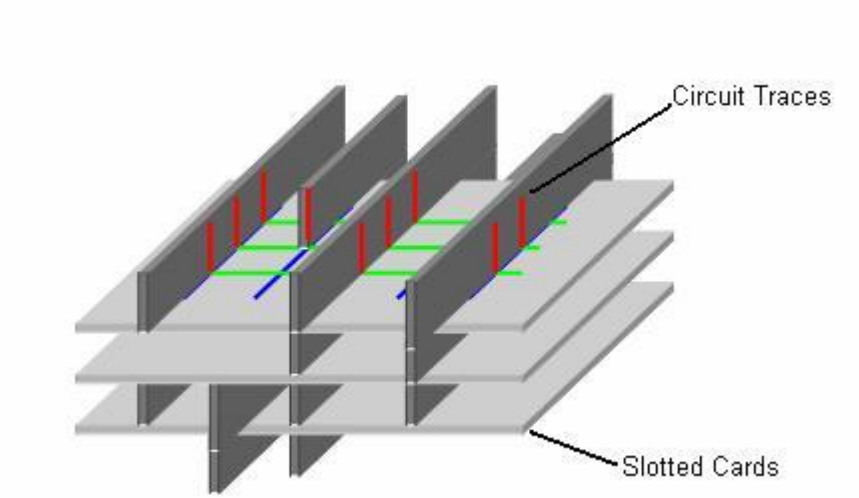

Figure 4-21 Slotted Card Concept

The slotted card concept was developed from the idea of printing circuit traces onto flex circuit material, cutting slots halfway through the length of the card and assembling the cards perpendicular to each other by sliding the cards together at the slots. The vertical geometry of the antenna elements are represented by vertical cards and the horizontal geometry of the antenna elements are represented by horizontal cards. Conductive epoxy is placed at each location where a vertical circuit trace intersects a horizontal circuit trace. The entire assembly can be filled with EPS foam or epoxy to increase the structural properties of the antenna.

A third concept termed the card and rod concept was developed and is shown in Figure 4-22.

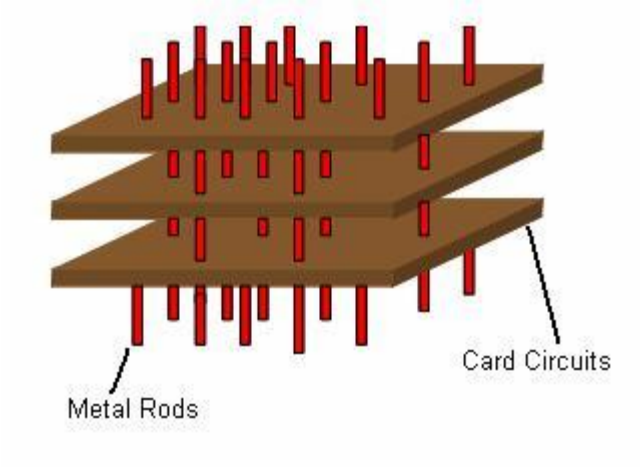

Figure 4-22 Card and Rods Concept

The card and rods concept was developed from the idea of printing circuit traces on flex circuit material and then inserting metallic rods perpendicularly through the cards. Conductive epoxy is used to mechanically and electrically join the rods and cards at locations where the metallic rods intersect the flex circuit traces. The horizontal geometry of the antenna are represented by the circuit traces on the cards and the vertical geometry of the antenna elements are represented by the metallic rods.

The assembly method of the card and rod concept is shown in Figure 4-23.

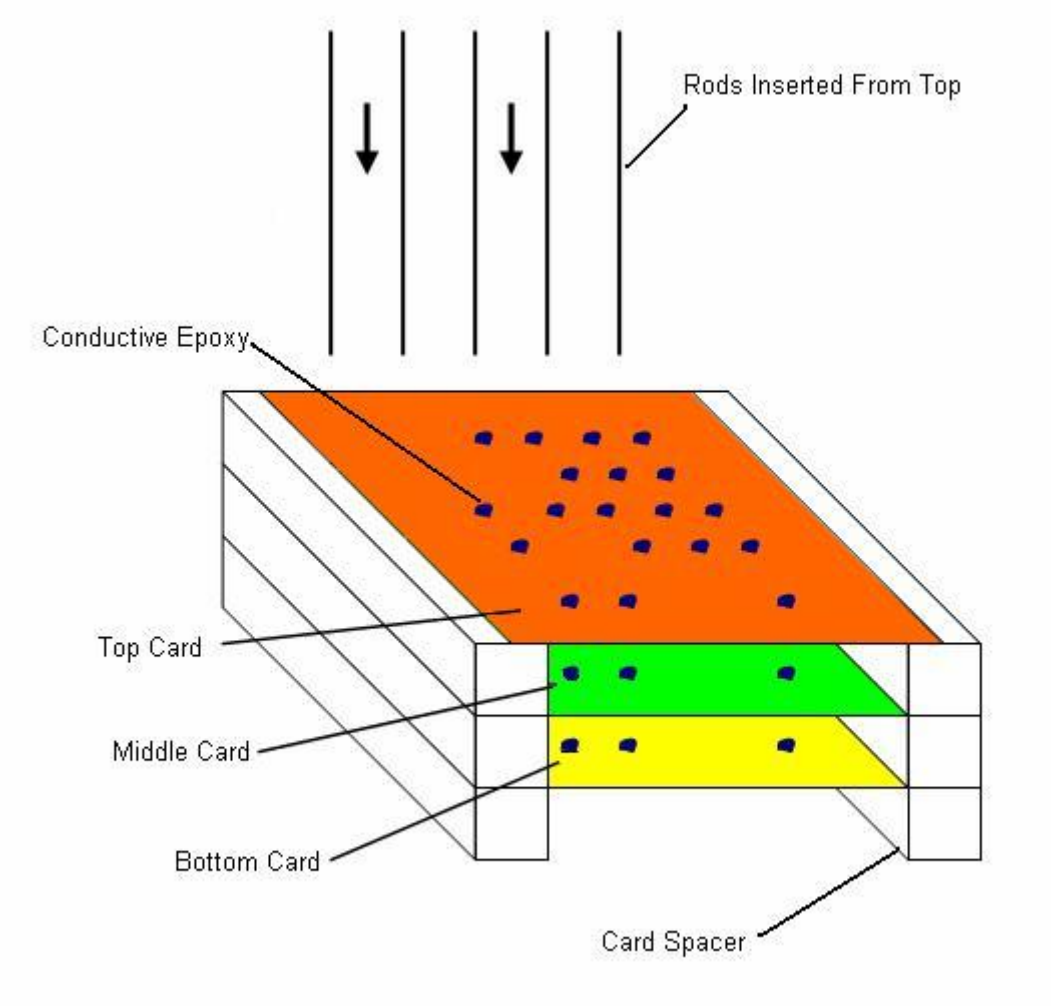

Figure 4-23 Card and Rod Assembly Method

The three cards that contained the horizontal geometry of the antenna were drilled in the areas where the metallic rods would pass. The size of the bit was selected such that the metallic rod fit tightly into the hole in the card. Conductive epoxy dollops were placed on top of the holes in the cards. The cards then were stacked on top of each other, separated by spacers that positioned the cards so that the circuit traces on them would line up with the horizontal antenna elements. The metallic rods were inserted into the holes in

the cards, passing through the conductive epoxy, and forming an electrical and mechanical connection between the cards, circuit traces, and the rods.

The fourth concept developed was the bends and L-shapes concept and is shown in Figure 4-24.

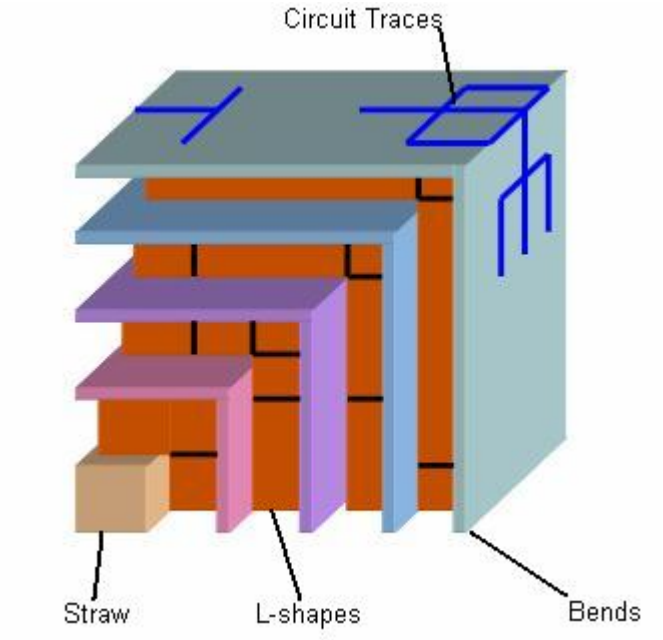

Figure 4-24 Bends and L-shapes Concept

The bends and L-shapes concept was developed around the idea of bending rectangular pieces of flex circuit material in half and assembling them with L-shaped pieces. The bends and the L-shaped pieces are covered in circuit traces, and when assembled represent the geometry of the antenna elements. One straw is used in this model in place of the smallest bend, as this substitution makes the model much more rigid. The bends and L-shapes are

joined with conductive epoxy at intersecting circuit traces of the bends and the L-shapes.

Figure 4-25 shows an assembly detail of the bends and L-shapes concept.

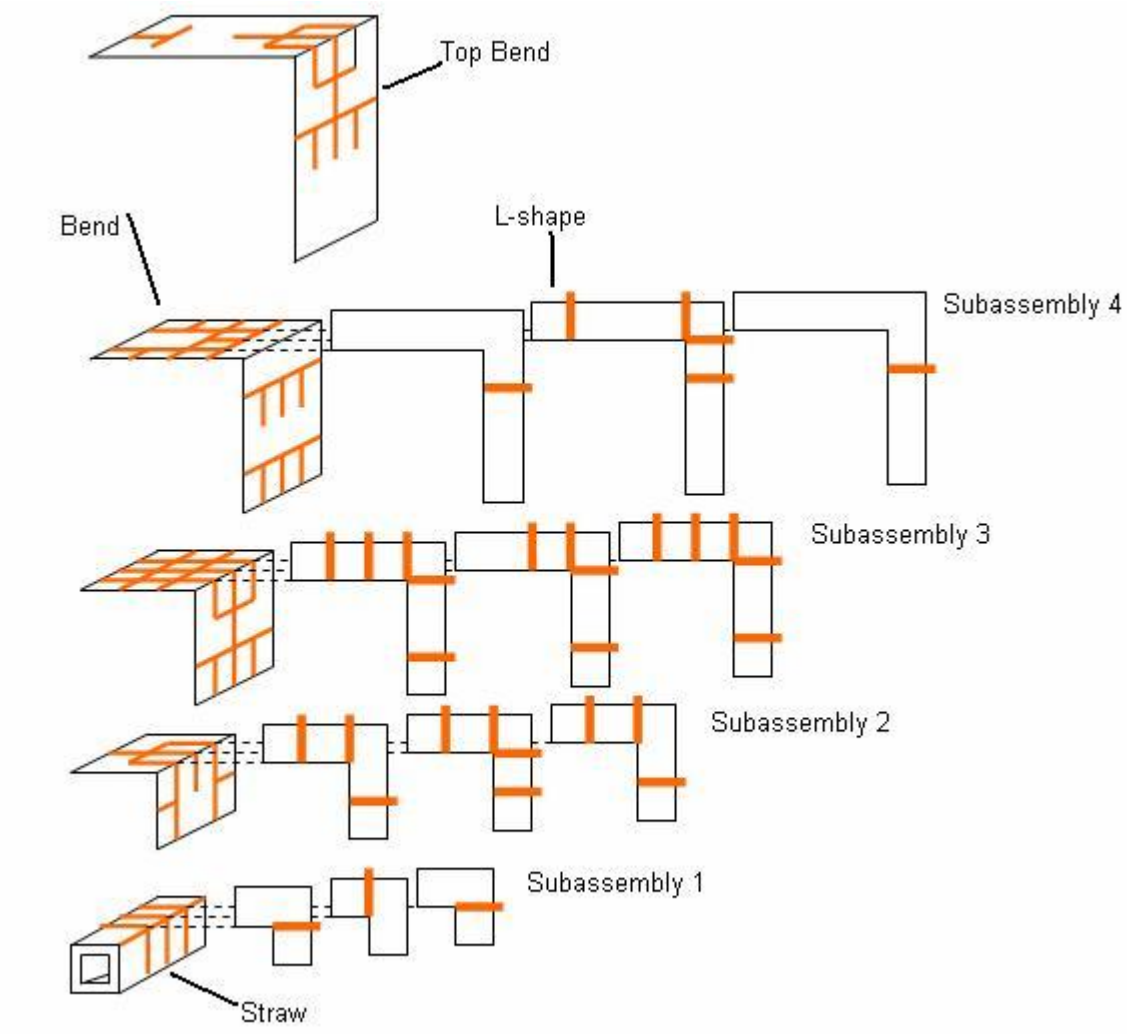

Figure 4-25 Bend and L-shapes Assembly Detail

The bends and L-shape concept was divided into several portions to facilitate assembly. The straw and three small bend pieces were joined to L-shapes to form subassembly 1. The three bends and L-shapes of corresponding size

were joined to form subassembly 2, subassembly 3 and subassembly 4. The subassemblies were then joined starting with subassembly 1 and adding subassembly 2. Subassembly 3 and subassembly 4 were added in similar fashion. The top bend was added as the last component. The components of the subassemblies were joined with conductive epoxy.

The multiple flex circuit concepts were narrowed down to two concepts deemed most suitable to the three dimensional antenna application, which would be subject to further development. Table 4-2 shows the concept selection chart.

Table 4-2 Concept Selection Chart

	Straws		Cards and Rods		Cards		Bends and L-shapes	
	Score		Score		Score		Score	
Number of Unique Parts	12	3	3	1	8	2	13	4
Total Number of Parts	12	2	22	4	8	1	17	3
Ease of Component Construction	Good	2	Excellent	1	Good	2	Good	2
Ease of Component Assembly	Excellent	1	Excellent	1	Poor	4	Fair	3
Geometric Stability	Good	2	Good	2	Poor	4	Good	2
Joint Strength	Good	2	Fair	3	Poor	4	Good	2
Complete Antenna Geometry	Pass	N/A	Pass	N/A	Pass	N/A	Pass	N/A
Allowance for Circuit Chips	Pass	N/A	Fail	N/A	Pass	N/A	Pass	N/A
Total Score		12		12		17		16

The selection criteria comprised the number of unique parts, total number of parts, ease of component construction, ease of component assembly, geometric stability, joint strength, complete antenna geometry and allowance for circuit chips. The concepts were given a ranking and a score for each criterion. The decision chart was set up such that the lowest score of any given concept was the best selection.

The antenna concepts comprised several parts. Some of these parts are common and can be used in multiple locations of the concept. The fewer unique parts that are to be made, the less the cost. The concepts' number of unique parts were counted and given ranking scores relative to each other on a one to four scale with one representing the lowest unique part count and four the highest unique part count.

A higher number of total parts of a concept will result in a higher material cost and a higher manufacturing cost. The concepts' total number of parts were counted and given a ranking score relative to each other on a one to four scale with one representing the lowest part count and four the highest part count.

Ease of component construction and ease of component assembly will result in shorter component manufacturing and assembly times and lower costs. The concepts were evaluated in these criteria and given a performance ranking of excellent, good, fair and poor with a corresponding score of 1, 2, 3 and 4,

respectively. The performance ratings were determined from experiences encountered while building models of the concepts.

The geometric stability and the joint strength represent the structural requirements of the concept. If the concept is lacking in geometric stability, then the potential exists for the concept to deform and alter the location of the representative antenna elements resulting in the degradation of the performance of the antenna. If the concept is lacking in joint strength, then joints will break and the required connections between representative antenna elements will be unattainable, therefore resulting in the degradation of the performance of the antenna. The concepts were evaluated in these criteria and given a ranking of excellent, good, fair and poor with a corresponding score of 1, 2, 3 and 4, respectively. The performance ratings were determined from experiences encountered while building models of the concepts.

The criterion of complete antenna geometry was a pass or fail measure to determine if the concept was capable of representing all of the elements of the antenna. For a concept to be chosen for further development, it must pass this criterion.

The criterion of allowance for circuit chips was added after the initial concepts were developed. This criterion was a pass or fail measure to determine if the

concept was capable of having circuit chips attached to elements. For a concept to be chosen for further development, it must pass this criterion.

All of the scores for the concepts were added and the two lowest scores were the straw concept and the cards and rods concept. However the cards and rods concept failed the "allowance for circuit chips" criterion. Therefore, the two concepts that were selected for further development were the straw concept and the bends and L-shapes concept.

Further development of the straws concept resulted in a prototype antenna shown in Figure 4-26.

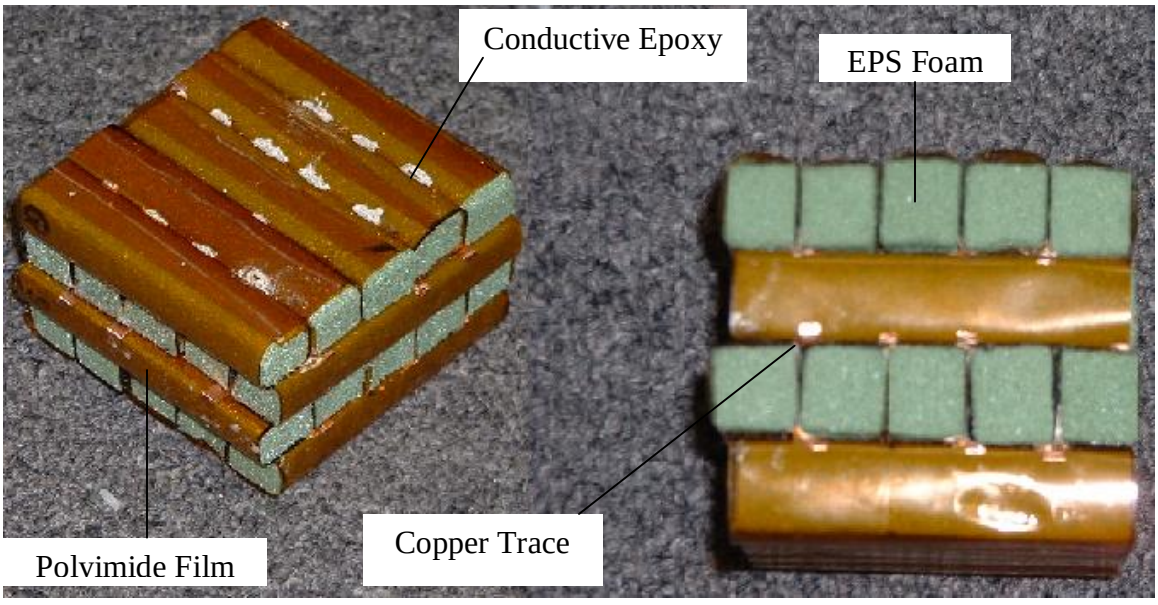

Figure 4-26 Straw Concept Prototype Antenna

In this model, copper tape was placed on polyimide film to represent antenna elements. The film with traces was folded four times and joined with

cyanoacrylate to form a rectangular straw shape. These straws were joined mechanically and electrically with conductive epoxy. The antenna could be constructed with blank spaces in between the straws. It was decided that these blank spaces should be filled with additional straws with the appropriate circuit traces to increase the structural properties of the model as well as to create redundancy in the copper traces.

Further development of the bends and L-shapes concept resulted in a prototype antenna shown in Figure 4-27.

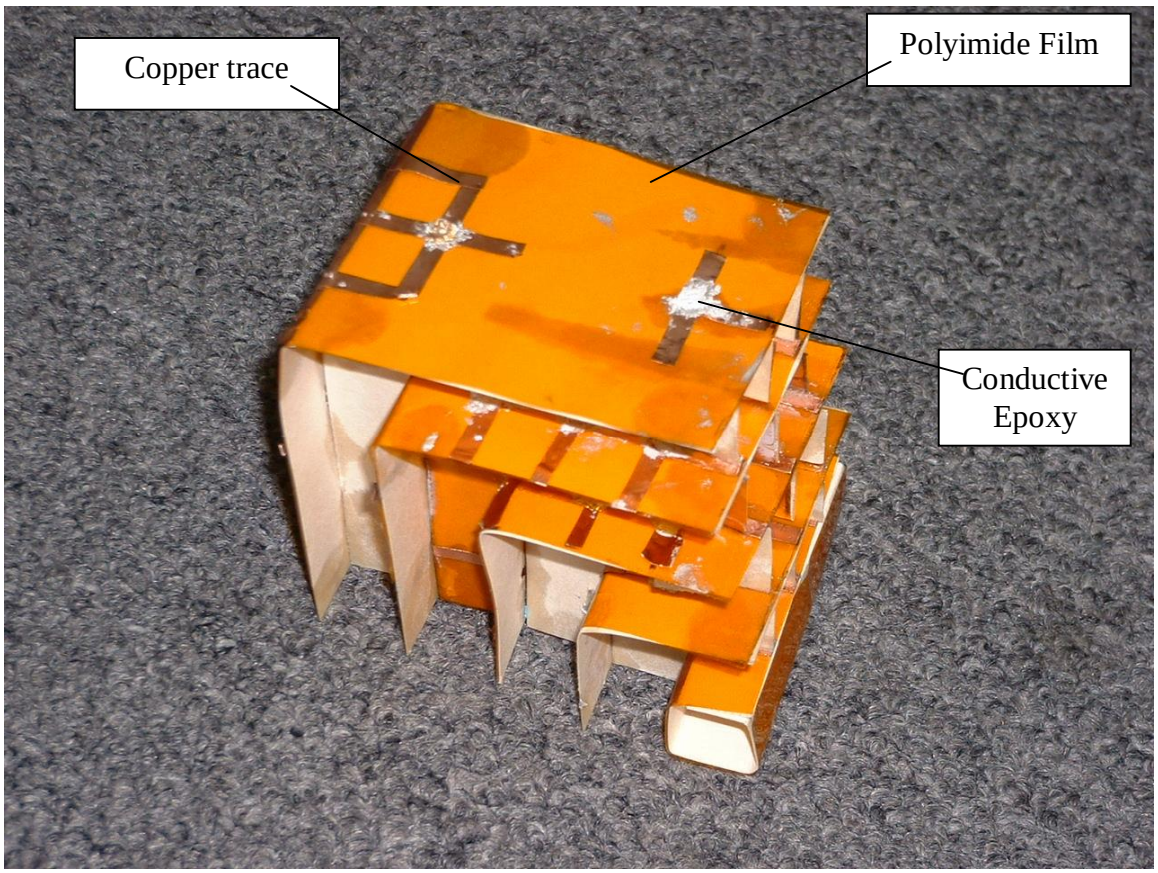

Figure 4-27 Bends and L-shapes Concept Prototype Antenna

In this model copper tape was placed onto polyimide film to represent antenna elements. Card stock material was joined to the back of the polyimide material to increase the stiffness of the material to ease in assembly. The individual components were electrically and mechanically joined with conductive epoxy.

4.5.3 Flex Circuit Formation and Bending

The two concepts for manufacturing antennas from flexible circuit material that were selected for further development required bending the flexible circuit material containing circuit traces into a shape that contains the geometry of the antenna. The flexible circuit material is a composite of thin copper and polyimide sheets laminated together with an acrylic adhesive as shown in Figure 4-28.

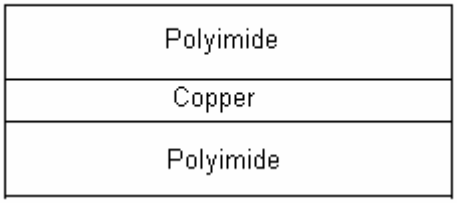

Figure 4-28 Flexible Circuit Material Cross-section

The procedure for constructing the material to be used in the antenna application is first to obtain a piece of flexible circuit material which is constructed from a layer of copper and a layer of polyimide with a binding

layer of adhesive. The required antenna geometry is etched onto the copper sheet and a protective coverlay sheet comprised of a layer of polyimide and adhesive is laminated onto the circuit. The resulting material is a layer of copper circuit with polyimide layers on either side, bonded with layers of adhesive [1].

A 12 inch by 12 inch sheet of flexible circuit material was purchased from Innovative Circuits, Inc. located in Alpharetta, Georgia. The sheet was made from Pyralux LF9120R single sided copper clad flex circuit laminated to Pyralux LF0120 coverlay. The sheet was cut into 0.5 inch by 2 inch test strips. The strips were then bent by a compressive method in an Instron Model 4400 Universal Testing System shown in Figure 4-29.

Figure 4-29 Instron Model 4400 Universal Testing Machine

A fixture for testing the specimens was constructed as shown in Figure 4-30.

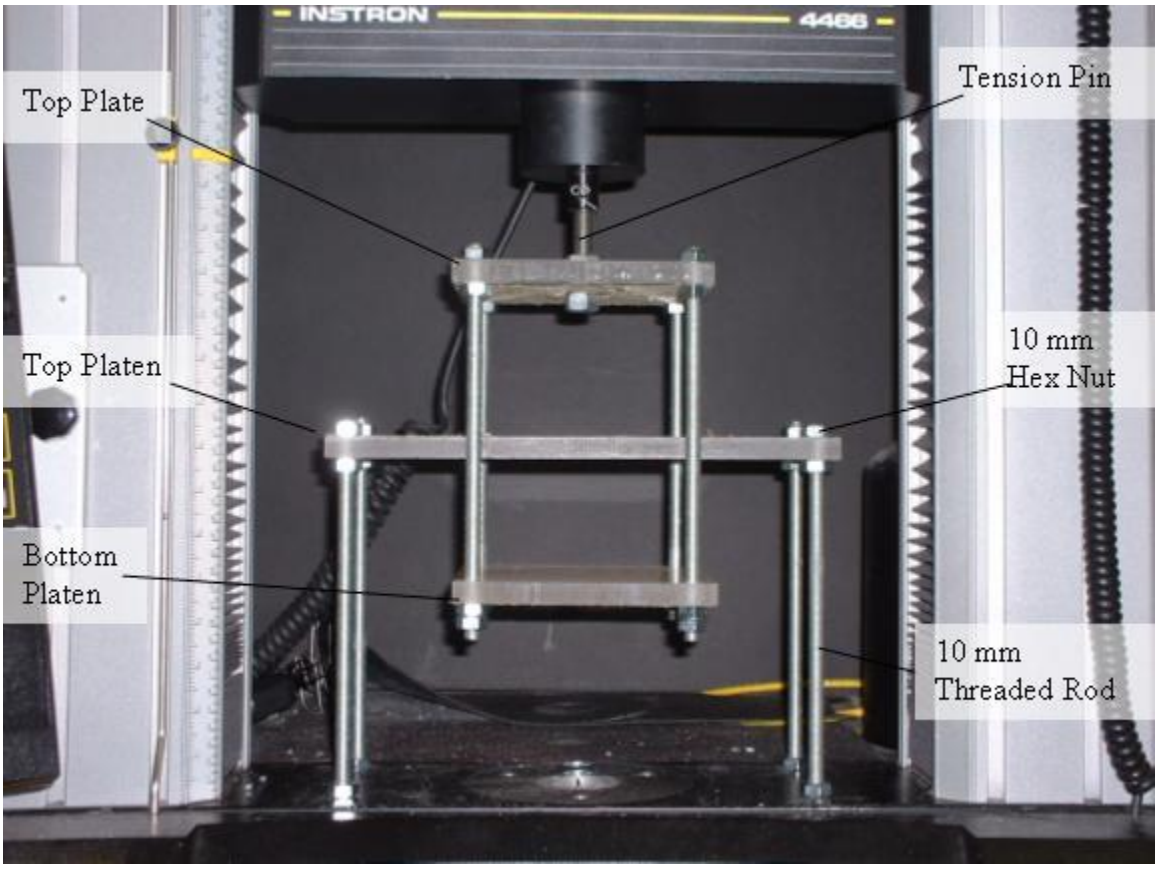

Figure 4-30 Instron Test Fixture

Dimensions of the bending fixture are shown in Figure 4-31.

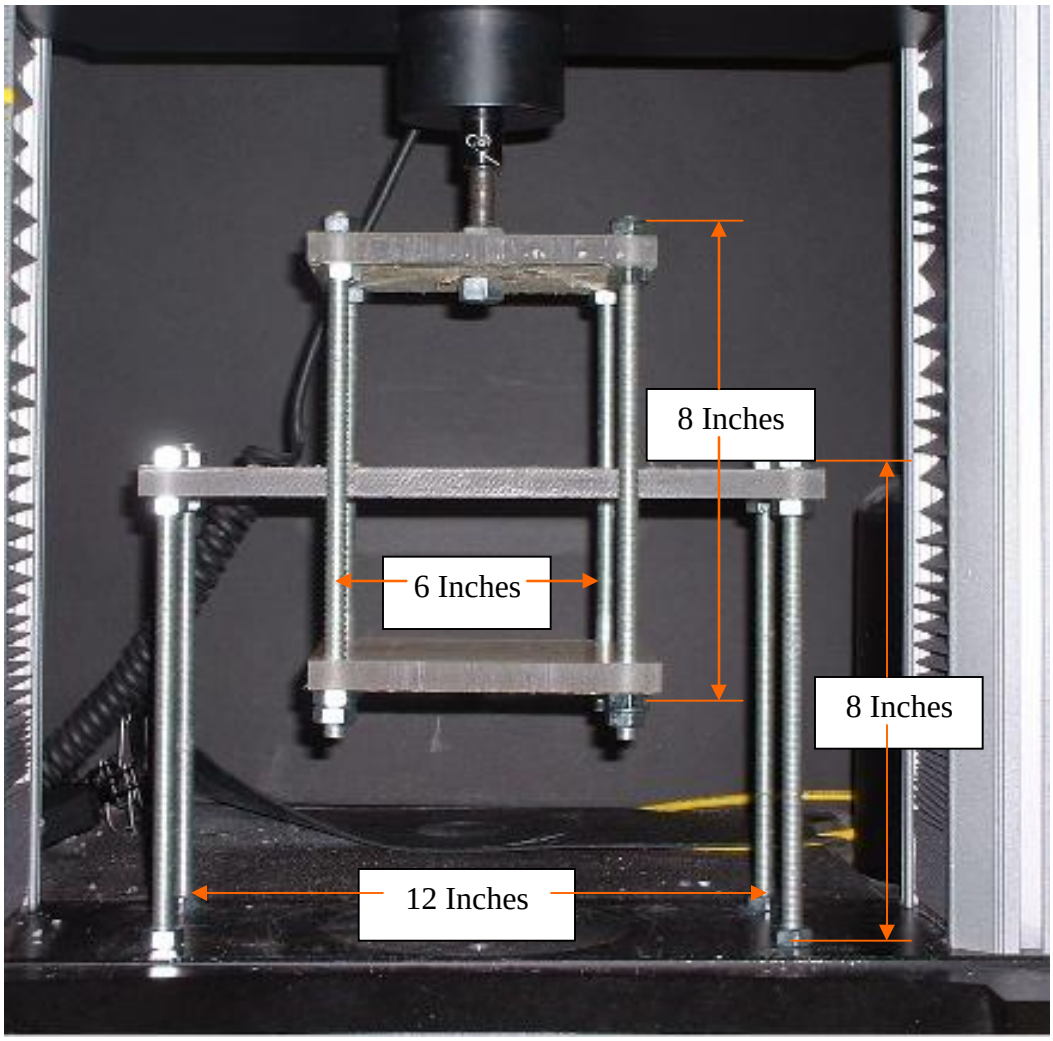

Figure 4-31 Dimensions of Bending Fixture

The fixture is made from 10 mm threaded rod, 10 mm hex nuts and 0.05 inch acrylic plate. Four 10 mm threaded rods are screwed into the base of the Instron and secured with four 10 mm hex nuts. The top platen is secured to the top of the four 10 mm threaded rods, which are attached to the base of the Instron, with eight 10 mm hex nuts. The bottom platen and the top plate are secured to four 10 mm threaded rods with sixteen 10 mm hex nuts. The tension pin is secured to the center of the top plate with two 10 mm hex nuts and is pinned to the load cell of the Instron.

In this fixture design, the top platen is fixed to the base of the Instron. The top plate is fixed to the movable head of the Instron. The Instron then can apply a tensile load to the fixture, moving the bottom platen towards the top platen. This tensile method of compression ensures that the top platen and bottom platen are parallel when loaded.

The distance between the two platens is controlled by inserting two stacks of steel shims between the platens as shown in Figure 4-32. The compression height is equal to the thickness of the shim stacks. The strips of flex circuit are placed in between the steel shim stacks and are compressed to the thickness of the steel shim stacks.

The test strips of flex circuit were subjected to compression bending at various heights using the Instron Model 4400 Universal Testing Machine at a speed of 20 inches per minute. The test was set up so that when the two platens contacted the steel shim stacks the compression would stop. This was accomplished by setting a cutoff force on the Instron. A cutoff force of 5 pounds was sufficient for complete contact of the steel shim stacks and the platens. Maximum travel limits were adjusted to prevent damage to the machine and test fixture in the event the cutoff force failed to stop the test. Figure 4-32 shows the test fixture compressed with a 5 pound load.

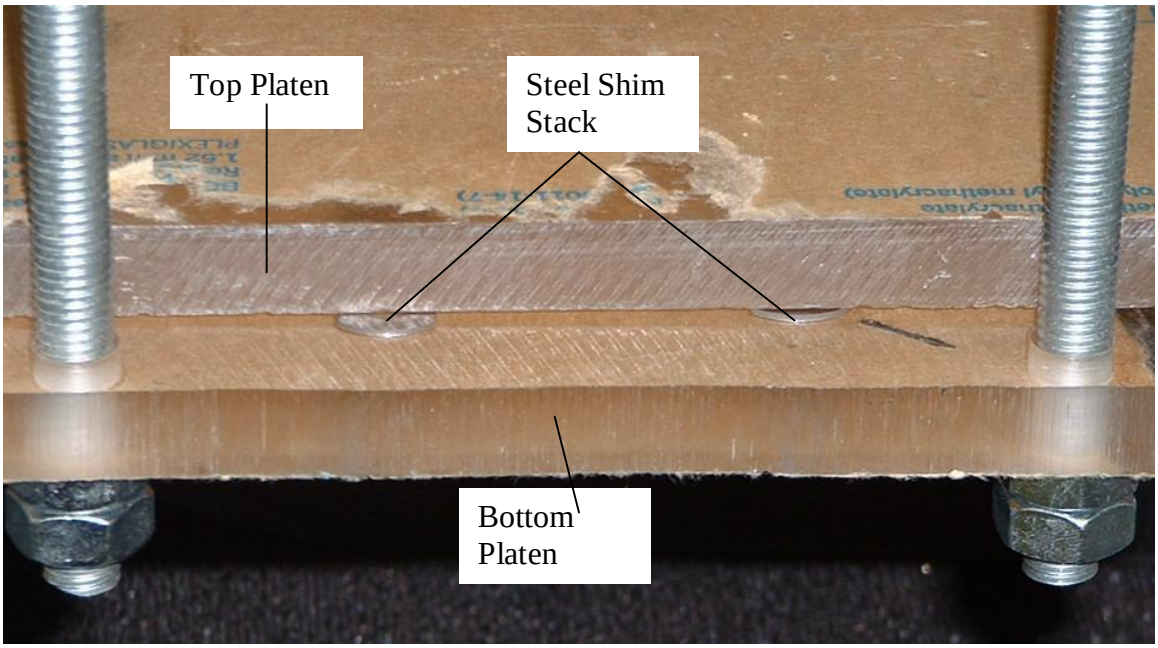

Figure 4-32 Test Fixture Compressed

Bending tests were conducted over a range of compression heights within the bending constraints listed in Table 4-3.

Table 4-3 Compression Heights

Compression Heights (inch)
0.016
0.018
0.020
0.021
0.022
0.023
0.024
0.025
0.026
0.027
0.028
0.029
0.030
0.031
0.032
0.033
0.034
0.035
0.036
0.037
0.038
0.039
0.040
0.042
0.044
0.049
0.054
0.064

After the test strip was compressed, it was measured with a protractor to determine the final bent angle. Ten test strips were bent for every setting of compression height.

4.5.4 Rapid Prototyping Models

The rapid prototyping technologies of stereolithography and selective laser sintering were used to make the two different types of three dimensional

antennas. A solid model of the two designs was created. Several different photopolymer resins were used to build antennas via stereolithography. The antennas then were coated with conductive coatings.

4.5.4.1 Solid Model Development

As the antenna designs were quite complicated, and the elements numerous, it was not feasible to hand draw every component of the antenna model into a three dimensional solid model. A program was developed using Matlab that generated Autocad commands from the data in the element and node list. The source code of the program is shown in Appendix B. These commands were then inserted into Autocad and a solid model was produced.

4.5.4.2 Stereolithography Model

From the solid model a STL file was created. Figure 4-33 shows a solid model of the second three dimensional design.

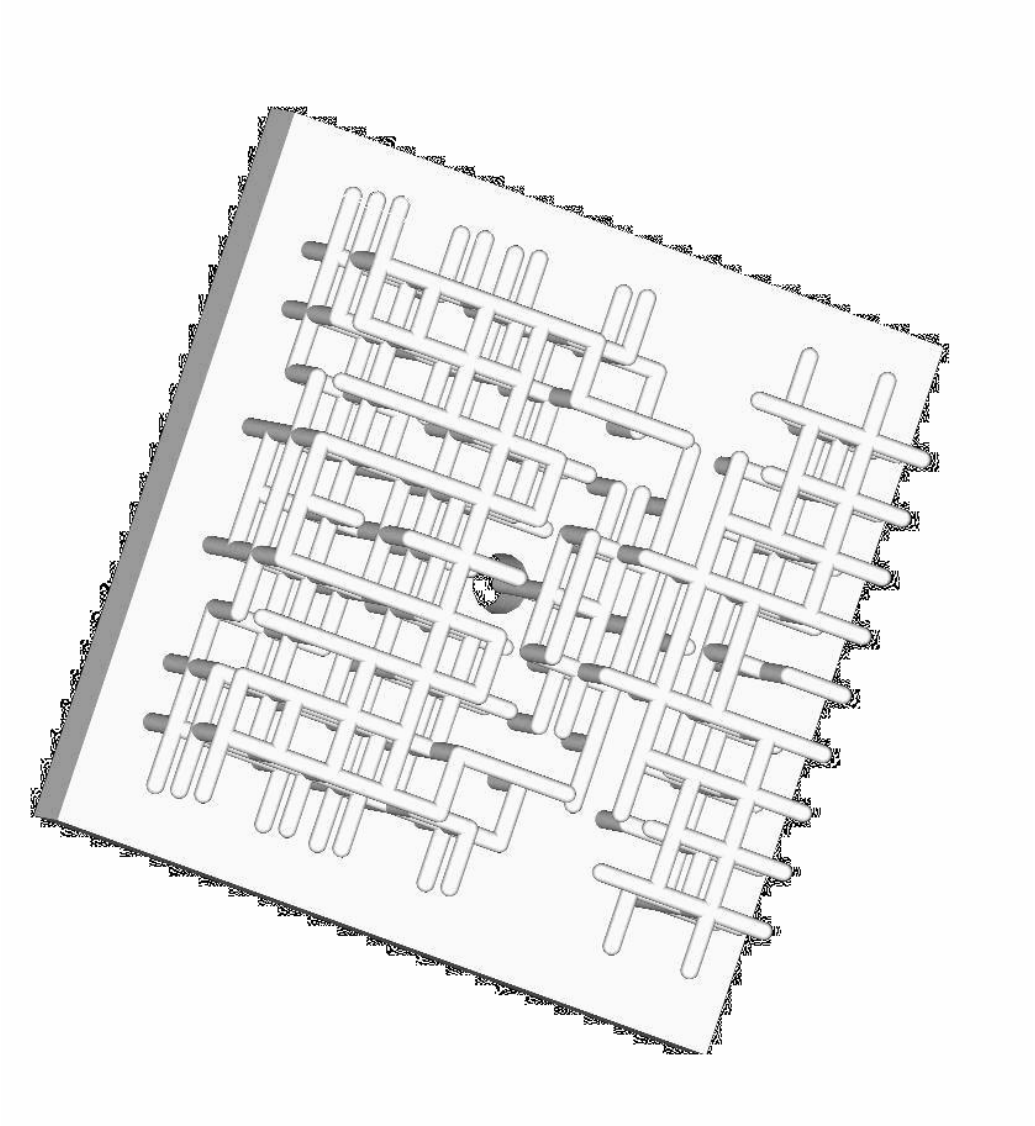

Figure 4-33 Solid Model of Second Three Dimensional Design

This file was processed with 3D Lightyear software to generate a part build file. The part build file was loaded into an SLA 3500 stereolithography machine manufactured by 3D Systems, Valencia, California. The antenna was then constructed. When the part was finished, it was allowed to rest in the machine so that excess resin could drip off of the part. The part was washed with an isopropyl alcohol solution followed by a water rinse. The

part then was placed in a UV oven for one hour so that the part would fully cure. The part was taken from the oven and the supports were removed.

Figure 4-34 shows the first three dimensional antenna design made via SLA with SL 7510 resin, manufactured by 3D Systems, Valencia, California.

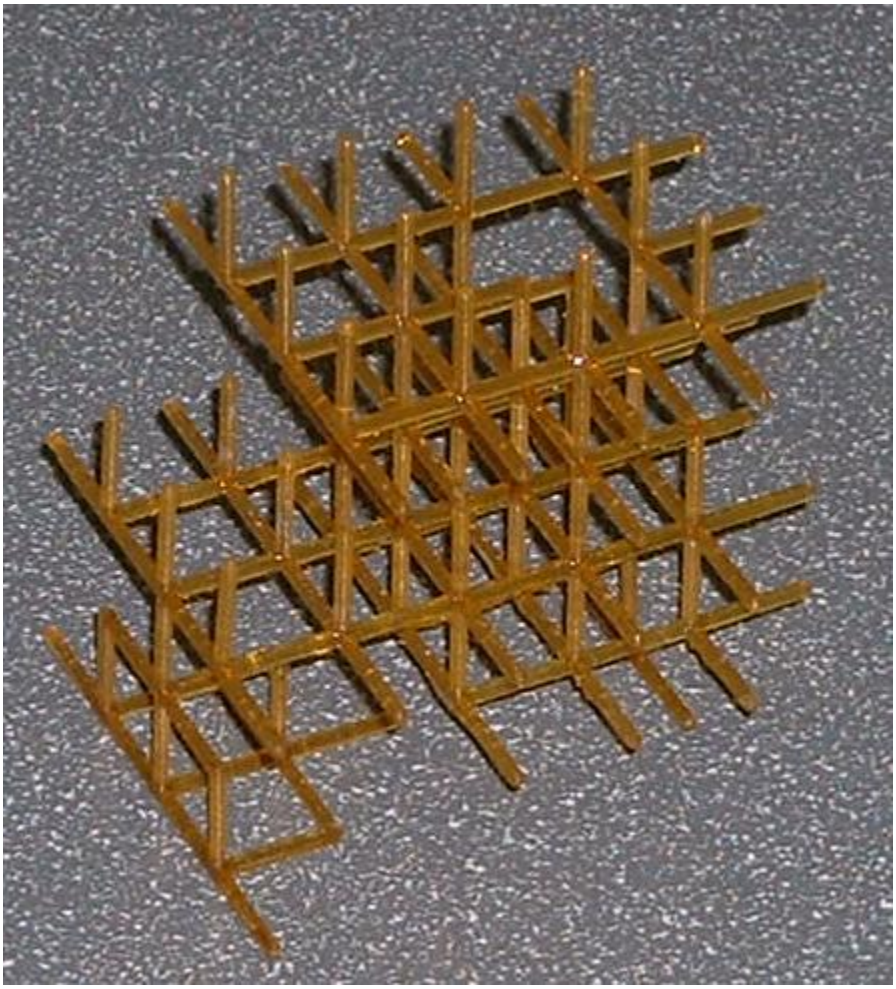

Figure 4-34 First Three Dimensional Design Made From SL 7510 Resin

SL 7510 is a general purpose epoxy resin. This material has a tensile strength of 6500 psi (44 MPa), a flexural strength of 11,900 psi (82 MPa) and a Shore

D hardness of 87 [10]. The supports were easily removed from the part and the antenna elements were intact after support removal.

Figure 4-35 shows the second three dimensional antenna design made via SLA with 8120 resin manufactured by DSM Somos, New Castle, Delaware.

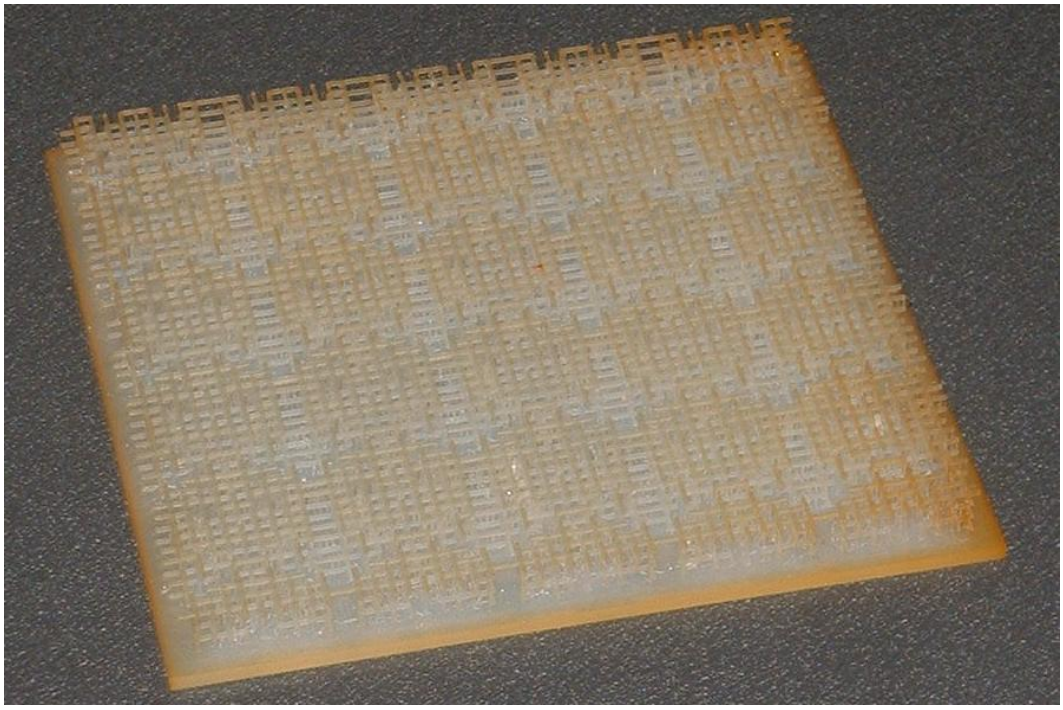

Figure 4-35 Second Three Dimensional Design Made From 8120 Resin

8120 is a photopolymer resin with properties similar to polyethylene. This material has a tensile strength of 3800 psi (26 MPa), a flexural strength of 3800 psi (26 MPa) and a Shore D hardness of 76 [11]. The supports were difficult to remove from the part and the antenna elements were not intact after support removal.

Figure 4-36 shows the second three dimensional antenna design made via SLA with SL 7560 resin, manufactured by Vantico AG, Basel, Switzerland.

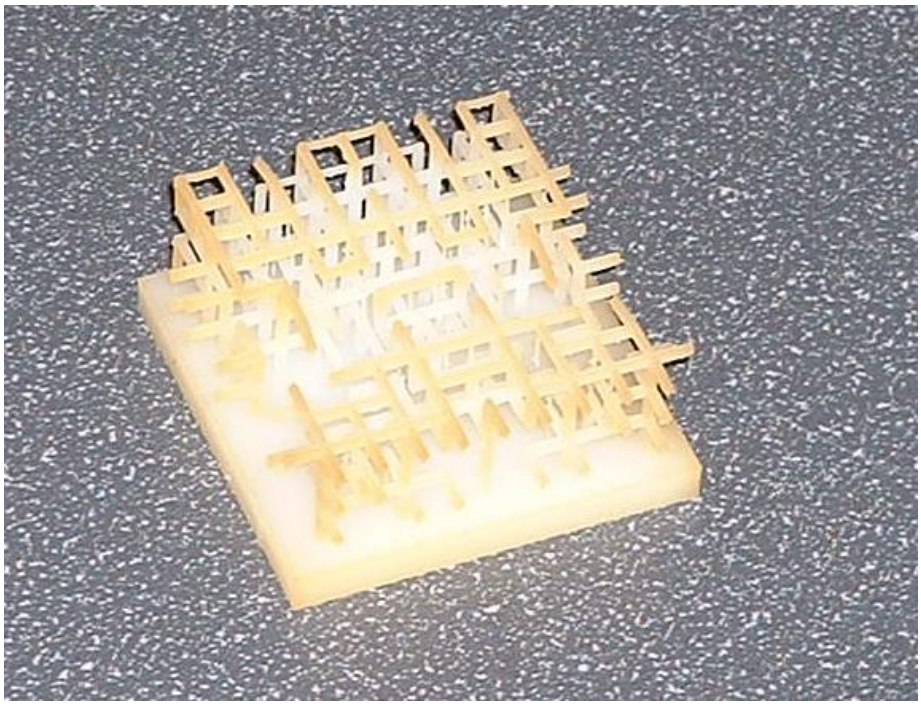

Figure 4-36 Second Three Dimensional Design Made From SL 7560 Resin

SL 7560 is a photopolymer resin with properties similar to ABS. This material has a tensile strength of 6,000 psi (42 MPa), a flexural strength of 12,000 psi (83 MPa) and a Shore D hardness of 86 [12]. The supports were difficult to remove from the part and the antenna elements were not intact after support removal.

Figure 4-37 shows the second three dimensional antenna design made via SLA with 10120 resin.

Figure 4-37 Second Three Dimensional Design Made From 10120 Resin

10120 is a photopolymer resin with properties similar to polycarbonate. This material has a tensile strength of 3,736 psi (26 MPa), a flexural strength of 5726 psi (39.5 MPa) and a Shore D hardness of 81 [13]. The supports were difficult to remove from the part and the antenna elements were not intact after support removal.

SLA parts of the first three dimensional antenna design were sent to coating companies to be coated with conductive paints. Figure 4-38 shows a SLA part coated with a nickel based paint.

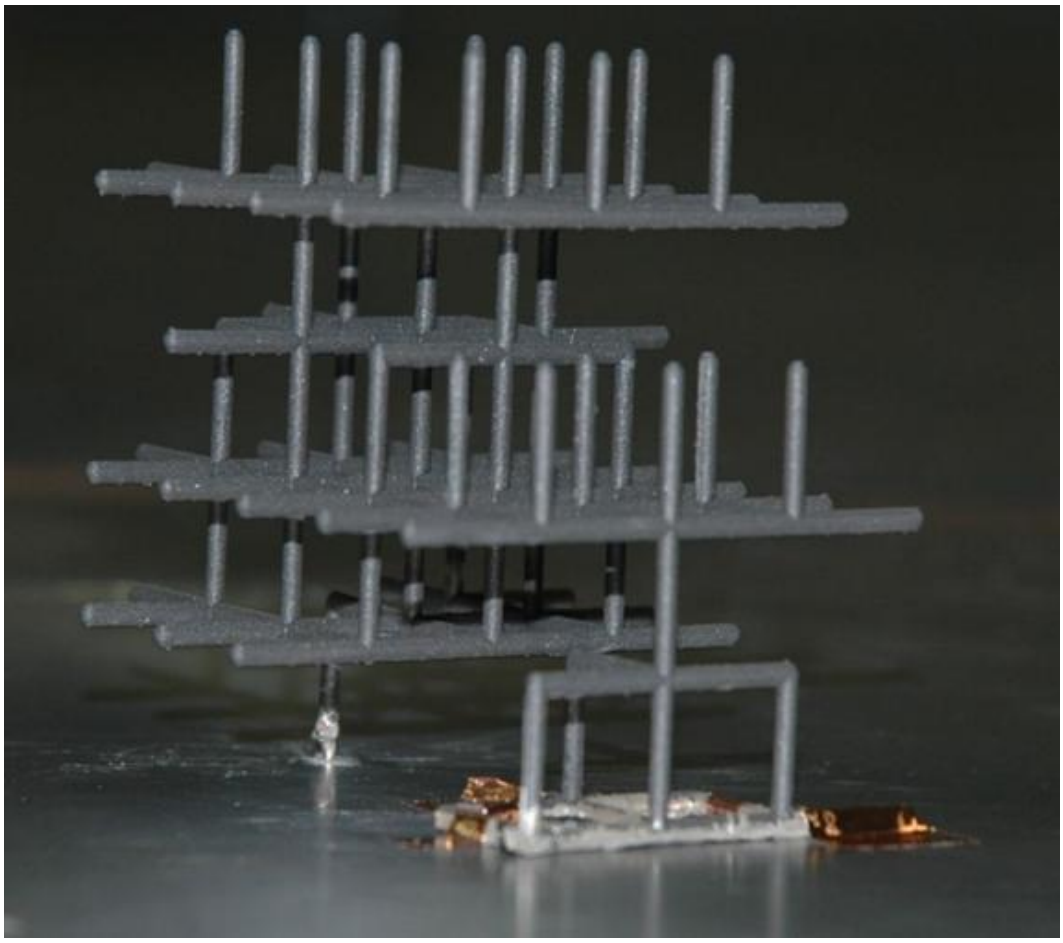

Figure 4-38 First Three Dimensional Design Coated With Nickel Paint

The nickel coating of the first three dimensional antenna design was completed by Atlanta Metal Coating Inc., located in Doraville, Georgia.

The nickel coated antenna was tested, with an imageplane measurement system, by driving the antenna over a frequency range of 0 GHz to 3.5 GHz. The maximum antenna gain was recorded over this frequency range.

Figure 4-39 shows a SLA part coated with a silver based paint.

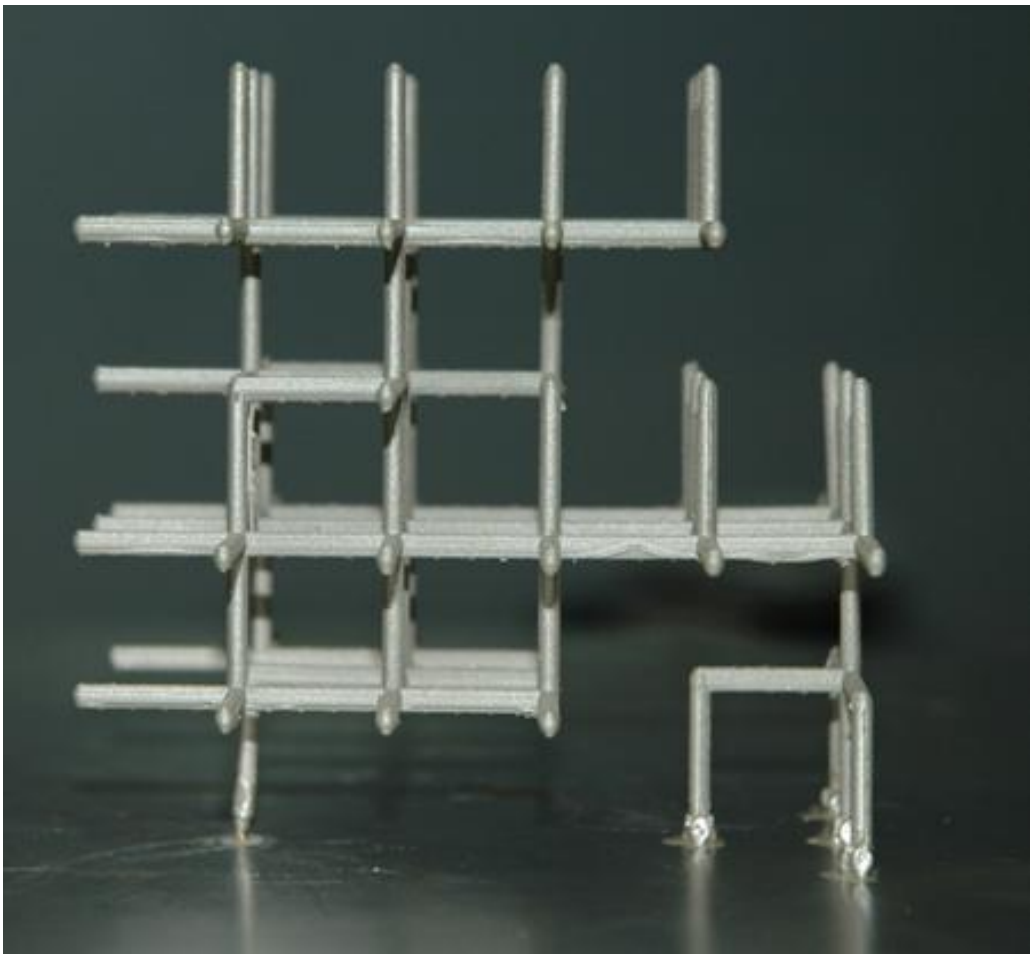

Figure 4-39 First Three Dimensional Design Coated With Silver Paint

The silver coating of the first three dimensional antenna design was performed by Thermospray Company Inc., located in Sarasota, Florida.

The silver coated antenna was tested, with an image plane measurement system, by driving the antenna over a frequency range of 0 GHz to 3.5 GHz. The maximum antenna gain was recorded over this frequency range.

4.5.4.3 Selective Laser Sintering Model

From the solid model of the second three dimensional antenna design, a STL file was created. This STL file was sent to the Rapid Prototyping Center at the University of Louisville located in Louisville, Kentucky to have an antenna created via SLS because there are no SLS machines at Georgia Tech. Figure 4-40 shows the completed SLS antenna.

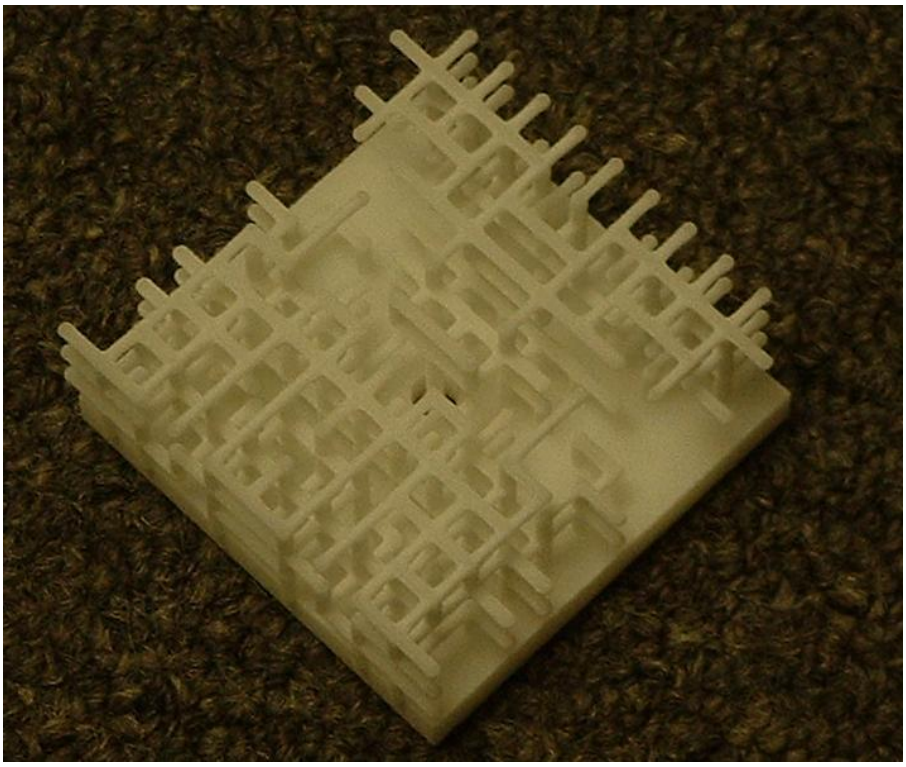

Figure 4-40 SLS Antenna

The SLS antenna was made from Duraform PA thermoplastic powder manufactured by 3D Systems, Valencia California. This material is an unfilled nylon powder with a tensile strength of 6,400 psi (44 MPa). The finished part had a good surface finish as shown in Figure 4-41.

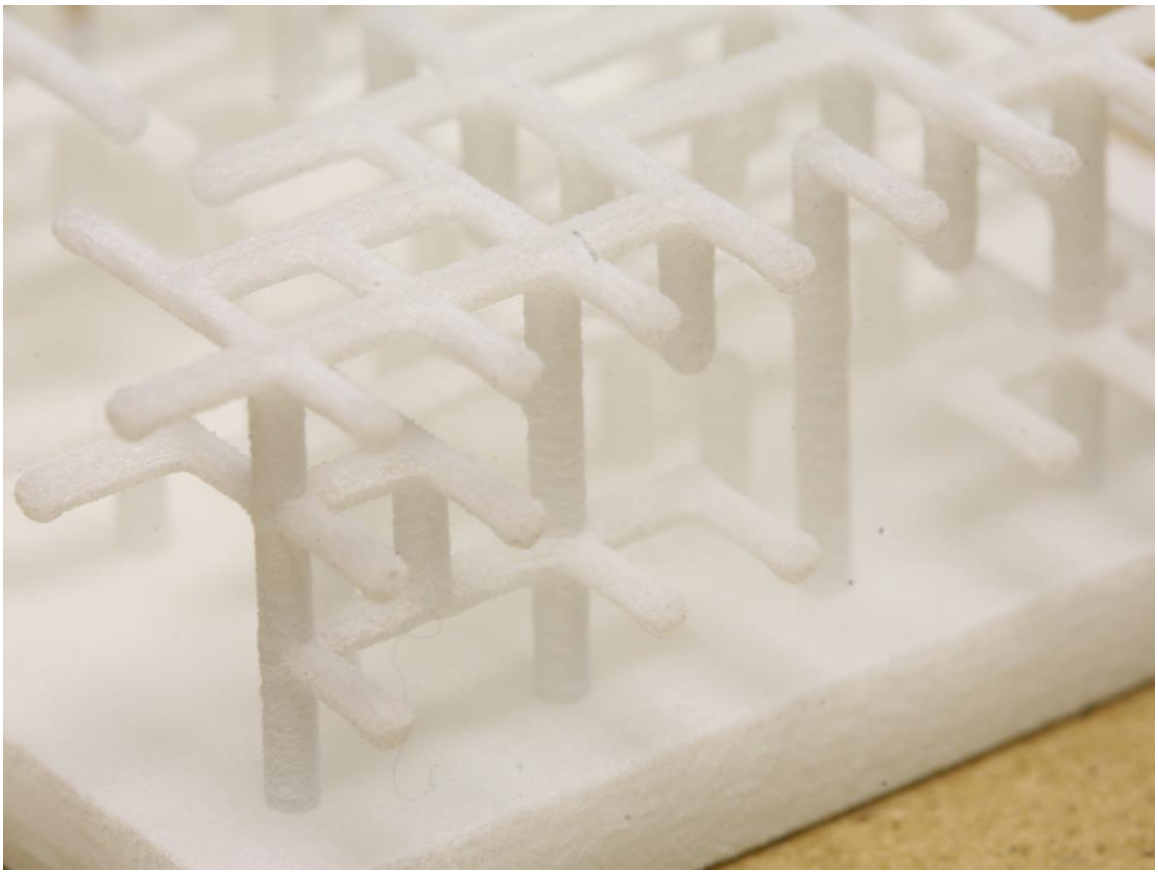

Figure 4-41 Surface Finish of SLS Antenna

The SLS antenna has not been coated with a conductive coating or tested at the time of completion of this work.

4.6 Summary

In this chapter experimental procedures used to test the bending of the flex circuit material were presented. A bending fixture was designed and a bending procedure for bending flex circuit material was developed. Epoxy encapsulation testing was performed. Models of epoxy encapsulated antenna designs were constructed.

Concepts for three dimensional antenna designs manufactured from flex circuit were discussed. Models of three dimensional antennas constructed from flex circuit material were created. Methods of manufacturing three dimensional antennas via rapid prototyping were presented.

Chapter 5 presents the results of the experimental procedures discussed in Chapter 4. Results of the experimental bending tests of the flex circuit is provided and analyzed. The predicted values of strain, due to bending of flex circuit material are compared to the experimental bending results. An evaluation of the flex circuit material, after bending, is conducted. Discussion of models of the epoxy encapsulated antenna designs is provided. Models of three dimensional antennas manufactured from flex circuit material are discussed. Testing results of three dimensional antennas manufactured via SLA are provided and discussed.

5 RESULTS AND DISCUSSION

5.1 Introduction

In this chapter the results of the bending tests are presented and analyzed. These results are compared to the predicted values of the theoretical bending model. A material analysis is provided to show that the physical limits of the flex circuit material were not exceeded. The epoxy encapsulated antenna models are discussed. The flex circuit models are discussed and conductivity results provided. The SLS antenna testing is discussed and antenna gain results provided.

5.2 Bending Model Results

Figure 5-1 shows the results of the compression bend tests of the test strips.

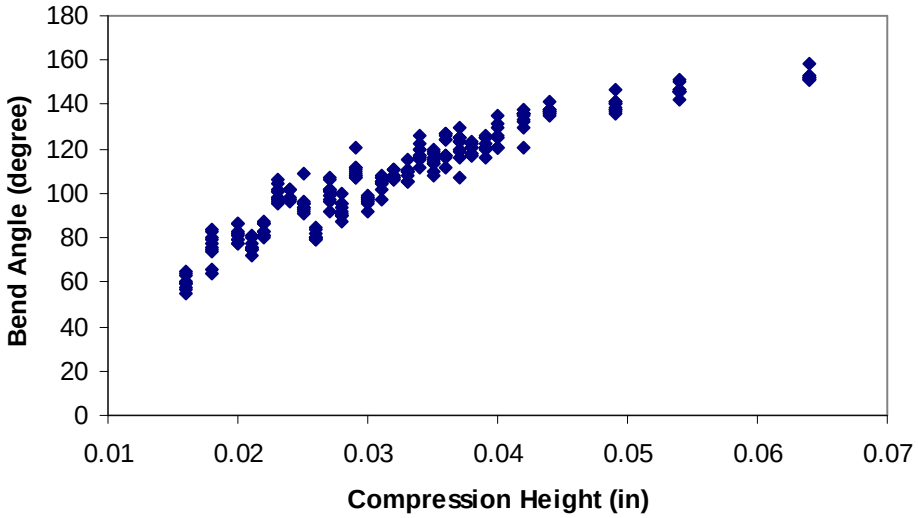

Figure 5-1 Results of Test Strip Compression Bend Test

The compression bend test data are also provided in Appendix D. The experimental data were analyzed and the bend angles were used to calculate the strain in the material at various compression heights as shown below. This was possible by assuming that the length of the neutral axis remains constant throughout the bending process. The radius of the neutral axis of the compressed material was compressed was calculated at each compression height by Equation 5-1.

$$R_x = \frac{h_c - t}{2}$$

Equation 5-1

The effective punch radius was calculated at each compression height with Equation 5-2.

$$r_p = \frac{h_c - 2 * t}{2}$$

Equation 5-2

The effective punch radius after the material was released was calculated at each compression height with Equation 5-3.

$$r'_p = \frac{R_x * \pi}{\alpha} - \frac{t}{2}$$

Equation 5-3

The bent strain, the strain when the material is compressed, was calculated at each compression height with Equation 5-4.

$$\varepsilon_{bent} = \frac{1}{1 + \frac{2 * r_p}{t}}$$

Equation 5-4

The final strain, the strain in the material when it is released from compression, was calculated at each compression height using Equation 5-5.

$$\varepsilon_{final} = \frac{1}{1 + \frac{2 * r'_p}{t}}$$

Equation 5-5

The amount of recovery strain was the difference between the bent strain and the final strain. Figure 5-2 shows the bent strain, final strain and recovery strain for the experimental data. This data is also provided in Appendix E.

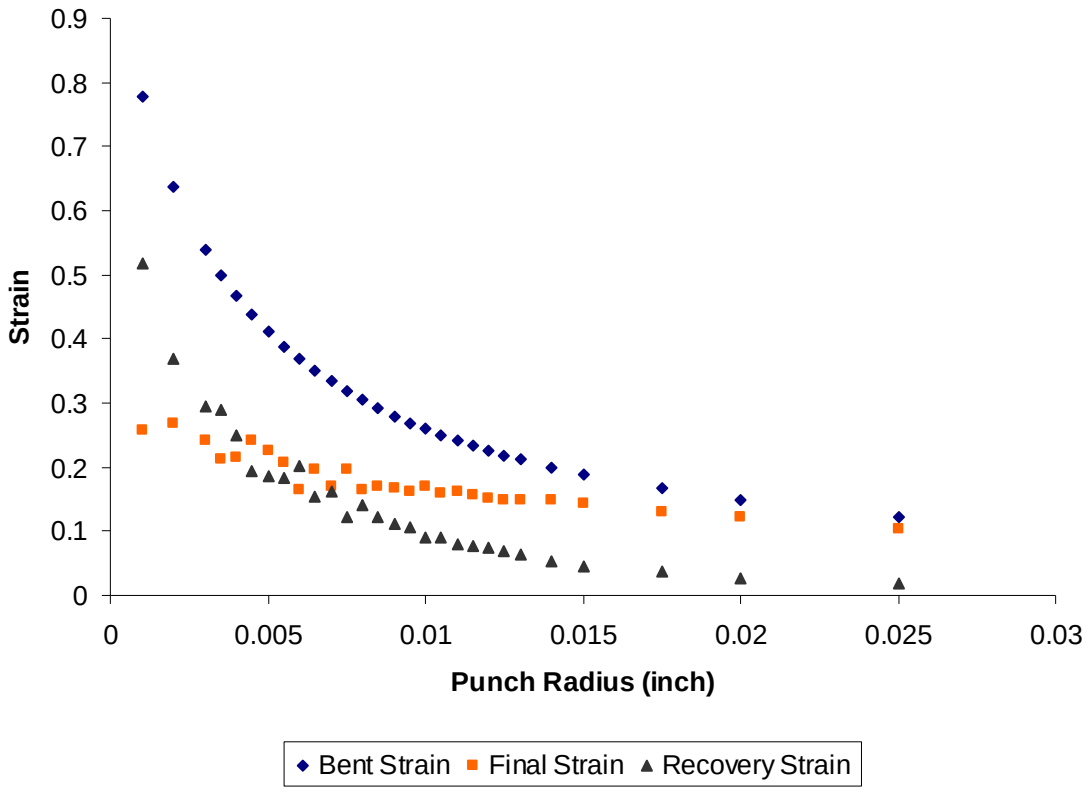

Figure 5-2 Experimental Strain Results

The experimental data were then compared to the predicted values from the analytical bending model. Figure 5-3 shows the final strain of the experimental data compared to the final strain predicted by the analytical model. This data is also provided in Appendix F.

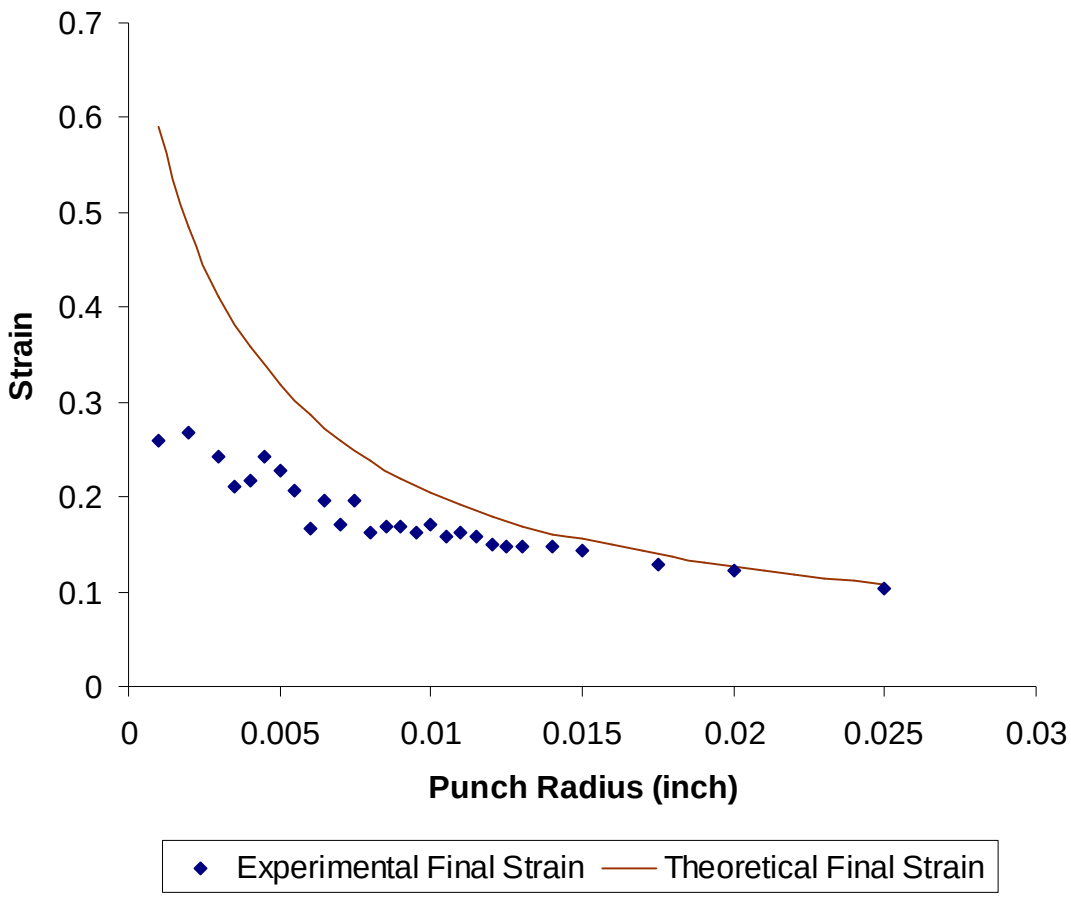

Figure 5-3 Experimental and Theoretical Final Strain Comparison

Figure 5-3 shows the experimental final strain data compared to the theoretical final strain predicted by the analytical model. As the punch radius decreases the difference between the experimental data and theoretical data increases. This difference was attributed to the bulging of the flex circuit material and adhesive mandating the development of a bulging model. A bulging model was developed and is discussed in Section 3.3.

The bulging model was incorporated into the analytical model and the bulging corrected theoretical final strain is compared to the experimental results in Figure 5-4. The corrected final strain data are also provided in Appendix G.

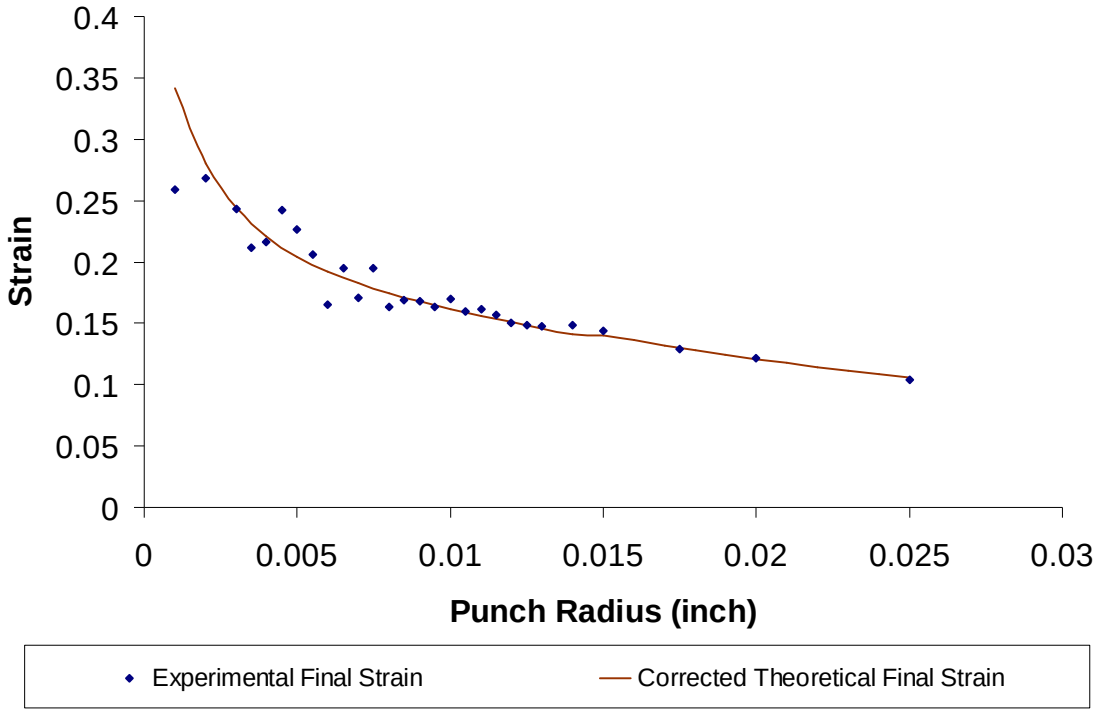

Figure 5-4 Bulging Corrected Comparison of Final Strain

This figure shows the experimental final strain data compared to the bulging corrected theoretical final strain that is predicted by the analytical model. The predicted value of the final strain is very close to the experimental values, validating the bulging model and enabling one to predict the final conditions of the material.

Bending copper polyimide composites can lead to cracking and delamination. The bent specimens were inspected visually, and with the aide of an Intel Model QX3

Computer Microscope manufactured by Intel Inc., Santa Clara, California. The specimens were examined for cracks and layer separation both parallel and perpendicular to the plane of the bend. The specimens were examined by eyesight and with a microscope setting of 10x, 60x and 200x. No cracks or evidence of layer separation was found, as can be seen in Figure 5-5, a cross-sectional view of the bent area at 200x.

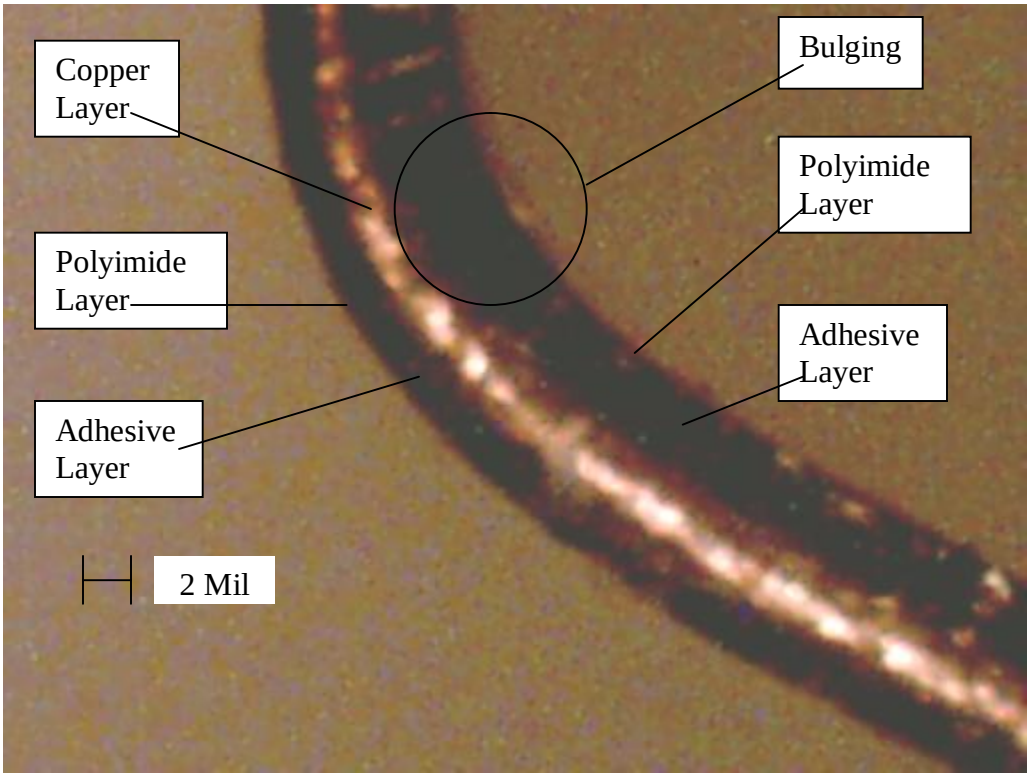

Figure 5-5 200x Image of Bent Area

It can be concluded from these observations that the deformation processes used did not exceed the physical limits of the flex circuit. Figure 5-5 also shows the bulging of the inner layer of polyimide and adhesive which supports the bulging model.

5.3 *Epoxy Encapsulated Antennas*

The development of models of the epoxy encapsulated hemispheres model and the fragmented slot antenna were intended to prove that it was possible to manufacture these two concepts. All of the models met the requirements that the epoxy structure be clear and free from voids and met the geometry of the concept. This was accomplished by careful control of the epoxy encapsulation procedure. Both of the hemispherical concepts possessed locations that radiators could be placed. Incorporating copper mesh reflective back planes and fiberglass cloth into the epoxy structure was performed on the models and proven feasible. The FR4 circuit based hemisphere antenna model proved to be easier to manufacture as the hemispheres were fixed onto a single circuit structure, enabling them to be located properly, and more easily than the four individual hemispheres of the other design. The fragmented slot antenna design was proven possible to manufacture by the development of the model. No antenna testing was conducted on these models.

5.4 Flex Circuit Models

Two flex circuit prototype models were produce. Figure 5-6 shows a straw concept prototype.

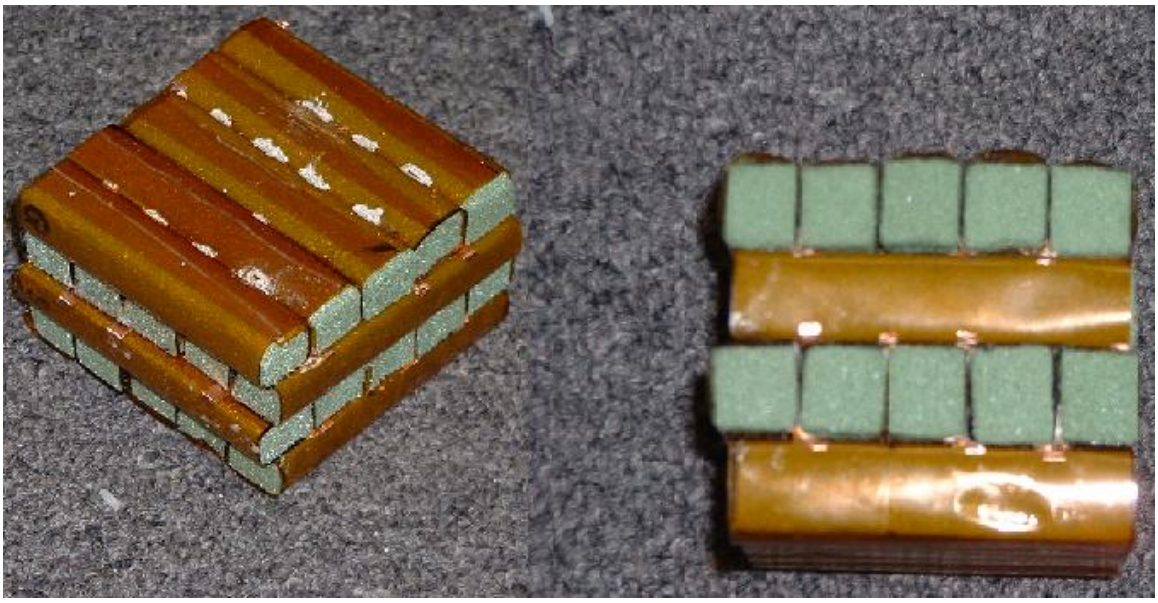

Figure 5-6 Straw Concept Prototype

The straw concept prototype was easier to manufacture than the other flex circuit concepts because it was much easier to line up the antenna components so that the copper traces would represent the antenna geometry. This prototype had a resistance of 1.7 Ohms from corner to corner of the model. This is well below the desired value of three Ohms. There was some problem with the copper tape sticking to the flex circuit material. In an actual part this would not be a problem as there is a very good connection between the copper and the polyimide in the flex circuit material.

Figure 5-7 shows the bends and L-shapes prototype.

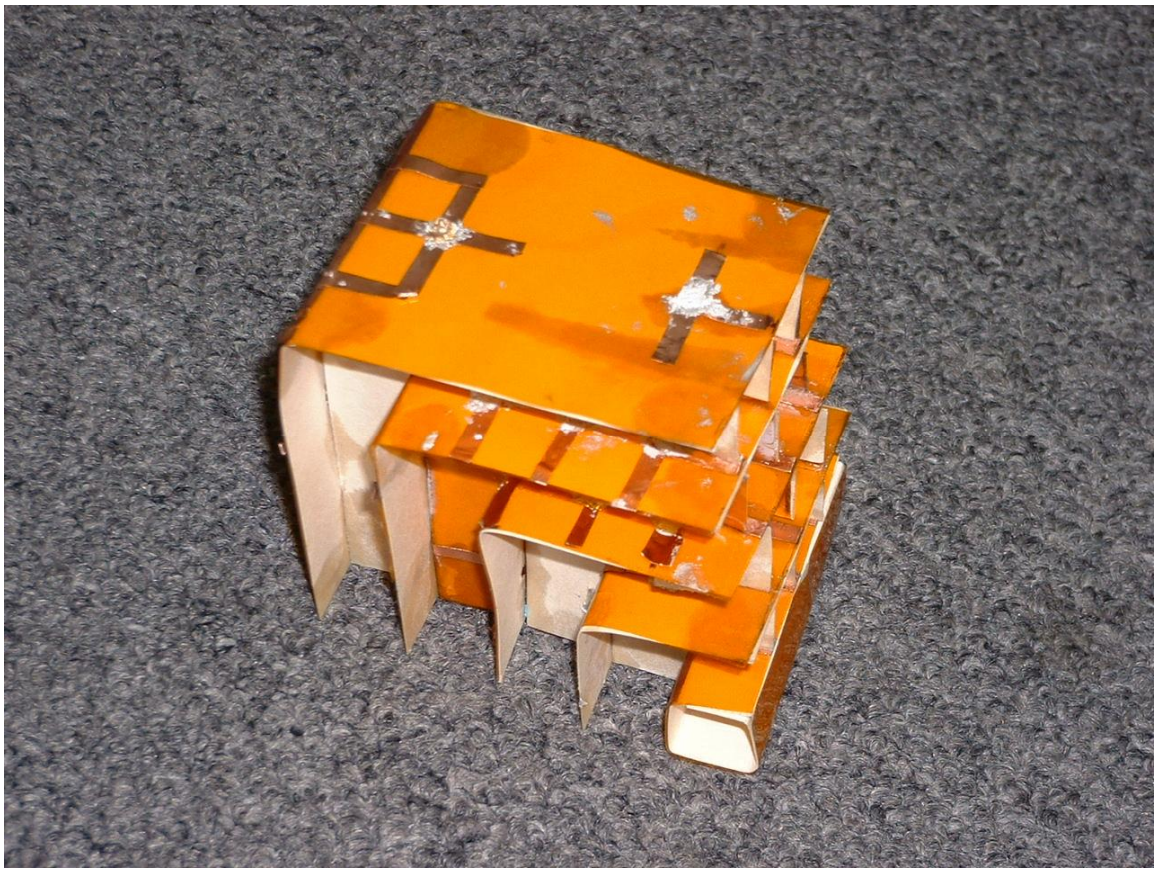

Figure 5-7 Bends and L-shapes Prototype

The bends and L-shapes concept prototype antenna was difficult to manufacture. It was very difficult to line up the antenna components so that the copper traces would represent the antenna geometry. The conductive epoxy was also difficult to place on the model as one had to reach into the crevices of the antenna to place it. This prototype had a resistance of 2.75 Ohms from corner to corner. It was also noticed that not all of the elements were electrically connected due to some joints that disconnected.

5.5 *Rapid Prototyping Models*

The rapid prototyping models were very easy to manufacture and were an exact match with the antenna geometry. There were no concerns with individual elements lining up properly. The SLA models had the difficulty of removing the supports without breaking the antenna elements. The SLA method was successful for the first three dimensional antenna design as the antenna elements were significantly larger than the supports and did not break when the supports were removed. The second design was not able to undergo the support removal procedure as the smaller elements broke when the supports were removed. The SLS prototype circumvented the support removal issue making a model without attached supports. Both of these methods can be successful in manufacturing three dimensional antenna designs, however, SLA is limited in the applicable designs by requiring antenna elements that are significantly larger than the supports.

The nickel coated antenna had a corner to corner resistance of 300 Ohms. This was significantly above the required resistance of 3 Ohms. The silver coated antenna had a corner to corner resistance of 0.85 Ohms which is within the 3 Ohm requirement. The silver and nickel antennas were tested to determine their antenna gain which is shown in Figure 5-8.

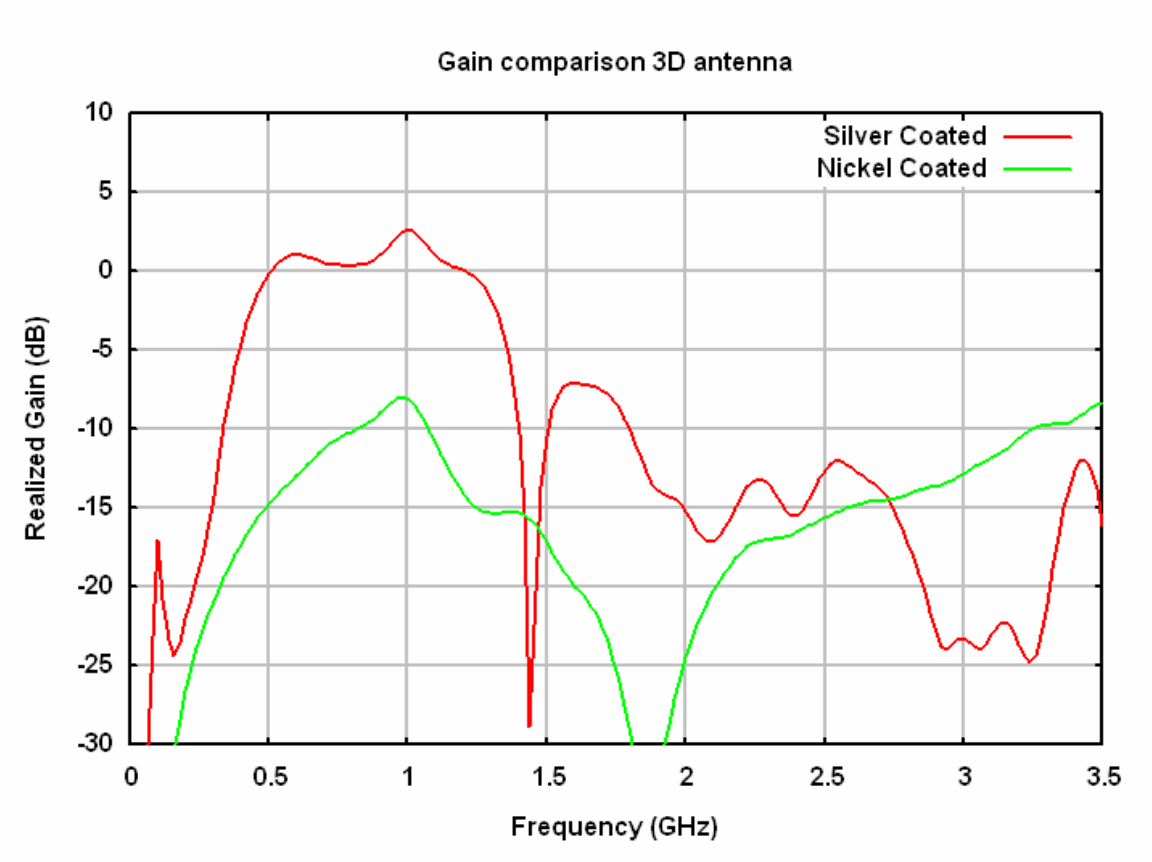

Figure 5-8 Silver and Nickel Antenna Gain

From Figure 5-8, one can see the obvious better performance of the silver coated antenna as compared to the nickel coated antenna by observing the larger area under the silver antenna gain plot as compared to the nickel antenna gain plot over the 0 GHz to 3.5 GHz frequency test range. This signifies that overall, the silver antenna performed better than the nickel antenna over the frequency range tested.

Figure 5-9 shows good agreement between the theoretical antenna performance, performed by others, and the actual measured performance of an antenna, made from wires, over a test frequency range of 0GHz to 1GHz, validating the performance of the three dimensional models.

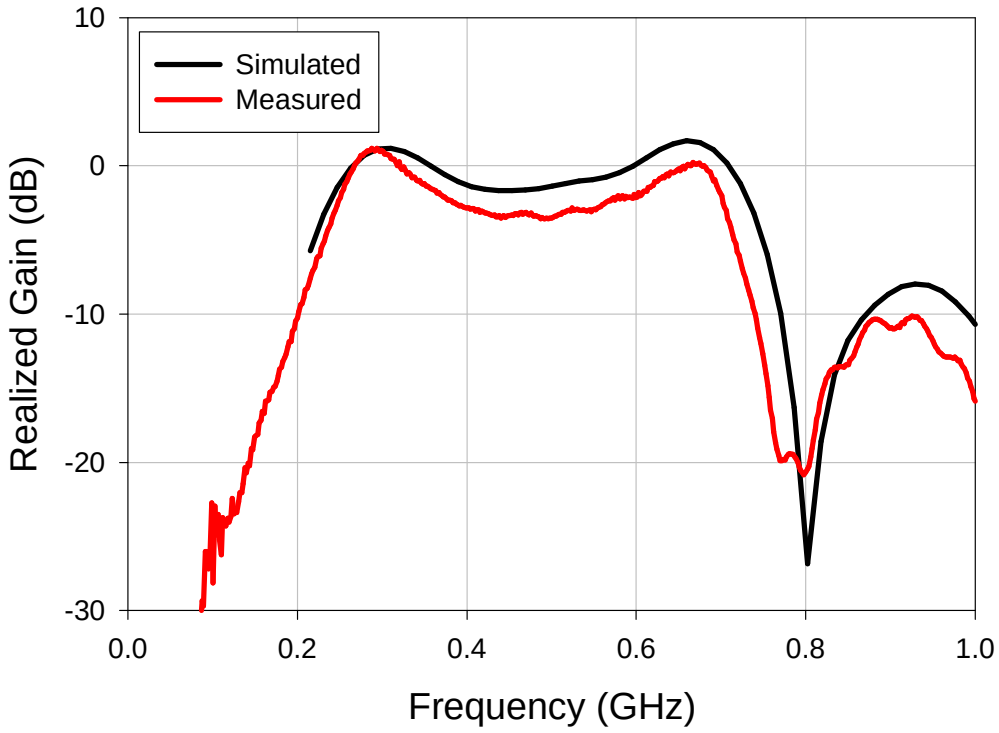

Figure 5-9 Simulated and Measured Antenna Performance

5.6 Summary

This chapter presented the results of the experimental procedures discussed in Chapter 4. Results of the experimental bending tests of the flex circuit were provided and analyzed. The predicted values of stain, for the bending of flex circuit material, were compared to the experimental bending results. It was found that with a bulging model incorporated into the bending model, the strain in the material can be approximated. An evaluation of the flex circuit material, after bending, was conducted. It was found that the materials bulge while bending and the materials do not exceed their physical limits. Models of the epoxy encapsulated antenna designs were constructed. Models of three dimensional antennas manufactured from flex

circuit material were constructed. Testing results of three dimensional antennas manufactured via SLA was provided and discussed. It was found that the three dimensional antennas perform well and agree with theory.

Chapter 6 provides a brief summary of the findings of this work. Recommendations for continuing research on three dimensional antenna manufacturing are also provided.

6 CONCLUSIONS AND RECOMMENDATIONS

This chapter provides a brief summary of the findings of this work. Recommendations for continuing research on three dimensional antenna manufacturing are provided.

6.1 Conclusions

With further development of phased array antennas, new designs become increasingly complex. The manufacturing techniques utilized to create these designs must be developed, and techniques sought to allow the complexity of the antenna designs, as traditional manufacturing operations such as injection molding, machining or bulk deformation processes are not well suited to create the small details and complex three dimensional lattice designs of the antenna.

Several possible manufacturing techniques were developed and analyzed for each antenna design to determine the methods suitable to manufacture the antennas. The manufacturing techniques include forming flex circuit material into different configurations that incorporate the geometry of the antenna design. In one design the flex circuit material was folded into hollow rectangular shapes that contain a portion of the geometry of the antenna. A second design that utilizes the flex circuit material was created by constructing folded planes and L-shapes that contain a portion of the antenna geometry.

An analytical bending model of bending of the flex circuit material was developed. Experimental testing of flex circuit bending was conducted. The theoretical values and the experimental data were compared and determined to agree closely.

Stereolithography was another manufacturing technique that was investigated. In this method a solid model of the antenna's lattice structure was created and a part was manufactured from photopolymer resin on a 3D Systems SLA 3500 machine. This part was then coated with a conductive material.

Another antenna design was manufactured by affixing coaxial cables to hollow plastic hemispheres. These hemispheres and cables were then cast into epoxy for support. Layers of copper wire mesh and fiberglass cloth were then cast into the epoxy structure to compliment the performance and strength of the antenna, respectively.

The requirement of the three dimensional antenna design was that it be conductive, on the order of 3 Ohms from corner to corner. The antennas were subjected to an electrical test to determine if they meet the three ohm conductivity requirement. Both of the three dimensional antennas constructed from the flex circuit material and the silver coated SLA antenna passed this requirement. The SLA antennas were tested to see how well they can send and receive signals. The gains of the nickel and silver coated SLA three dimensional antennas were measured over a frequency range. Both models agreed with theoretical antenna performance,

however, the silver coated SLA antenna had a larger area under the gain curve indicating that it performed better than the nickel coated SLA antenna

6.2 Recommendations for Further Work

In order to obtain a better understanding of the bending of flex circuit material, it is recommended that the thickness of the materials which comprise the flex circuit material be changed, experimental bending tests conducted, and the results compared to theoretical values predicted by the analytical model.

For further work on the three dimensional antennas constructed from flex circuit, the next step would be to have circuits manufactured commercially, and develop a large scale bending system and an automated method of assembly. It is recommended that work be continued on the straw concept three dimensional antenna as this design proved to be easier to manufacture than the bends and L-shapes concept.

Rapid prototyping technologies proved to be sound methods of manufacturing three dimensional antennas. With use of the Matlab program that generates Autocad commands from the element node locations, little resources and time are required to develop a new solid model. Also, there would be virtually no overhead cost for tooling changes if a different three dimensional design were to be implemented as compared to the three dimensional antennas manufactured with flex circuit material which would require a significant overhead cost to manufacture a different three

dimensional design, provided that automated manufacturing methods were employed. The SLS antennas were superior to those made via SLA in that there were no supports to remove and the antenna elements were not damaged as a result. It is the general view of the author that this was the best method for manufacturing three dimensional antenna designs and future efforts should be focused on this method.

.

APPENDIX A: MATLAB BENDING MODEL SOURCE CODE

```
clear;

%material data for polyimide (psi)
Epi=370000;
yieldpi=10000;
sigyieldpi=yieldpi/Epi;
Tpi=.003;
kpi=32714;
%kpi=1;

%material data for copper (psi)
Ecu=17e6;
yieldcu=10000;
sigyieldcu=yieldcu/Ecu;
Tcu=.001;
kcu=62500;
%kcu=1;

%bend width
b=1;

%punch radius limits
rmin=.001;
rmax=.025;
step=.001;
N=(rmax-rmin)/step;

fprintf('\npunch radius  bent strain   recovery      final strain\n')

%calculates bending moment with elastic strain hardening model
for n=1:1:(N+1);
   %increment punch radius
   r(n)=rmax-(n-1)*step;

   %calculate max engineering strain in polyimide
   sigmax(n)=1/(((2*r(n))/(2*Tpi+Tcu))+1);

   %calcualte strain at transition point; max of copper
   sigtrans(n)=Tcu/(2*r(n)+2*Tpi+Tcu);
```

```
%calculate bending moments

%determine elastic extent for polyimide

ap(n)=sigyieldpi/sigmax(n)*(Tcu+2*Tpi);

%calculates bending moment for polyimide
if r(n) > .015

    Mp1(n)= b*(ap(n)/2-Tcu/2)*((yieldpi-Epi*sigtrans(n))/2)*(2/3*(ap(n)/2-
Tcu/2)+Tcu/2);
    Mp2(n)= b*(ap(n)/2-Tcu/2)*(Epi*sigtrans(n))*(1/2*(ap(n)/2-Tcu/2)+Tcu/2);
    Mp3(n)= b*(Tpi+Tcu/2-ap(n)/2)*yieldpi*(1/2*(Tpi+Tcu/2-ap(n)/2)+ap(n)/2);
    Mp4(n)= b*(Tpi+Tcu/2-ap(n)/2)*(kpi*sigmax(n)/2)*(2/3*(Tpi+Tcu/2-
ap(n)/2)+ap(n)/2);

    Mp(n)=Mp1(n)+Mp2(n)+Mp3(n)+Mp4(n);

end

if r(n) <= .015

    Mp5(n)=b*Tpi*(yieldpi+kpi*sigtrans(n))*(Tpi/2+Tcu/2);
    Mp6(n)=b*Tpi*((kpi*sigmax(n)-kpi*sigtrans(n))/2)*(2/3*Tpi+Tcu/2);

    Mp(n)=Mp5(n)+Mp6(n);

end

%determine elastic extent for copper
ac(n)=sigyieldcu/sigtrans(n)*Tcu;

%calculates bending moment for copper
Mc1(n)=b*ac(n)/2*(yieldcu/2)*(2/3*(ac(n)/2));
Mc2(n)=b*(Tcu/2-ac(n)/2)*yieldcu*(1/2*(Tcu/2-ac(n)/2)+ac(n)/2);
Mc3(n)=b*(Tcu/2-ac(n)/2)*(kcu*sigtrans(n)/2)*(2/3*(Tcu/2-ac(n)/2)+ac(n)/2);

Mc(n)=Mc1(n)+Mc2(n)+Mc3(n);


BendingMoment(n)=Mc(n)+Mp(n);


%solve for elastic recovery strain
%x=1;
%E1(n)=b*(Tcu/2)*((Ecu*x/(Tpi+Tcu/2)*Tcu/2)/2)*(2/3*Tcu/2);
```

```
    %E2(n)=b*(Tpi)*(Epi*x/(Tpi+Tcu/2)*(Tcu/2))*(Tpi/2+Tcu/2);
    %E3(n)=b*(Tpi)*((Epi*x-Epi*x/(Tpi+Tcu/2)*Tcu/2)/2)*(2/3*Tpi*Tcu/2);


recoverystrain(n)=12*BendingMoment(n)*(2*Tpi+Tcu)/b/Tcu/(4*Tpi^3*Epi+6*Tpi^2*
Epi+6*Tpi*Epi*Tcu+Tcu^2*Ecu)-.13+(.3017*exp(-195.24*r(n)));

    finalstrain(n)=sigmax(n)-recoverystrain(n);

    %fprintf('%1.8f\n',recoverystrain(n));

    fprintf('%1.8f\n',sigmax(n));
    %fprintf('%3.3f,        %1.8f,   %1.8f,    %1.8f\n',r(n), sigmax(n),
recoverystrain(n),finalstrain(n));

end

hold on

plot(r,sigmax);
plot(r,recoverystrain,'g:');
plot(r,finalstrain,'r.');
title('Strain vs Bend Radius of Polyimide, t=0.005"');
xlabel('Bend Radius');
ylabel('Strain');
legend('Bending Strain','Elastic Recovery Strain','Final Strain');
hold off
```

APPENDIX B: MATLAB AUTOCAD COMMAND

PROGRAM SOURCE CODE

```
% x1,y1,z1 units are meters
% x2,y2,z2 units are meters

% unit cell size is .015 meters in x, .050 meters in y and .050 meters in z



%number of wires
N=419;

%wire diameter
D=0.0015;


load wirelist.m;

x1=wirelist(:,1);
y1=wirelist(:,2);
z1=wirelist(:,3);
x2=x1+wirelist(:,4);
y2=y1+wirelist(:,5);
z2=z1+wirelist(:,6);

fprintf('\n\n\n list of cylinders \n');
%plot cylinders
for n= 1:1:N;
   xi(n)=x1(n,1);
   yi(n)=y1(n,1);
   zi(n)=z1(n,1);

   xf(n)=x2(n,1);
   yf(n)=y2(n,1);
   zf(n)=z2(n,1);

   fprintf('cylinder %1.4f,%1.4f,%1.4f d %1.4f c %1.4f,%1.4f,%1.4f \n',...
      xi(n), yi(n), zi(n), D, xf(n), yf(n), zf(n));
end

fprintf('\n\n\n list of spheres \n');
```

```
%plot spheres
for n= 1:1:N;
   fprintf('sphere %1.4f,%1.4f,%1.4f d %1.4f \n', xi(n), yi(n), zi(n), D);

   fprintf('sphere %1.4f,%1.4f,%1.4f d %1.4f \n', xf(n), yf(n), zf(n), D);
end

%make holes
fprintf('\n\n\n list of spheres to remove y=0 plane \n');
for n= 1:1:N;

   if yi(n)==0
      fprintf('sphere %1.4f,%1.4f,%1.4f d %1.4f \n', xi(n), yi(n), zi(n), D);
   end
end


fprintf('\n\n\n list of cylinders to remove z=0.05 plane \n');
for x=.005:.005:.015;
   yint=-.005;
   yfin=.055;
   z=.05;

fprintf('cylinder %1.4f,%1.4f,%1.4f d %1.4f c %1.4f,%1.4f,%1.4f \n',...
      x, yint, z, D, x, yfin, z);

end

fprintf('\n\n\n more cylinders to remove z=0.05 plane \n');
for y=.005:.005:.045;
   xint=-.005;
   xfin=.02;
   z=.05;

fprintf('cylinder %1.4f,%1.4f,%1.4f d %1.4f c %1.4f,%1.4f,%1.4f \n',...
      xint, y, z, D, xfin, y, z);

end

%remove spheres from base
fprintf('\n\n\n remove spheres from base \n');
fprintf('sphere %1.4f,%1.4f,%1.4f d %1.4f \n', 0, .005, .05, D);
fprintf('sphere %1.4f,%1.4f,%1.4f d %1.4f \n', 0, .01, .05, D);
fprintf('sphere %1.4f,%1.4f,%1.4f d %1.4f \n', 0, .02, .05, D);
fprintf('sphere %1.4f,%1.4f,%1.4f d %1.4f \n', 0, .03, .05, D);
```

```
fprintf('sphere %1.4f,%1.4f,%1.4f d %1.4f \n', 0, .04, .05, D);
fprintf('sphere %1.4f,%1.4f,%1.4f d %1.4f \n', 0, .045, .05, D);

xps=[ x1.' ; x2.'];
yps=[ y1.' ; y2.'];
zps=[ z1.' ; z2.'];

plot3(xps,yps,zps,'r');
axis equal
```

APPENDIX C: ELEMENT LOCATIONS

Element #	X_0 (m)	Y_0 (m)	Z_0 (m)	X_1 (m)	Y_1 (m)	Z_1 (m)
1	0.000	0.005	0.000	0.005	0.000	0.000
2	0.010	0.005	0.000	0.005	0.000	0.000
3	0.010	0.005	0.005	0.005	0.000	0.000
4	0.000	0.005	0.010	0.005	0.000	0.000
5	0.010	0.005	0.010	0.005	0.000	0.000
6	0.000	0.005	0.015	0.005	0.000	0.000
7	0.005	0.005	0.015	0.005	0.000	0.000
8	0.000	0.005	0.020	0.005	0.000	0.000
9	0.005	0.005	0.020	0.005	0.000	0.000
10	0.000	0.005	0.025	0.005	0.000	0.000
11	0.005	0.005	0.025	0.005	0.000	0.000
12	0.000	0.005	0.045	0.005	0.000	0.000
13	0.005	0.005	0.045	0.005	0.000	0.000
14	0.010	0.005	0.045	0.005	0.000	0.000
15	0.000	0.010	0.000	0.005	0.000	0.000
16	0.005	0.010	0.000	0.005	0.000	0.000
17	0.005	0.010	0.005	0.005	0.000	0.000
18	0.010	0.010	0.005	0.005	0.000	0.000
19	0.000	0.010	0.010	0.005	0.000	0.000
20	0.000	0.010	0.015	0.005	0.000	0.000
21	0.005	0.010	0.015	0.005	0.000	0.000
22	0.000	0.010	0.020	0.005	0.000	0.000
23	0.005	0.010	0.020	0.005	0.000	0.000
24	0.010	0.010	0.020	0.005	0.000	0.000
25	0.000	0.010	0.030	0.005	0.000	0.000
26	0.000	0.010	0.040	0.005	0.000	0.000
27	0.005	0.010	0.045	0.005	0.000	0.000
28	0.005	0.015	0.000	0.005	0.000	0.000
29	0.005	0.015	0.005	0.005	0.000	0.000
30	0.010	0.015	0.005	0.005	0.000	0.000
31	0.000	0.015	0.015	0.005	0.000	0.000
32	0.005	0.015	0.015	0.005	0.000	0.000
33	0.005	0.015	0.020	0.005	0.000	0.000
34	0.000	0.015	0.030	0.005	0.000	0.000
35	0.000	0.015	0.035	0.005	0.000	0.000
36	0.000	0.015	0.045	0.005	0.000	0.000
37	0.005	0.015	0.045	0.005	0.000	0.000
38	0.010	0.015	0.045	0.005	0.000	0.000
39	0.000	0.020	0.000	0.005	0.000	0.000
40	0.005	0.020	0.000	0.005	0.000	0.000
41	0.010	0.020	0.000	0.005	0.000	0.000
42	0.005	0.020	0.005	0.005	0.000	0.000
43	0.010	0.020	0.005	0.005	0.000	0.000

44	0.000	0.020	0.010	0.005	0.000	0.000
45	0.005	0.020	0.010	0.005	0.000	0.000
46	0.010	0.020	0.010	0.005	0.000	0.000
47	0.000	0.020	0.015	0.005	0.000	0.000
48	0.005	0.020	0.015	0.005	0.000	0.000
49	0.000	0.020	0.020	0.005	0.000	0.000
50	0.010	0.020	0.025	0.005	0.000	0.000
51	0.000	0.020	0.030	0.005	0.000	0.000
52	0.010	0.020	0.030	0.005	0.000	0.000
53	0.010	0.020	0.035	0.005	0.000	0.000
54	0.010	0.020	0.040	0.005	0.000	0.000
55	0.010	0.020	0.045	0.005	0.000	0.000
56	0.005	0.025	0.005	0.005	0.000	0.000
57	0.010	0.025	0.005	0.005	0.000	0.000
58	0.000	0.025	0.010	0.005	0.000	0.000
59	0.005	0.025	0.010	0.005	0.000	0.000
60	0.010	0.025	0.010	0.005	0.000	0.000
61	0.000	0.025	0.015	0.005	0.000	0.000
62	0.005	0.025	0.015	0.005	0.000	0.000
63	0.000	0.025	0.025	0.005	0.000	0.000
64	0.000	0.025	0.025	0.005	0.000	0.000
65	0.005	0.025	0.025	0.005	0.000	0.000
66	0.005	0.025	0.030	0.005	0.000	0.000
67	0.000	0.025	0.035	0.005	0.000	0.000
68	0.000	0.025	0.040	0.005	0.000	0.000
69	0.010	0.025	0.040	0.005	0.000	0.000
70	0.000	0.025	0.045	0.005	0.000	0.000
71	0.005	0.025	0.045	0.005	0.000	0.000
72	0.010	0.025	0.045	0.005	0.000	0.000
73	0.000	0.030	0.000	0.005	0.000	0.000
74	0.005	0.030	0.000	0.005	0.000	0.000
75	0.010	0.030	0.000	0.005	0.000	0.000
76	0.005	0.030	0.005	0.005	0.000	0.000
77	0.010	0.030	0.005	0.005	0.000	0.000
78	0.000	0.030	0.010	0.005	0.000	0.000
79	0.005	0.030	0.010	0.005	0.000	0.000
80	0.010	0.030	0.010	0.005	0.000	0.000
81	0.000	0.030	0.015	0.005	0.000	0.000
82	0.005	0.030	0.015	0.005	0.000	0.000
83	0.000	0.030	0.020	0.005	0.000	0.000
84	0.010	0.030	0.025	0.005	0.000	0.000
85	0.000	0.030	0.030	0.005	0.000	0.000
86	0.010	0.030	0.030	0.005	0.000	0.000
87	0.010	0.030	0.035	0.005	0.000	0.000
88	0.010	0.030	0.040	0.005	0.000	0.000
89	0.010	0.030	0.045	0.005	0.000	0.000
90	0.005	0.035	0.000	0.005	0.000	0.000

91	0.005	0.035	0.005	0.005	0.000	0.000
92	0.010	0.035	0.005	0.005	0.000	0.000
93	0.000	0.035	0.015	0.005	0.000	0.000
94	0.005	0.035	0.015	0.005	0.000	0.000
95	0.005	0.035	0.020	0.005	0.000	0.000
96	0.000	0.035	0.030	0.005	0.000	0.000
97	0.000	0.035	0.035	0.005	0.000	0.000
98	0.000	0.035	0.045	0.005	0.000	0.000
99	0.005	0.035	0.045	0.005	0.000	0.000
100	0.010	0.035	0.045	0.005	0.000	0.000
101	0.000	0.040	0.000	0.005	0.000	0.000
102	0.005	0.040	0.000	0.005	0.000	0.000
103	0.005	0.040	0.005	0.005	0.000	0.000
104	0.010	0.040	0.005	0.005	0.000	0.000
105	0.000	0.040	0.010	0.005	0.000	0.000
106	0.000	0.040	0.015	0.005	0.000	0.000
107	0.005	0.040	0.015	0.005	0.000	0.000
108	0.000	0.040	0.020	0.005	0.000	0.000
109	0.005	0.040	0.020	0.005	0.000	0.000
110	0.010	0.040	0.020	0.005	0.000	0.000
111	0.000	0.040	0.030	0.005	0.000	0.000
112	0.000	0.040	0.040	0.005	0.000	0.000
113	0.005	0.040	0.045	0.005	0.000	0.000
114	0.000	0.045	0.000	0.005	0.000	0.000
115	0.010	0.045	0.000	0.005	0.000	0.000
116	0.010	0.045	0.005	0.005	0.000	0.000
117	0.000	0.045	0.010	0.005	0.000	0.000
118	0.010	0.045	0.010	0.005	0.000	0.000
119	0.000	0.045	0.015	0.005	0.000	0.000
120	0.005	0.045	0.015	0.005	0.000	0.000
121	0.000	0.045	0.020	0.005	0.000	0.000
122	0.005	0.045	0.020	0.005	0.000	0.000
123	0.000	0.045	0.025	0.005	0.000	0.000
124	0.005	0.045	0.025	0.005	0.000	0.000
125	0.000	0.045	0.045	0.005	0.000	0.000
126	0.005	0.045	0.045	0.005	0.000	0.000
127	0.010	0.045	0.045	0.005	0.000	0.000
128	0.005	0.000	0.000	0.000	0.005	0.000
129	0.005	0.005	0.000	0.000	0.005	0.000
130	0.005	0.010	0.000	0.000	0.005	0.000
131	0.005	0.020	0.000	0.000	0.005	0.000
132	0.005	0.025	0.000	0.000	0.005	0.000
133	0.005	0.035	0.000	0.000	0.005	0.000
134	0.005	0.040	0.000	0.000	0.005	0.000
135	0.005	0.045	0.000	0.000	0.005	0.000
136	0.005	0.010	0.005	0.000	0.005	0.000
137	0.005	0.015	0.005	0.000	0.005	0.000

138	0.005	0.030	0.005	0.000	0.005	0.000
139	0.005	0.035	0.005	0.000	0.005	0.000
140	0.005	0.000	0.010	0.000	0.005	0.000
141	0.005	0.015	0.010	0.000	0.005	0.000
142	0.005	0.030	0.010	0.000	0.005	0.000
143	0.005	0.045	0.010	0.000	0.005	0.000
144	0.005	0.000	0.015	0.000	0.005	0.000
145	0.005	0.005	0.015	0.000	0.005	0.000
146	0.005	0.010	0.015	0.000	0.005	0.000
147	0.005	0.015	0.015	0.000	0.005	0.000
148	0.005	0.020	0.015	0.000	0.005	0.000
149	0.005	0.025	0.015	0.000	0.005	0.000
150	0.005	0.030	0.015	0.000	0.005	0.000
151	0.005	0.035	0.015	0.000	0.005	0.000
152	0.005	0.040	0.015	0.000	0.005	0.000
153	0.005	0.045	0.015	0.000	0.005	0.000
154	0.005	0.005	0.020	0.000	0.005	0.000
155	0.005	0.010	0.020	0.000	0.005	0.000
156	0.005	0.035	0.020	0.000	0.005	0.000
157	0.005	0.040	0.020	0.000	0.005	0.000
158	0.005	0.000	0.025	0.000	0.005	0.000
159	0.005	0.045	0.025	0.000	0.005	0.000
160	0.005	0.005	0.030	0.000	0.005	0.000
161	0.005	0.015	0.030	0.000	0.005	0.000
162	0.005	0.030	0.030	0.000	0.005	0.000
163	0.005	0.040	0.030	0.000	0.005	0.000
164	0.005	0.010	0.035	0.000	0.005	0.000
165	0.005	0.015	0.035	0.000	0.005	0.000
166	0.005	0.020	0.035	0.000	0.005	0.000
167	0.005	0.025	0.035	0.000	0.005	0.000
168	0.005	0.030	0.035	0.000	0.005	0.000
169	0.005	0.035	0.035	0.000	0.005	0.000
170	0.005	0.005	0.045	0.000	0.005	0.000
171	0.005	0.010	0.045	0.000	0.005	0.000
172	0.005	0.015	0.045	0.000	0.005	0.000
173	0.005	0.030	0.045	0.000	0.005	0.000
174	0.005	0.035	0.045	0.000	0.005	0.000
175	0.005	0.040	0.045	0.000	0.005	0.000
176	0.010	0.000	0.000	0.000	0.005	0.000
177	0.010	0.005	0.000	0.000	0.005	0.000
178	0.010	0.015	0.000	0.000	0.005	0.000
179	0.010	0.020	0.000	0.000	0.005	0.000
180	0.010	0.025	0.000	0.000	0.005	0.000
181	0.010	0.030	0.000	0.000	0.005	0.000
182	0.010	0.040	0.000	0.000	0.005	0.000
183	0.010	0.045	0.000	0.000	0.005	0.000
184	0.010	0.005	0.005	0.000	0.005	0.000

185	0.010	0.010	0.005	0.000	0.005	0.000
186	0.010	0.015	0.005	0.000	0.005	0.000
187	0.010	0.020	0.005	0.000	0.005	0.000
188	0.010	0.025	0.005	0.000	0.005	0.000
189	0.010	0.030	0.005	0.000	0.005	0.000
190	0.010	0.035	0.005	0.000	0.005	0.000
191	0.010	0.040	0.005	0.000	0.005	0.000
192	0.010	0.000	0.010	0.000	0.005	0.000
193	0.010	0.010	0.010	0.000	0.005	0.000
194	0.010	0.020	0.010	0.000	0.005	0.000
195	0.010	0.025	0.010	0.000	0.005	0.000
196	0.010	0.035	0.010	0.000	0.005	0.000
197	0.010	0.045	0.010	0.000	0.005	0.000
198	0.010	0.000	0.015	0.000	0.005	0.000
199	0.010	0.005	0.015	0.000	0.005	0.000
200	0.010	0.020	0.015	0.000	0.005	0.000
201	0.010	0.025	0.015	0.000	0.005	0.000
202	0.010	0.040	0.015	0.000	0.005	0.000
203	0.010	0.045	0.015	0.000	0.005	0.000
204	0.010	0.010	0.020	0.000	0.005	0.000
205	0.010	0.015	0.020	0.000	0.005	0.000
206	0.010	0.030	0.020	0.000	0.005	0.000
207	0.010	0.035	0.020	0.000	0.005	0.000
208	0.010	0.000	0.025	0.000	0.005	0.000
209	0.010	0.020	0.025	0.000	0.005	0.000
210	0.010	0.025	0.025	0.000	0.005	0.000
211	0.010	0.045	0.025	0.000	0.005	0.000
212	0.010	0.015	0.030	0.000	0.005	0.000
213	0.010	0.020	0.030	0.000	0.005	0.000
214	0.010	0.025	0.030	0.000	0.005	0.000
215	0.010	0.030	0.030	0.000	0.005	0.000
216	0.010	0.020	0.035	0.000	0.005	0.000
217	0.010	0.025	0.035	0.000	0.005	0.000
218	0.010	0.000	0.040	0.000	0.005	0.000
219	0.010	0.015	0.040	0.000	0.005	0.000
220	0.010	0.020	0.040	0.000	0.005	0.000
221	0.010	0.025	0.040	0.000	0.005	0.000
222	0.010	0.030	0.040	0.000	0.005	0.000
223	0.010	0.045	0.040	0.000	0.005	0.000
224	0.010	0.005	0.045	0.000	0.005	0.000
225	0.010	0.040	0.045	0.000	0.005	0.000
226	0.015	0.000	0.000	0.000	0.005	0.000
227	0.015	0.005	0.000	0.000	0.005	0.000
228	0.015	0.020	0.000	0.000	0.005	0.000
229	0.015	0.025	0.000	0.000	0.005	0.000
230	0.015	0.040	0.000	0.000	0.005	0.000
231	0.015	0.045	0.000	0.000	0.005	0.000

232	0.015	0.005	0.005	0.000	0.005	0.000
233	0.015	0.040	0.005	0.000	0.005	0.000
234	0.015	0.005	0.010	0.000	0.005	0.000
235	0.015	0.010	0.010	0.000	0.005	0.000
236	0.015	0.035	0.010	0.000	0.005	0.000
237	0.015	0.040	0.010	0.000	0.005	0.000
238	0.015	0.005	0.015	0.000	0.005	0.000
239	0.015	0.010	0.015	0.000	0.005	0.000
240	0.015	0.015	0.015	0.000	0.005	0.000
241	0.015	0.020	0.015	0.000	0.005	0.000
242	0.015	0.025	0.015	0.000	0.005	0.000
243	0.015	0.030	0.015	0.000	0.005	0.000
244	0.015	0.035	0.015	0.000	0.005	0.000
245	0.015	0.040	0.015	0.000	0.005	0.000
246	0.015	0.005	0.020	0.000	0.005	0.000
247	0.015	0.015	0.020	0.000	0.005	0.000
248	0.015	0.030	0.020	0.000	0.005	0.000
249	0.015	0.040	0.020	0.000	0.005	0.000
250	0.015	0.020	0.025	0.000	0.005	0.000
251	0.015	0.025	0.025	0.000	0.005	0.000
252	0.015	0.010	0.035	0.000	0.005	0.000
253	0.015	0.015	0.035	0.000	0.005	0.000
254	0.015	0.020	0.035	0.000	0.005	0.000
255	0.015	0.025	0.035	0.000	0.005	0.000
256	0.015	0.030	0.035	0.000	0.005	0.000
257	0.015	0.035	0.035	0.000	0.005	0.000
258	0.015	0.005	0.040	0.000	0.005	0.000
259	0.015	0.010	0.040	0.000	0.005	0.000
260	0.015	0.020	0.040	0.000	0.005	0.000
261	0.015	0.025	0.040	0.000	0.005	0.000
262	0.015	0.035	0.040	0.000	0.005	0.000
263	0.015	0.040	0.040	0.000	0.005	0.000
264	0.015	0.000	0.045	0.000	0.005	0.000
265	0.015	0.005	0.045	0.000	0.005	0.000
266	0.015	0.010	0.045	0.000	0.005	0.000
267	0.015	0.015	0.045	0.000	0.005	0.000
268	0.015	0.030	0.045	0.000	0.005	0.000
269	0.015	0.035	0.045	0.000	0.005	0.000
270	0.015	0.040	0.045	0.000	0.005	0.000
271	0.015	0.045	0.045	0.000	0.005	0.000
272	0.005	0.005	0.000	0.000	0.000	0.005
273	0.005	0.005	0.005	0.000	0.000	0.005
274	0.005	0.005	0.015	0.000	0.000	0.005
275	0.005	0.005	0.020	0.000	0.000	0.005
276	0.005	0.005	0.025	0.000	0.000	0.005
277	0.005	0.005	0.045	0.000	0.000	0.005
278	0.005	0.010	0.000	0.000	0.000	0.005

279	0.005	0.010	0.010	0.000	0.000	0.005
280	0.005	0.010	0.040	0.000	0.000	0.005
281	0.005	0.015	0.000	0.000	0.000	0.005
282	0.005	0.015	0.005	0.000	0.000	0.005
283	0.005	0.015	0.015	0.000	0.000	0.005
284	0.005	0.015	0.020	0.000	0.000	0.005
285	0.005	0.015	0.040	0.000	0.000	0.005
286	0.005	0.015	0.045	0.000	0.000	0.005
287	0.005	0.020	0.000	0.000	0.000	0.005
288	0.005	0.020	0.015	0.000	0.000	0.005
289	0.005	0.020	0.020	0.000	0.000	0.005
290	0.005	0.020	0.030	0.000	0.000	0.005
291	0.005	0.020	0.045	0.000	0.000	0.005
292	0.005	0.025	0.000	0.000	0.000	0.005
293	0.005	0.025	0.005	0.000	0.000	0.005
294	0.005	0.025	0.015	0.000	0.000	0.005
295	0.005	0.025	0.025	0.000	0.000	0.005
296	0.005	0.030	0.000	0.000	0.000	0.005
297	0.005	0.030	0.015	0.000	0.000	0.005
298	0.005	0.030	0.020	0.000	0.000	0.005
299	0.005	0.030	0.030	0.000	0.000	0.005
300	0.005	0.030	0.045	0.000	0.000	0.005
301	0.005	0.035	0.000	0.000	0.000	0.005
302	0.005	0.035	0.005	0.000	0.000	0.005
303	0.005	0.035	0.015	0.000	0.000	0.005
304	0.005	0.035	0.020	0.000	0.000	0.005
305	0.005	0.035	0.040	0.000	0.000	0.005
306	0.005	0.035	0.045	0.000	0.000	0.005
307	0.005	0.040	0.000	0.000	0.000	0.005
308	0.005	0.040	0.010	0.000	0.000	0.005
309	0.005	0.040	0.040	0.000	0.000	0.005
310	0.005	0.045	0.000	0.000	0.000	0.005
311	0.005	0.045	0.005	0.000	0.000	0.005
312	0.005	0.045	0.015	0.000	0.000	0.005
313	0.005	0.045	0.020	0.000	0.000	0.005
314	0.005	0.045	0.025	0.000	0.000	0.005
315	0.005	0.045	0.045	0.000	0.000	0.005
316	0.010	0.005	0.000	0.000	0.000	0.005
317	0.010	0.005	0.005	0.000	0.000	0.005
318	0.010	0.005	0.010	0.000	0.000	0.005
319	0.010	0.005	0.020	0.000	0.000	0.005
320	0.010	0.005	0.040	0.000	0.000	0.005
321	0.010	0.005	0.045	0.000	0.000	0.005
322	0.010	0.010	0.000	0.000	0.000	0.005
323	0.010	0.010	0.005	0.000	0.000	0.005
324	0.010	0.010	0.010	0.000	0.000	0.005
325	0.010	0.010	0.015	0.000	0.000	0.005

326	0.010	0.010	0.040	0.000	0.000	0.005
327	0.010	0.010	0.045	0.000	0.000	0.005
328	0.010	0.015	0.015	0.000	0.000	0.005
329	0.010	0.015	0.020	0.000	0.000	0.005
330	0.010	0.015	0.040	0.000	0.000	0.005
331	0.010	0.020	0.000	0.000	0.000	0.005
332	0.010	0.020	0.005	0.000	0.000	0.005
333	0.010	0.020	0.015	0.000	0.000	0.005
334	0.010	0.020	0.025	0.000	0.000	0.005
335	0.010	0.020	0.040	0.000	0.000	0.005
336	0.010	0.025	0.025	0.000	0.000	0.005
337	0.010	0.025	0.040	0.000	0.000	0.005
338	0.010	0.030	0.000	0.000	0.000	0.005
339	0.010	0.030	0.005	0.000	0.000	0.005
340	0.010	0.030	0.015	0.000	0.000	0.005
341	0.010	0.030	0.025	0.000	0.000	0.005
342	0.010	0.030	0.040	0.000	0.000	0.005
343	0.010	0.035	0.015	0.000	0.000	0.005
344	0.010	0.035	0.020	0.000	0.000	0.005
345	0.010	0.035	0.040	0.000	0.000	0.005
346	0.010	0.040	0.000	0.000	0.000	0.005
347	0.010	0.040	0.005	0.000	0.000	0.005
348	0.010	0.040	0.010	0.000	0.000	0.005
349	0.010	0.040	0.015	0.000	0.000	0.005
350	0.010	0.040	0.040	0.000	0.000	0.005
351	0.010	0.040	0.045	0.000	0.000	0.005
352	0.010	0.045	0.000	0.000	0.000	0.005
353	0.010	0.045	0.005	0.000	0.000	0.005
354	0.010	0.045	0.010	0.000	0.000	0.005
355	0.010	0.045	0.020	0.000	0.000	0.005
356	0.010	0.045	0.040	0.000	0.000	0.005
357	0.010	0.045	0.045	0.000	0.000	0.005
358	0.015	0.005	0.000	0.000	0.000	0.005
359	0.015	0.005	0.005	0.000	0.000	0.005
360	0.015	0.005	0.010	0.000	0.000	0.005
361	0.015	0.005	0.015	0.000	0.000	0.005
362	0.015	0.005	0.035	0.000	0.000	0.005
363	0.015	0.005	0.040	0.000	0.000	0.005
364	0.015	0.005	0.045	0.000	0.000	0.005
365	0.015	0.010	0.000	0.000	0.000	0.005
366	0.015	0.010	0.005	0.000	0.000	0.005
367	0.015	0.010	0.010	0.000	0.000	0.005
368	0.015	0.010	0.020	0.000	0.000	0.005
369	0.015	0.010	0.025	0.000	0.000	0.005
370	0.015	0.010	0.040	0.000	0.000	0.005
371	0.015	0.010	0.045	0.000	0.000	0.005
372	0.015	0.015	0.000	0.000	0.000	0.005

373	0.015	0.015	0.005	0.000	0.000	0.005
374	0.015	0.015	0.010	0.000	0.000	0.005
375	0.015	0.015	0.015	0.000	0.000	0.005
376	0.015	0.015	0.035	0.000	0.000	0.005
377	0.015	0.015	0.040	0.000	0.000	0.005
378	0.015	0.015	0.045	0.000	0.000	0.005
379	0.015	0.020	0.000	0.000	0.000	0.005
380	0.015	0.020	0.005	0.000	0.000	0.005
381	0.015	0.020	0.010	0.000	0.000	0.005
382	0.015	0.020	0.015	0.000	0.000	0.005
383	0.015	0.020	0.030	0.000	0.000	0.005
384	0.015	0.020	0.035	0.000	0.000	0.005
385	0.015	0.020	0.040	0.000	0.000	0.005
386	0.015	0.020	0.045	0.000	0.000	0.005
387	0.015	0.025	0.000	0.000	0.000	0.005
388	0.015	0.025	0.010	0.000	0.000	0.005
389	0.015	0.025	0.015	0.000	0.000	0.005
390	0.015	0.025	0.045	0.000	0.000	0.005
391	0.015	0.030	0.000	0.000	0.000	0.005
392	0.015	0.030	0.005	0.000	0.000	0.005
393	0.015	0.030	0.010	0.000	0.000	0.005
394	0.015	0.030	0.015	0.000	0.000	0.005
395	0.015	0.030	0.030	0.000	0.000	0.005
396	0.015	0.030	0.035	0.000	0.000	0.005
397	0.015	0.030	0.040	0.000	0.000	0.005
398	0.015	0.030	0.045	0.000	0.000	0.005
399	0.015	0.035	0.000	0.000	0.000	0.005
400	0.015	0.035	0.005	0.000	0.000	0.005
401	0.015	0.035	0.010	0.000	0.000	0.005
402	0.015	0.035	0.015	0.000	0.000	0.005
403	0.015	0.035	0.035	0.000	0.000	0.005
404	0.015	0.035	0.040	0.000	0.000	0.005
405	0.015	0.035	0.045	0.000	0.000	0.005
406	0.015	0.040	0.000	0.000	0.000	0.005
407	0.015	0.040	0.005	0.000	0.000	0.005
408	0.015	0.040	0.010	0.000	0.000	0.005
409	0.015	0.040	0.020	0.000	0.000	0.005
410	0.015	0.040	0.025	0.000	0.000	0.005
411	0.015	0.040	0.040	0.000	0.000	0.005
412	0.015	0.040	0.045	0.000	0.000	0.005
413	0.015	0.045	0.000	0.000	0.000	0.005
414	0.015	0.045	0.005	0.000	0.000	0.005
415	0.015	0.045	0.010	0.000	0.000	0.005
416	0.015	0.045	0.015	0.000	0.000	0.005
417	0.015	0.045	0.035	0.000	0.000	0.005
418	0.015	0.045	0.040	0.000	0.000	0.005
419	0.015	0.045	0.045	0.000	0.000	0.005

APPENDIX D: BENDING TEST DATA

TEST#	TEST HEIGHT (inch)	BEND ANGLE (degree)
1	0.016	55
2	0.016	64
3	0.016	60
4	0.016	59
5	0.016	58
6	0.016	57
7	0.016	65
8	0.016	59
9	0.016	59
10	0.016	63
11	0.021	72
12	0.021	75
13	0.021	76
14	0.021	76
15	0.021	80
16	0.021	81
17	0.021	75
18	0.021	75
19	0.021	77
20	0.021	75
21	0.026	80
22	0.026	80
23	0.026	80
24	0.026	79
25	0.026	79
26	0.026	80
27	0.026	80
28	0.026	82
29	0.026	84
30	0.026	85
31	0.028	95
32	0.028	90
33	0.028	100
34	0.028	95
35	0.028	94
36	0.028	92
37	0.028	90
38	0.028	90
39	0.028	91
40	0.028	87
41	0.03	99
42	0.03	97
43	0.03	92

44	0.03	98
45	0.03	97
46	0.03	98
47	0.03	95
48	0.03	98
49	0.03	96
50	0.03	96
51	0.031	104
52	0.031	107
53	0.031	107
54	0.031	105
55	0.031	108
56	0.031	104
57	0.031	105
58	0.031	105
59	0.031	97
60	0.031	102
61	0.032	107
62	0.032	107
63	0.032	108
64	0.032	108
65	0.032	106
66	0.032	111
67	0.032	107
68	0.032	111
69	0.032	111
70	0.032	106
71	0.033	111
72	0.033	110
73	0.033	105
74	0.033	110
75	0.033	108
76	0.033	105
77	0.033	105
78	0.033	110
79	0.033	110
80	0.033	115
81	0.034	112
82	0.034	117
83	0.034	117
84	0.034	116
85	0.034	116
86	0.034	120
87	0.034	115
88	0.034	122
89	0.034	126
90	0.034	120
91	0.035	108

92	0.035	113
93	0.035	113
94	0.035	115
95	0.035	110
96	0.035	114
97	0.035	119
98	0.035	118
99	0.035	116
100	0.035	120
101	0.036	124
102	0.036	124
103	0.036	116
104	0.036	117
105	0.036	117
106	0.036	112
107	0.036	117
108	0.036	126
109	0.036	127
110	0.036	127
111	0.037	123
112	0.037	107
113	0.037	119
114	0.037	125
115	0.037	125
116	0.037	116
117	0.037	125
118	0.037	130
119	0.037	120
120	0.037	123
121	0.038	117
122	0.038	118
123	0.038	123
124	0.038	118
125	0.038	121
126	0.038	121
127	0.038	121
128	0.038	122
129	0.038	117
130	0.038	122
131	0.039	125
132	0.039	116
133	0.039	121
134	0.039	122
135	0.039	121
136	0.039	120
137	0.039	125
138	0.039	125
139	0.039	126

140	0.039	121
141	0.04	135
142	0.04	121
143	0.04	125
144	0.04	121
145	0.04	126
146	0.04	121
147	0.04	125
148	0.04	130
149	0.04	121
150	0.04	131
151	0.042	121
152	0.042	133
153	0.042	132
154	0.042	136
155	0.042	135
156	0.042	136
157	0.042	136
158	0.042	130
159	0.042	138
160	0.042	136
161	0.044	136
162	0.044	137
163	0.044	138
164	0.044	141
165	0.044	135
166	0.044	138
167	0.044	137
168	0.044	137
169	0.044	138
170	0.044	136
171	0.049	138
172	0.049	138
173	0.049	139
174	0.049	140
175	0.049	140
176	0.049	141
177	0.049	137
178	0.049	136
179	0.049	141
180	0.049	147
181	0.054	146
182	0.054	146
183	0.054	146
184	0.054	146
185	0.054	151
186	0.054	146
187	0.054	142

188	0.054	147
189	0.054	147
190	0.054	150
191	0.064	152
192	0.064	152
193	0.064	151
194	0.064	151
195	0.064	152
196	0.064	152
197	0.064	151
198	0.064	153
199	0.064	153
200	0.064	158
201	0.029	107
202	0.029	111
203	0.029	108
204	0.029	109
205	0.029	112
206	0.029	121
207	0.029	107
208	0.029	112
209	0.029	108
210	0.029	110
211	0.027	92
212	0.027	96
213	0.027	106
214	0.027	107
215	0.027	102
216	0.027	99
217	0.027	101
218	0.027	97
219	0.027	102
220	0.027	102
221	0.025	94
222	0.025	96
223	0.025	109
224	0.025	93
225	0.025	94
226	0.025	95
227	0.025	92
228	0.025	95
229	0.025	95
230	0.025	91
231	0.024	102
232	0.024	97
233	0.024	102
234	0.024	98
235	0.024	96

236	0.024	97
237	0.024	102
238	0.024	98
239	0.024	102
240	0.024	97
241	0.023	98
242	0.023	102
243	0.023	95
244	0.023	97
245	0.023	106
246	0.023	96
247	0.023	104
248	0.023	101
249	0.023	98
250	0.023	101
251	0.022	81
252	0.022	86
253	0.022	81
254	0.022	80
255	0.022	83
256	0.022	81
257	0.022	87
258	0.022	86
259	0.022	83
260	0.022	86
261	0.02	77
262	0.02	77
263	0.02	86
264	0.02	81
265	0.02	79
266	0.02	79
267	0.02	82
268	0.02	83
269	0.02	86
270	0.02	82
271	0.018	66
272	0.018	64
273	0.018	76
274	0.018	77
275	0.018	79
276	0.018	75
277	0.018	83
278	0.018	80
279	0.018	84
280	0.018	74

APPENDIX E: BENDING TEST STRAIN DATA

Punch Radius (inch)	Bent Strain	Final Strain	Recovery Strain
0.0250	0.1228	0.1040	0.0188
0.0200	0.1489	0.1214	0.0276
0.0175	0.1667	0.1294	0.0373
0.0150	0.1892	0.1443	0.0449
0.0140	0.2000	0.1481	0.0519
0.0130	0.2121	0.1480	0.0641
0.0125	0.2188	0.1485	0.0702
0.0120	0.2258	0.1505	0.0753
0.0115	0.2333	0.1572	0.0761
0.0110	0.2414	0.1619	0.0795
0.0105	0.2500	0.1592	0.0908
0.0100	0.2593	0.1701	0.0892
0.0095	0.2692	0.1629	0.1063
0.0090	0.2800	0.1683	0.1117
0.0085	0.2917	0.1692	0.1225
0.0080	0.3043	0.1633	0.1410
0.0075	0.3182	0.1953	0.1229
0.0070	0.3333	0.1711	0.1622
0.0065	0.3500	0.1952	0.1548
0.0060	0.3684	0.1656	0.2028
0.0055	0.3889	0.2061	0.1828
0.0050	0.4118	0.2267	0.1851
0.0045	0.4375	0.2426	0.1949
0.0040	0.4667	0.2162	0.2504
0.0035	0.5000	0.2117	0.2883
0.0030	0.5385	0.2429	0.2956
0.0020	0.6364	0.2680	0.3684
0.0010	0.7778	0.2588	0.5190

APPENDIX F: THEORETICAL FINAL STRAIN DATA

Punch Radius (inch)	Final Strain
0.0250	0.1081
0.0240	0.1113
0.0230	0.1147
0.0220	0.1185
0.0210	0.1225
0.0200	0.1269
0.0190	0.1318
0.0180	0.1371
0.0170	0.1429
0.0160	0.1493
0.0150	0.1565
0.0140	0.1607
0.0130	0.1697
0.0120	0.1799
0.0110	0.1914
0.0100	0.2047
0.0090	0.2201
0.0080	0.2382
0.0070	0.2597
0.0060	0.2857
0.0050	0.3179
0.0040	0.3587
0.0030	0.4120
0.0020	0.4847
0.0010	0.5897

APPENDIX G: CORRECTED FINAL STRAIN DATA

Punch Radius (inch)	Corrected Final Strain
0.0250	0.1058
0.0240	0.1085
0.0230	0.1113
0.0220	0.1143
0.0210	0.1175
0.0200	0.1209
0.0190	0.1244
0.0180	0.1281
0.0170	0.1320
0.0160	0.1361
0.0150	0.1404
0.0140	0.1411
0.0130	0.1459
0.0120	0.1509
0.0110	0.1562
0.0100	0.1619
0.0090	0.1680
0.0080	0.1749
0.0070	0.1828
0.0060	0.1922
0.0050	0.2043
0.0040	0.2205
0.0030	0.2440
0.0020	0.2805
0.0010	0.3415

REFRENCES

[1] Alan T. Zehnder and Anthony R. Ingraffea, “Reinforcing Effect of Coverlayers on the Fatigue Life of Copper-Kapton Flex Cables,” IEEE Transactions on Components, Packaging, and Manufacturing Technology – Part B, Vol. 18, pp. 704 – 708, 1995.

[2] Pyralux Technical Manual. E. I. du Pont de Nemours and Company. 1993.

[3] Stephen J. Meschter, “Cover Sheet Wrinkling of Rigid Flex Printed Circuits,” American Society of Mechanical Engineers, EEP, V4-1, Advances in Electronic Packaging, pp. 269-276, 1993.

[4] http://www.epoxyproducts.com/chemistry.html, Date Accessed: November 2005.

[5] Denny F. Bardoliwalla, “Fast Curing, Low Exotherm Epoxy Potting and Encapsulating Systems,” Electrical/Electronics Insulation Conference, IEEE, 1997, pp. 245-247.

[6] Serope Kalpakjian and Steven R. Schmid, *Manufacturing Processes for Engineering Materials*, 4th ed., Pearson Education, Inc., NJ, 2003.

[7] S. K. Kaldor and I. C. Noyan, “Differentiating between elastically bent rectangular beams and plates,” Applied Physics Letters, Vol. 80, No. 13, 2002, pp. 2284-2286.

[8] http://www.hcrosscompany.com/metals/copper.htm, Date Accessed: Februrary 2006.

[9] Publication 300674A, E. I. du Pont de Nemours and Company. 1997.

[10] SL 7510 Resin, Material Data Sheet P/N 70356, 3D Systems, 1999.

[11] Somos 8120 Epoxy Photopolymer, Material Data Sheet, DSM Somos.

[12] RenShape SL 7560, Material Data Sheet, Vantico AG, 2003.

[13] WaterClear 10120, Material Data Sheet, DSM Somos.

[14] Gilleo, Ken, “Packaging Problems,” Printed Circuit Fabrication, Vol. 21, Iss. 9, 1998, pp 18-22.